Progress in Oceanography 182 (2020) 102266

Contents lists available at ScienceDirect

Progress in Oceanography

journal homepage: www.elsevier.com/locate/pocean

Seasonal dynamics of midwater zooplankton and relation to particle cycling in the North Pacific Subtropical Gyre

Cecelia C.S. Hannides[a,*], Brian N. Popp[a], Hilary G. Close[a,c], Claudia R. Benitez-Nelson[d], Cassie A. Ka'apu-Lyons[a], Kristen Gloeckler[b], Natalie Wallsgrove[a], Blaire Umhau[d], Emily Palmer[d], Jeffrey C. Drazen[b]

[a] Department of Earth Sciences, University of Hawaii at Manoa, 1680 East West Road, Honolulu, HI 96822, USA
[b] Department of Oceanography, University of Hawaii at Manoa, 1000 Pope Road, Honolulu, HI 96822, USA
[c] Rosenstiel School of Marine and Atmospheric Science, University of Miami, 4600 Rickenbacker Causeway, Miami, FL 33149, USA
[d] School of the Earth, Ocean and Environment, University of South Carolina, 701 Sumter Street, Columbia, SC 29208, USA

ARTICLE INFO

Keywords:
Mesopelagic ecosystem
CSIA-AA
Stable isotope analysis
Station ALOHA
Food webs

ABSTRACT

Midwater zooplankton are major agents of biogeochemical transformation in the open ocean; however their characteristics and activity remain poorly known. Here we evaluate midwater zooplankton biomass, amino acid (AA)-specific stable isotope composition (δ^{15}N values) using compound-specific isotope analysis of amino acids (CSIA-AA), trophic position, and elemental composition in the North Pacific Subtropical Gyre (NPSG). We focus on zooplankton collected in the winter, spring, and summer to evaluate midwater trophic dynamics over a seasonal cycle. For the first time we find that midwater zooplankton respond strongly to seasonal changes in production and export in the NPSG. In summer, when export from the euphotic zone is elevated and this 'summer pulse' material is transported rapidly to depth, CSIA-AA indicates that large particles (> 53 μm) dominate the food web base for zooplankton throughout the midwaters, and to a large extent even into the upper bathypelagic zone. In winter, when export is low, zooplankton in the mid-mesopelagic zone continue to rely on large particle basal resources, but resident zooplankton in the lower mesopelagic and upper bathypelagic zones switch to include smaller particles (0.7–53 μm) in their food web base, or even a subset of the small particle pool. Midwater zooplankton migration patterns also vary with season, with migrants distributed more evenly at night through the euphotic zone in summer as compared to being more compressed in the upper mixed layer in winter. Deeper zooplankton migration within the mesopelagic zone is also reduced in late summer, likely due to the increased magnitude of large particle material available at depth during this season. Our observed seasonal change in activity and trophic dynamics drives modestly greater biomass in summer than winter through the mesopelagic zone. In contrast midwater zooplankton carbon (C), nitrogen (N), and phosphorus (P) composition does not change with season. Instead we find increasing C:N, C:P, and N:P ratios with greater depths, likely due to decreases in proteinaceous structures and organic P compounds and increases in storage lipids with depth. Our study highlights the importance and diversity of feeding strategies for small zooplankton in NPSG midwaters. Many small zooplankton, such as oncaeid and oithonid copepods, are able to access small particle resources at depth and may be an important trophic link between the microbial loop and deep dwelling micronekton species that also rely on small particle-based food webs. Our observed midwater zooplankton trophic response to export-driven variation in the particle field at depth has important implications for midwater metabolism and the export of C to the deep sea.

1. Introduction

Zooplankton living in the ocean's 'twilight zone' are key components of an ecologically understudied habitat. In this midwater environment, between the base of the euphotic zone and 1000 m depth, particles sinking from surface waters are consumed, repackaged, and remineralized, thus changing the transfer efficiency of the biological pump (Buesseler and Boyd, 2009). A significant contributor to particle attenuation in this realm are resident midwater zooplankton, as the amount of carbon (C) needed to support their metabolism is equivalent

* Corresponding author.
E-mail address: cecelia.hannides@gmail.com (C.C.S. Hannides).

https://doi.org/10.1016/j.pocean.2020.102266
Received 3 February 2019; Received in revised form 4 January 2020; Accepted 12 January 2020
Available online 16 January 2020

to (Hannides et al., 2015) or greater than (Steinberg et al., 2008b) the reduction in sinking particulate flux over these depths. Particle flux is also affected by zooplankton migrating to midwaters on a diel cycle through the production of fecal pellets. Here zooplankton act as a vertical shunt (Buesseler and Boyd, 2009), moving C efficiently from the surface waters where they feed at night to their resting depths in the mesopelagic zone. At the same time migrant zooplankton excrete dissolved organic material at depth, which likely contributes to the metabolism of midwater microbial populations (Hannides, 2014; Steinberg et al., 2000). Ultimately, resident and migrant zooplankton are a major food source for mesopelagic micronekton (Clarke, 1978) which in turn feed commercially important fish species (Brodeur and Yamamura, 2005). By respiring, repackaging, or excreting C originally produced in surface waters, zooplankton act as agents of biogeochemical transformation in the mesopelagic zone.

Despite their important role within the mesopelagic ecosystem, the characteristics and biological activity of deep pelagic zooplankton remain poorly known (Robison, 2004). A key conundrum is how zooplankton consume enough C to support their metabolism at depth. As noted above, Steinberg et al. (2008b) found zooplankton metabolic C demand to be 1–2 times and 3–9 times greater than the attenuation of sinking particle fluxes in the North Pacific Subtropical Gyre (NPSG) and in the subarctic Pacific, respectively. In the NPSG, Steinberg et al. (2008b) evaluated attenuation as losses of sinking particulate organic C (POC) measured using sediment traps, and calculated metabolic demand by applying models of zooplankton metabolism to estimates of midwater zooplankton biomass. Even when global-bathymetric models of zooplankton metabolism are applied, zooplankton metabolic C demand in the NPSG remains roughly equivalent to (0.4–1.9 times) the loss in sinking particle flux through the midwaters (Hannides et al., 2015). This imbalance between sinking particle supply and zooplankton respiratory demand is greatest in the lower mesopelagic zone (Giering et al., 2014). Thus midwater zooplankton must have alternative sources of C fueling their activity, particularly deep in the midwaters. Steinberg et al. (2008b) suggested zooplankton carnivory on vertical migrants as an alternative feeding mechanism, which would allow for midwater consumption of C originally produced in the euphotic zone. A recent review by Steinberg and Landry (2017) reiterated that migrant zooplankton were an important source of surface-derived C for resident zooplankton carnivores in the mesopelagic zone. Thus research to date supports the view of midwater zooplankton as consumers of large, sinking particles, or other migrant zooplankton, at depth.

A potential alternate source of C fueling midwater zooplankton food webs are small, slowly setting particles. Recent work has shown that small, slowly settling particles significantly contribute to C flux throughout the world's oceans (Baker et al., 2017; Close et al., 2013; Puigcorbe et al., 2015; Richardson and Jackson, 2007). For example, small or slowly settling particles contributed over 60% of particulate organic C (POC) flux in the Canary Current region in the summer and fall (Alonso-Gonzalez et al., 2010), and were responsible for more than a third of the total C flux throughout the year in the Sargasso Sea (Durkin et al., 2015). In the NPSG the contribution of slowly settling particles to POC flux can be 15–50% (Trull et al., 2008) or potentially higher (Alonso-Gonzalez et al., 2010). Small particles in turn drive a significant proportion of microbial metabolism at depth (Baltar et al., 2009), fueling a deep microbial loop that could, in theory, support resident midwater zooplankton. Findings to date, however, have been equivocal. Small particles form up to 80% of the food web base for select zooplanktivorous micronekton in the NPSG (Choy et al., 2015), suggesting mesopelagic zooplankton are an important conduit for the transfer of energy between small particles and micronekton at depth. In contrast, Steinberg et al. (2008b) found that small particle C was inadequate to meet mesopelagic zooplankton C demand in the subarctic Pacific during summer. Moreover Hannides et al. (2013) found that deep small particles were not a significant basal resource for mesopelagic zooplankton in the NPSG during summer, and instead 62–88% of the nitrogen (N) supporting midwater zooplankton food webs during this time period was surface-derived.

Conflicting conclusions regarding the importance of small particles as a basal resource for midwater zooplankton food webs may be due in part to seasonal dynamics, at least in the NPSG. Once considered 'monotonously' stable (McGowan and Walker, 1979), more recent time-series research has revealed a unique annual cycle in the surface ocean of this system. Primary production in the NPSG is generally higher during summer when the water column is highly stratified (Church et al., 2013; Karl et al., 1996). This seasonality is driven in part by diazotrophic (N_2-fixing) plankton (Church et al., 2009; Dore et al., 2002) that increase in biomass during summer (Pasulka et al., 2013). It is hypothesized that the peak in N_2-supported new production results in a higher biomass of zooplankton in the surface ocean during summer (Landry et al., 2001). At the same time, a highly predictable and rapid late summer export pulse, fueled by these diazotrophs, has been observed in deep-sea (4000 m) sediment traps (Karl et al., 2012). This annual variability in new production and export conditions in the surface ocean likely impacts mesopelagic populations. For example, as noted above, Hannides et al. (2013) found that a significant proportion of the organic matter sustaining midwater zooplankton in the NPSG is surface-derived. However this study was conducted in late summer when large particle fluxes are maximal and thus likely dominated zooplankton nutrition at depth. Small, slowly settling particles could be a more important basal food web resource for zooplankton during the winter, spring, and fall when these particles likely dominate export (Richardson and Jackson, 2007).

An added complexity to the size of material contributing to zooplankton nutrition is the composition of the material itself. Large particles generally sink rapidly and are thought to be comprised of fresher organic matter and/or fecal pellets while smaller, slowly sinking particles are subject to a longer exposure of microbial alteration. While several studies suggest that small particles are simply the result of disaggregation, more recent work indicates that small and large particles below the euphotic zone are fundamentally different. For example, Abramson et al. (2010) found that sinking and suspended particles maintained distinctly different pigment, amino acid, and lipid compositions to depths of 1900 m in the Mediterranean Sea. Moreover, differences were more pronounced during the high flux period in spring in the Mediterranean, as compared to the low flux period in summer (Abramson et al., 2010). Duret et al. (2019) also found, based on 16S rRNA sequencing, that prokaryotic communities were distinctly different on mesopelagic suspended versus sinking particles. Finally, analysis of particle samples collected by Multiple Unit Large Volume *in situ* Filtration (MULVFS) indicates that differences in mesopelagic particle source is driven by changes in community composition in the overlying euphotic zone (Lam et al., 2011).

Evaluating the basal resources supporting midwater zooplankton food webs remains logistically challenging, due in large part to the remote nature of the environment. However new biochemical tracer techniques such as compound-specific isotope analysis of amino acids (CSIA-AA) are improving our knowledge of deep ocean ecology. The utility of this technique lies in the evaluation of $^{15}N/^{14}N$ ($\delta^{15}N$ values) in 'source' and 'trophic' amino acids (AAs; McClelland and Montoya, 2002; Popp et al., 2007). Source AAs (Src-AA) retain their $\delta^{15}N$ value with each trophic transfer, and thus reflect baseline $\delta^{15}N$ values even when measured in consumers at the top of the food chain. For example, measurement of Src-AA $\delta^{15}N$ values in a secondary consumer can be used to determine baseline Src-AA $\delta^{15}N$ values underlying the whole food web (Fig. 1). In contrast, 'trophic' AAs (Tr-AA) are ^{15}N enriched by up to 8‰ with each trophic step (Chikaraishi et al., 2009, 2010), due to fractionation associated with *de novo* synthesis or metabolic transamination and deamination (Fuller and Petzke, 2017; O'Connell, 2017). For example, Tr-AA $\delta^{15}N$ values measured in a secondary consumer will be much greater than Tr-AA $\delta^{15}N$ values measured at the base of its food web (Fig. 1). These trophic fractionations are consistent across many

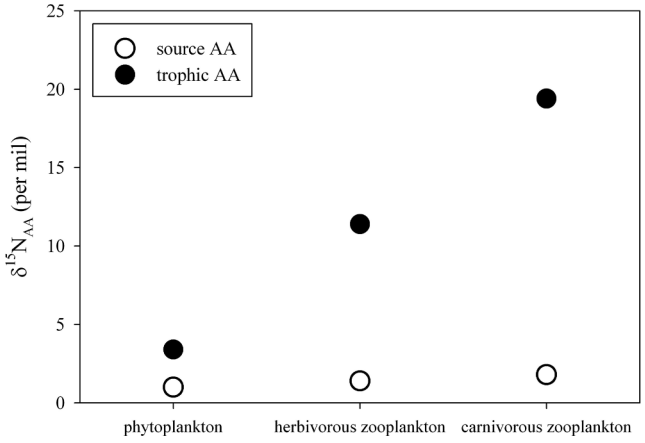

Fig. 1. Schematic illustration of the relationship between the nitrogen isotopic composition of amino acids and trophic level in a simple marine food web. Source AAs change very little in $\delta^{15}N$ value with each trophic transfer, thus source AA $\delta^{15}N$ values measured in a consumer will reflect source AA $\delta^{15}N$ values at the base of its food web. In contrast trophic AAs increase greatly in $\delta^{15}N$ value with each trophic transfer, thus comparison of source and trophic AA $\delta^{15}N$ values in a single consumer can be used to determine its trophic level.

different trophic level taxa (Nielsen et al., 2015), thus trophic positions for a wide variety of consumers can be quantified by comparing trophic $\delta^{15}N_{AA}$ and source $\delta^{15}N_{AA}$ values from a single sample (Chikaraishi et al., 2009, 2010). In summary, by applying CSIA-AA to a single consumer, both Src-AAs $\delta^{15}N$ values at the base of its food web and the consumer's trophic position can be determined. Application of CSIA-AA to mesopelagic food webs thus allows a more direct measure of basal food web resources than previous indirect estimates of large particle attenuation and zooplankton metabolism. CSIA-AA research on mesopelagic food webs to date has yielded insight into the trophic position for midwater micronekton in diverse marine ecosystems (Choy et al., 2012), as well as the trophic structure of a pelagic micronekton assemblage in the NPSG (Choy et al., 2015; Gloeckler et al., 2017). The latter study (Gloeckler et al., 2017) further used Src-AA $\delta^{15}N$ values to argue that small particles were an important baseline resource for micronekton in the lower mesopelagic and upper bathypelagic zones.

Here we evaluate basal resources supporting midwater zooplankton food webs in the NPSG using CSIA-AA. We specifically assess whether alternate nutritional sources, such as carnivory on vertical migrants or feeding on a small particle-based food web, are significant for zooplankton in the mesopelagic and upper bathypelagic zones. We place our findings in the context of NPSG seasonality, evaluating whether alternate nutritional sources such as small particles become more prominent in the winter when large particle fluxes are reduced. CSIA-AA of specific taxa and the zooplankton community as a whole are determined to discern the range in basal resources supporting NPSG zooplankton food webs. We also focus on the potential role of small zooplankton taxa as a trophic link between small particles and micronekton at depth. The biomass structure of the mesopelagic zooplankton community and their C, N, and phosphorus (P) composition are further assessed in the winter, spring, and summer. We synthesize results to yield a holistic view of midwater zooplankton trophic function in the subtropical open ocean.

2. Materials and methods

2.1. Sample collection

Zooplankton were collected in the winter (19–28 February 2014), late summer (29 August–11 September 2014), and spring (2–11 May 2015) at Station (Sta.) ALOHA (22.45°N, 158°W) in the NPSG. This station is the study site for the Hawaii Ocean Time-series (HOT; Karl and Lukas, 1996) and biogeochemical aspects of this environment are very well characterized (Church et al., 2013; Karl and Church, 2014). Zooplankton were collected using a 1-m^2 MOCNESS (Multiple Opening/Closing Net and Environmental Sensing System; Wiebe et al., 1985) equipped with nine 0.2 mm mesh sampling nets and sensors to measure conductivity, temperature, pressure, fluorometry, flow past the net, and net angle. Plankton were collected by oblique 8 h tows at night (19:00–03:00 h) and during the day (07:00–15:00 h) over the following depth intervals from the surface to 1500 m: 0–50 m, 50–100 m, 100–150 m, 150–200 m, 200–300 m, 300–500 m, 500–700 m, 700–1000 m, and 1000–1500 m. Replicate (n = 2–4) night and day tows were conducted on each cruise. The intervals were chosen to capture assumed zooplankton migration depths (e.g., 300–700 m during the day) and to compare results with previous summer collections at Sta. ALOHA (Hannides et al., 2015; Steinberg et al., 2008a). A larger surface depth interval (0–100 m) was sampled in spring 2015 on several tows due to technical issues. Additionally, a 0.06 mm mesh net was used on a few tows to collect small zooplankton and juvenile stages, i.e., at 300–500 m in winter and 1000–1500 m in summer. Average volume of water filtered by each net ranged from 509 m^3 (0–50 m, day) to 4924 m^3 (1000–1500 m, night).

Immediately following collection, cod ends were retrieved and immersed in chilled surface seawater. For collection of zooplankton size fractions, cod end contents were wet sieved using stacked 0.2, 0.5, 1.0, 2.0 and 5.0 mm sieves, filtered onto acid-cleaned, pre-weighed 47 mm filters of 0.2 mm nitex mesh, and frozen at −80 °C. For samples collected with the small (0.06 mm) mesh net the same procedure was followed but a smaller mesh size (0.06 mm) was included for sieving and filtering. For collection of individual zooplankton taxa, the cod end contents of some tows were split into 1/2 or 1/4 fractions using a Folsom plankton splitter and that portion of the tow preserved in 4.5% borate-buffered formalin.

2.2. Sample processing

Size-fractioned zooplankton from the replicate day and night tows on each cruise (n = 2–4 per cruise) were processed for biomass and stable isotope analysis. Zooplankton filters were initially defrosted, weighed to determine wet weight (wet wt) biomass, and a portion of each size-fractioned sample removed for analysis of total zooplankton abundance (the latter done for only one target night tow per cruise). The samples were then lyophilized for 24–36 h and weighed again to determine dry weight (dry wt) biomass. Lyophilized zooplankton were scraped off each nitex filter, ground using an agate mortar and pestle, and weighed using an ultra microbalance. For C and N composition, all zooplankton size fractions were targeted from all depths on each cruise and ~0.5 mg of each sample packaged in tin capsules. For P composition, samples from the winter and spring cruises were targeted and 8–23 mg weighed into acid cleaned and combusted vials. Size fractions are referred to as: 0.06 mm = 0.06–0.2 mm fraction, 0.2 mm = 0.2–0.5 mm fraction, 0.5 mm = 0.5–1.0 mm, 1 mm = 1.0–2.0 mm, 2 mm = 2.0–5.0 mm, and 5 mm = > 5 mm. For CSIA-AA, 0.2 mm and 1 mm zooplankton were targeted from select depths (0–50 m, 100–150 m, 300–500 m, 700–1000 m, and 1000–1500 m) and 5–10 mg of each sample weighed into combusted hydrolysis vials.

Individual zooplankton taxa from winter and summer cruises were also targeted for CSIA-AA analysis. Whereas evaluation of size fractions allows insight into the entire zooplankton community, targeting individual taxa allows insight into specific zooplankton classes, such as mesopelagic residents or vertical migrators. Here we define 'resident' as any zooplankton found in surface waters during the day or found at mesopelagic and bathypelagic depths during the night. Target taxa were identified in formalin-preserved samples using stereomicroscopy, counted, and removed and washed in Milli-Q water using clean techniques. Taxa were sorted from a targeted day and night tow on each

cruise from three depths (0–50 m, 300–500 m, 1000–1500 m), and included small resident copepods (oithonids, oncaeids, and harpacticoids), vertical migrators (*Pleuromamma xiphias* and ostracods in surface waters), resident ostracods (at depth) and carnivores (chaetognaths). Specifically, copepods from the family Oithonidae (prosome length: 0.6–0.7 mm) were collected from 0 to 50 m (day) and 300–500 m (night). Copepods from the family Oncaeidae (prosome length: 0.5–0.6 mm) were collected from 0 to 50 m (day), 300–500 m (night), and 1000–1500 m (night). Harpacticoid copepods included *Macrosetella gracilis* (total length: 1.1–1.2 mm) collected from 0 to 50 m (day), and *Aegisthus* spp. (total length: 1.3–2.1 mm) collected from 300 to 500 m (night) and 1000–1500 m (night). The vertical migrator *P. xiphias* (prosome length: 2.9–3.0 mm) was collected from 0 to 50 m (night) and a few animals were found at 1000–1500 m (night). Ostracods (total length: 1.3–3.1 mm) were collected from 0 to 50 m (night), 300–500 m (night), and 1000–1500 m (night). Both large (total length: 18–24 mm) and small (total length: 7–12 mm) chaetognaths were collected from 0 to 50 m (day), 300–500 m (night), and 1000–1500 m (night). Numbers of individuals analyzed for CSIA-AA ranged from 577 (oncaeid copepods) to 4 (large chaetognaths), with each sample placed in combusted hydrolysis vials and lyophilized for 24 h.

2.3. Biomass analyses

Samples were measured for wet wt and dry wt biomass as described above. Migrant biomass was calculated as the difference between night and day biomass. Numbers of individuals (ind.) per filter were calculated from microscopic analysis of abundance samples, and dry wt conversion factors (dry wt ind.$^{-1}$) determined for each depth and size fraction.

2.4. Carbon, nitrogen and bulk stable isotope analyses

Elemental (C and N) composition was determined using a Costech elemental combustion system (Model 4010) coupled to a Thermo-Finnigan Delta Plus XP isotope ratio mass spectrometer (IRMS) through a Conflo IV interface. Bulk (whole animal) stable N isotope composition was measured simultaneously (see Appendix B).

2.5. Phosphorus analyses

Total particulate P (TPP) and particulate inorganic P (PIP) content was measured using a modification of the Aspila phosphomolybdate method (Aspila et al., 1976; Benitez-Nelson et al., 2007). Briefly, inorganic P was extracted from lyophilized and ground zooplankton using 10% hydrochloric acid, with samples for total P first combusted at 550 °C to convert all organic P to inorganic P. Particulate organic P (POP) content was then estimated by difference (TPP – PIP). A standard reference material (NIST #1573a, tomato leaves) was analyzed with each run to evaluate analytical accuracy and monitor run-to-run variability.

2.6. Compound-specific stable isotope analyses

Amino acid-specific stable N isotope composition was determined on samples that were hydrolyzed, derivatized, and analyzed according to Popp et al. (2007) and Hannides et al. (2009). Briefly, size-fractioned zooplankton material and target zooplankton taxa were hydrolyzed using trace metal-grade 6 M HCl and the resulting AAs purified using cation exchange chromatography. The samples were then esterified using 4:1 isopropanol:acetyl chloride and derivatized using 3:1 methylene chloride:trifluoroacetyl anhydride. The resulting trifluoroacetyl and isopropyl ester (TFA) derivatives were purified using chloroform extraction and stored at −20 °C for up to 1 month before analysis. This method yielded information for the following AAs: alanine (Ala), glycine (Gly), isoleucine (Ile), leucine (Leu), lysine (Lys), methionine (Met), phenylalanine (Phe), proline (Pro), serine (Ser), threonine (Thr), tyrosine (Tyr), and valine (Val). During acid hydrolysis asparagine (Asn) is converted to aspartic acid (Asp) and glutamine (Gln) is converted to glutamic acid (Glu), thus we also report information on the combined pools, termed Asx (Asn + Asp) and Glx (Gln + Glu), respectively.

TFA derivatives of AAs were analyzed for stable N isotope composition ($\delta^{15}N_{AA}$ values) following Hannides et al. (2013). AAs were analyzed using a Thermo Scientific Delta V Plus IRMS interfaced to a trace gas chromatograph (GC) fitted with a 60 m BPx5 capillary column through a GC-C III combustion furnace (980 °C), reduction furnace (680 °C) and liquid nitrogen cold trap. $\delta^{15}N_{AA}$ values were measured on 3–5 replicate injections with norleucine and aminoadipic acid with known $\delta^{15}N$ values as internal reference materials co-injected on each run. For replicate injections of zooplankton samples, $\delta^{15}N_{AA}$ standard deviations averaged 0.4‰ and ranged from 0.02 to 1.0‰. Full AA reference suites (15 AAs) were analyzed with each batch of samples, and the corresponding response factors (Vs [nmol AA]$^{-1}$) used to determine AA concentrations and AA mol% (i.e., mol AA_i/Σ mol AA × 100% for each AA *i*). A process blank (subject to the same taxa processing, hydrolysis, and derivatization steps) was analyzed in the same manner as individual zooplankton taxa and did not contain detectable AAs.

2.7. Stable isotope-based parameters

The 'weighted average $\delta^{15}N_{AA}$ value' refers to an average zooplankton $\delta^{15}N_{AA}$ value (e.g., average for a depth, season, or size fraction) weighted by the instrumental standard deviation of each $\delta^{15}N_{AA}$ value (Hayes et al., 1990). A composite source $\delta^{15}N_{AA}$ value was calculated by averaging a suite of AAs (e.g., $\delta^{15}N_{Src\text{-}AA}$ = average of Gly, Lys, Phe, and Ser $\delta^{15}N$ values). Here we include Phe, the canonical source AA (Chikaraishi et al., 2009; McClelland and Montoya, 2002), and Lys, a source AA that has shown negligible ^{15}N enrichment with trophic transfer (Bradley et al., 2014; Nielsen et al., 2015). We further include Gly and Ser, source AAs that have minimal ^{15}N enrichment in trophic transfers involving zooplankton consumers and their prey (Chikaraishi et al., 2009; McClelland and Montoya, 2002).

Zooplankton trophic positions (TP) were calculated based on multiple source and trophic $\delta^{15}N_{AA}$ values as recommended by Nielsen et al. (2015). That is, we calculate $TP_{Tr\text{-}Src} = 1 + (\delta^{15}N_{Tr\text{-}AA} - \delta^{15}N_{Src\text{-}AA} - \beta)/TDF$, where $\delta^{15}N_{Tr\text{-}AA}$ = average of Glx, Ala, and Leu $\delta^{15}N$ values and $\delta^{15}N_{Src\text{-}AA}$ = average of Phe and Lys $\delta^{15}N$ values. Glx, Ala, and Leu are trophic AAs that are ^{15}N enriched with trophic transfers between zooplankton consumers and their prey (Chikaraishi et al., 2009; McClelland and Montoya, 2002) and have consistently high TDFs (Bradley et al., 2014; Nielsen et al., 2015). Phe and Lys are source AAs as described above (Nielsen et al., 2015). In the $TP_{Tr\text{-}Src}$ calculation β is 2.2 ± 0.7‰ and the TDF is 6.3 ± 0.9‰ (derived from Chikaraishi et al. (2009)). For comparative purposes only (for example, evaluating formalin preservation in Appendix A), we also report zooplankton TP derived using Glx and Phe, $TP_{Glx\text{-}Phe}$. Here $TP_{Glx\text{-}Phe} = 1 + (\delta^{15}N_{Glx} - \delta^{15}N_{Phe} - \beta)/TDF$, where β is 3.4 ± 1.0‰ and the TDF is 7.6 ± 1.2‰ (Chikaraishi et al., 2009, 2010). Standard deviations were calculated for $TP_{Tr\text{-}Src}$ and $TP_{Glx\text{-}Phe}$ considering propagation of error (Bradley et al., 2015; Jarman et al., 2017). We note that the above formulations may underestimate zooplankton TP given the 'isotopic invisibility' of protistan consumer-prey interactions (Gutiérrez-Rodríguez et al., 2014). However our calculation of $TP_{Tr\text{-}Src}$ includes Ala, which is enriched in phagotrophic protistan consumer-prey interactions (Gutiérrez-Rodríguez et al., 2014). Thus our $TP_{Tr\text{-}Src}$ should be influenced by trophic steps involving both protists and zooplankton, which are significant components of community function in the NPSG (Calbet and Landry, 1999).

2.8. Particle collection and analyses

We compare our findings for midwater zooplankton to parallel research on particle cycling in the NPSG. Particles were collected on winter and summer cruises to Sta. ALOHA using *in situ* filtration (WTS-LV, McLane Research Laboratories). Specifically, particles were collected *in situ* at 8–12 discrete depths from 25 to 1200 m by filtering sequentially onto 53 μm nylon (Nitex) mesh and 0.7 μm pre-combusted glass microfiber filters (GF/F; double-stacked to improve particle retention) mounted on a mini-MULVFS 2-tiered filter holder. Particle collection by this method is designed to exclude swimmers but to include all other ambient, non-swimming particulate material (phytoplankton, bacteria, archaea, and protozoan biomass and detritus, fecal pellets, fragmented plankton carcasses, aggregates, and other visually unidentifiable particulate detritus; see Bishop et al. (2012; and references therein). Post-collection, large particles were resuspended in 0.2 μm filtered seawater, filtered onto combusted 47-mm GF/Fs, and inspected using microscopy to ensure complete removal of Nitex fibers and zooplankton, which were minimal. All filters were then freeze-dried and analyzed using CSIA-AA procedures as described above (Section 2.6) and in Hannides et al. (2013). For both large (> 53 μm) and small (0.7–53 μm) particles, $\delta^{15}N_{Src\text{-}AA}$ values and $TP_{Tr\text{-}Src}$ were calculated as described in Section 2.7. Average $\delta^{15}N_{Src\text{-}AA}$ values and $TP_{Tr\text{-}Src}$ for fresh surface material (large and small particles collected at 0–75 m), deep large particles (large particles collected from 250 to 1250 m), and deep small particles (small particles collected from 250 to 1250 m) were evaluated and used in this study. Here large particles were used as a proxy for more rapidly sinking particulate material, based on precedents set by Abramson et al. (2010) and Lam et al. (2011), among others. While sinking particles were also collected on our cruises using sediment traps, it is very difficult to separate small and large particles in sediment trap material due to the nature of collection. Moreover use of the WTS-LV pumps allowed us to sample small and large particles deep into the mesopelagic zone, as compared to sediment trap fluxes, which were only measured at 150 m (in this study).

3. Results

3.1. Zooplankton biomass

To evaluate the change in biomass across season, depth distributions of size fractionated zooplankton biomass and total zooplankton biomass in the winter, spring, and late summer were measured. Total zooplankton biomass at Sta. ALOHA ranged from 3.2 to 11.6 mg dry wt m^{-3} in surface waters (0–50 m) during the day and 7.0–13.8 mg dry wt m^{-3} at night (Fig. 2). Biomass was consistently highest in the upper 100 m; however differences in biomass between the upper euphotic zone (0–50 m) and the lower euphotic zone (100–150 m) were only significant during summer (day and night; Wilcoxon test, $W = 16$, df = 7, $p < 0.05$). When integrated over the whole euphotic zone (0–150 m), total biomass ranged from 0.4 to 0.9 g dry wt m^{-2} during the day and 0.7–1.3 g dry wt m^{-2} at night, which is within the range determined by the HOT program at Sta. ALOHA (0.2–3.1 g dry wt m^{-2}; HOT Data Organization and Graphical System (HOT-DOGS) website: http://hahana.soest.hawaii.edu/hot/hot-dogs/). As has been previously observed in the NPSG, zooplankton biomass decreased exponentially with depth through midwaters and the upper bathypelagic zone, such that by 1000–1500 m total zooplankton biomass was 0.06–0.2 mg dry wt m^{-3} during the day and 0.07–0.2 mg dry wt m^{-3} at night (Fig. 2).

To assess migrant zooplankton depth distributions and their relationship with particle dynamics, we first estimated migrant biomass as the difference between average night and day biomass and evaluated across specific depth ranges (Fig. 3). At night, total migrant biomass was consistently highest in the upper 50 m (2.7–3.6 mg dry wt m^{-3}) and at 50–100 m (0.9–2.6 mg dry wt m^{-3}). During the day, total migrant biomass was highest at 300–500 m (0.2–0.7 mg dry wt m^{-3}) and 500–700 m (0.5–1.9 mg dry wt m^{-3}). Total night biomass was significantly different than that measured during the day in summer in the euphotic zone (50–100 m) and in the deep mesopelagic zone (500–1000 m; Fig. 3; Wilcoxon test, $W \geq 0.0$, df = 7, $p < 0.05$). Based on samples collected in summer, the increase in migrant biomass in the upper 100 m at night is driven by 0.5 and 1 mm zooplankton (Table 1). However our data also indicates migration of 1 and 5 mm zooplankton into the upper mesopelagic zone at night, that is, just below the deep chlorophyll maximum (DCM; 150–200 m; Table 1). During the day migrants return to their resting depths, with smaller zooplankton (0.2 and 0.5 mm) migrating back down into the upper mesopelagic zone (200–300 m), and larger zooplankton (1– > 5 mm) migrating into the mid- to deep mesopelagic zone (300–1000 m; Table 1; Wilcoxon test, $W \geq 0.0$, df = 7, $p < 0.05$).

Based on zooplankton depth distributions observed in the winter, spring, and summer, modest seasonal changes in zooplankton biomass were observed at Sta. ALOHA. Overall seasonal differences were evaluated on a logarithmic scale, while controlling for the change in biomass with depth (uniform slopes were found in all cases day or night; ANCOVA, $p > 0.05$). Spring and summer zooplankton biomass were equivalent and significantly greater than winter biomass during both day and night (ANCOVA, $F_{2,74\text{-}77} = 7.8\text{–}9.8$, $p < 0.001$). Summer biomass was also consistently greater than winter biomass when evaluated at each depth interval in the euphotic zone (0–100 m), upper mesopelagic zone below the DCM (150–200 m), and lower mesopelagic zone (500–1000 m; Fig. 4, Table 2), although due to small sample size these seasonal differences were not significant (Wilcoxon test, $p > 0.05$). For migrant biomass, seasonal differences within the euphotic zone (0–150 m) and at depth (300–700 m) were not significant (winter and summer migrant biomass were within 2 standard deviations (SD) of each other). However the distribution of migrant biomass within the upper 100 m at night varied with season, i.e., in winter most of the 0–100 m migrants (80%) were constrained to the upper 50 m, whereas in summer the 0–100 m migrants were equally distributed throughout the upper 100 m (Fig. 3).

3.2. Zooplankton elemental composition

To evaluate potential seasonal change in zooplankton elemental composition, zooplankton C, N, and P content were determined for zooplankton size fractions and average elemental ratios were determined for the total zooplankton community. Over day and night and all depths and size fractions, zooplankton C:N ratios averaged 5.0 ± 0.05 and biomass-weighted average C:N ratios ranged from 4.6 to 5.6 (Fig. 5). Zooplankton C:N ratios did not change with season (when split by depth and size fraction: Kruskal-Wallis test, $p > 0.05$). However considerable variability was apparent when data from all seasons were combined (Table A.1).

There were significant differences in C:N ratios with size, depth, and time. In general, C:N ratios increased with both size and depth (ANCOVA, $F_{4,230\text{-}239} = 3.5\text{–}31.5$, $p < 0.01$ and $F_{1,46\text{-}48} = 16.5\text{–}80.6$, $p < 0.001$, Table A.1). When all size fractions were combined into biomass-weighted averages, C:N ratios increased significantly with depth for both day and night tows (Fig. 5; linear regression, $F_{1,24\text{-}25} = 10.3\text{–}50.1$, $p < 0.005$). Biomass-weighted average C:N ratios were generally further greater at night than during the day below 300 m, but these temporal differences were significant only at 300–500 m and 500–700 m (Fig. 5; Kruskal-Wallis test, $\chi^2 = 3.8$, $p < 0.05$). Below 700 m no significant temporal difference in biomass-weighted average C:N ratio was found (Kruskal-Wallis test, $p > 0.05$).

P composition for zooplankton was evaluated in the winter and spring at Sta. ALOHA. Over day and night and all depths and size fractions, molar (mol:mol) ratios averaged (± SEM) 115.0 ± 3.0 for C:TPP, 23.3 ± 0.6 for N:TPP, 255.5 ± 9.6 for C:POP, and 52.0 ± 1.7 for N:POP. Biomass-weighted average molar ratios ranged from 100.7

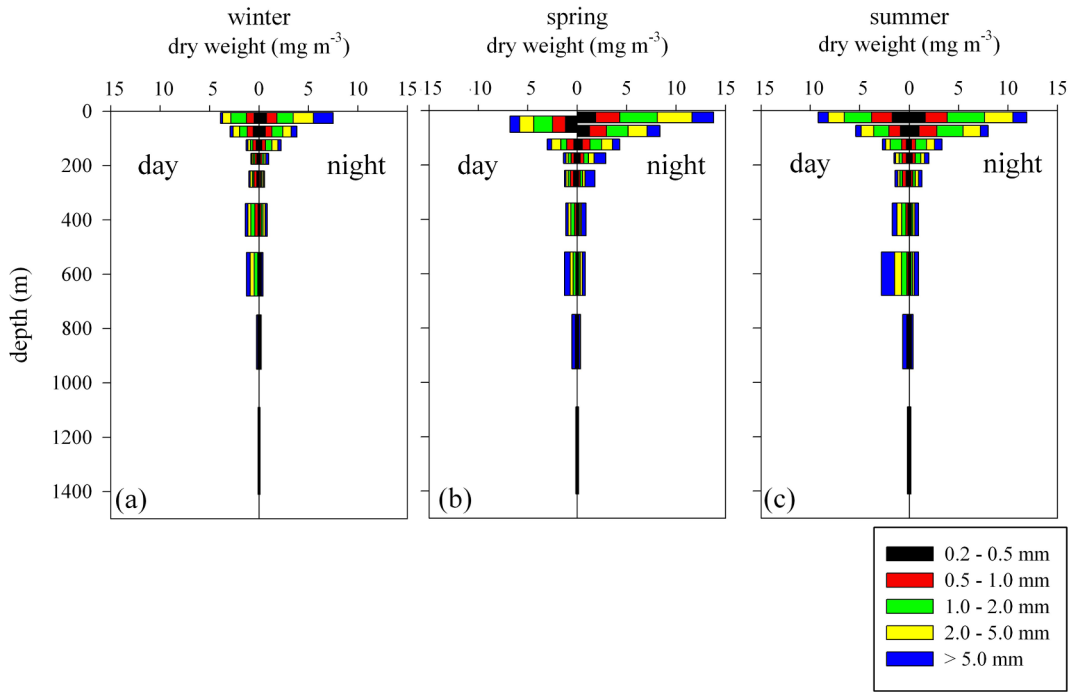

Fig. 2. Day and night size-fractioned zooplankton biomass (mg m^{-3}) at Sta. ALOHA in (a) winter (February 2014; n = 3), (b) spring (May 2015, n = 2), and (c) late summer (August – September 2014, n = 4). Zooplankton biomass is centered within each depth interval (0–50 m or 0–100 m in spring 2015, 50–100 m, 100–150 m, 150–200 m, 200–300 m, 300–500 m, 500–700 m, 700–1000 m, 1000–1500 m). Average CV% for each size fraction are 30% (0.2 mm), 28% (0.5 mm), 29% (1 mm), 29% (2 mm), and 48% (> 5 mm).

to 142.1 for C:TPP, 20.3–28.4 for N:TPP, 192.2–365.8 for C:POP, and 38.6–70.8 for N:POP (Fig. 5; Table A.2). Zooplankton P composition did not change with season (when split by depth and size fraction: Kruskal-Wallis test, $p > 0.05$).

Overall we found significant variation in zooplankton elemental composition with depth, driven primarily by changes in the mid-mesopelagic to upper bathypelagic zones (Fig. 5). For example, in several cases depth drove significant increases in C:TPP ratios (Table A.2; day: 0.2–2 mm; night: 0.2–2 mm; linear regression, $F_{1,13\text{-}23} = 5.8\text{–}53.0$, $p < 0.05$), and significant increases in N:TPP ratios during the day (Table A.2; day: 0.2–2 mm; linear regression, $F_{1,16\text{-}23} = 5.9\text{–}47.8$, $p < 0.05$). Significant increases in C:POP ratios were also observed for several size fractions (Table A.2; day: 1–2 mm; night: 0.2, 1–5; linear regression, $F_{1,13\text{-}23} = 4.9\text{–}19.0$, $p < 0.05$). When all size fractions were combined into biomass-weighted averages, modest changes with depth were found mostly for zooplankton collected during the day. Biomass-weighted average C:TPP and N:TPP ratios increased significantly with depth during the day (Fig. 5; linear regression, $F_{1,14} = 15.5$, $p < 0.005$, $F_{1,14} = 15.5$, $p < 0.005$). Biomass-weighted average C:POP ratios increased significantly with depth during both the day and night (Table A.2; linear regression, $F_{1,14\text{-}15} = 7.4\text{–}20.7$, $p < 0.05$), while biomass-weighted average N:POP ratios only increased significantly with depth during the day (Table A.2; linear regression, $F_{1,14} = 19.7$, $p < 0.001$).

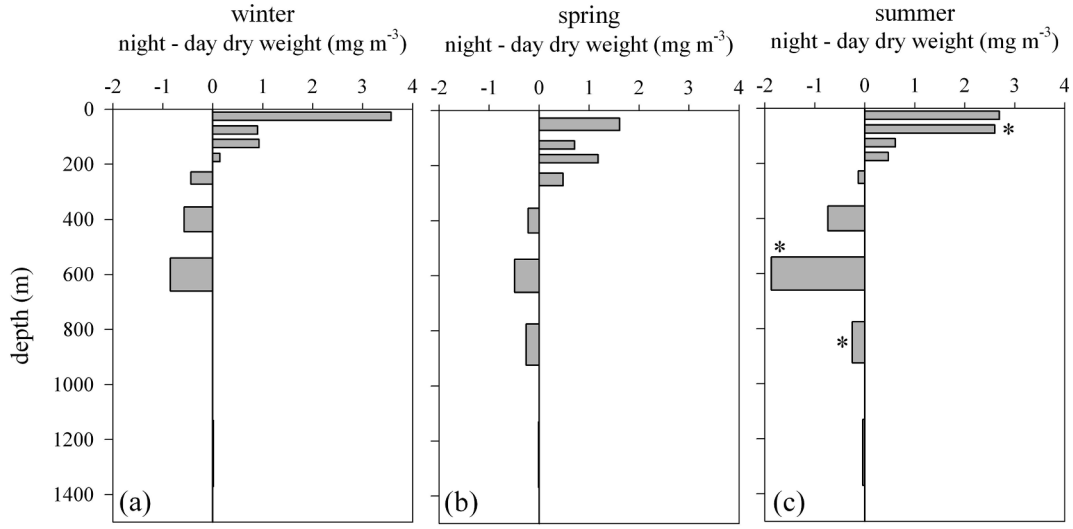

Fig. 3. Total migrant (night – day) zooplankton biomass (mg m^{-3}) at Station ALOHA in (a) winter (February 2014), (b) spring (May 2015), and (c) late summer (August–September 2014). Positive values indicate night > day zooplankton biomass, and negative values indicate day > night zooplankton biomass. Asterisks (*) indicate a significant difference between night versus day biomass (Wilcoxon test, p < 0.05).

Table 1
Size fractioned and total migrant (night – day) zooplankton biomass (mg m^{-3}) at Sta. ALOHA in winter (February 2014), spring (May 2015), and late summer (August–September 2014). Positive values indicate night > day zooplankton biomass, and negative values indicate day > night zooplankton biomass. Error is the standard deviation. Asterisks (*) indicate a significant difference between night versus day biomass (Wilcoxon test, $p < 0.05$).

Season	Depth (m)	0.2 mm	0.5 mm	1 mm	2 mm	5 mm	Total
Winter	0–50	0.249 ± 0.278	0.275 ± 0.339	0.089 ± 0.741	1.216 ± 0.384	1.745 ± 0.591	3.574 ± 0.862
	50–100	0.051 ± 0.129	0.078 ± 0.186	0.303 ± 0.210	0.194 ± 0.184	0.279 ± 0.469	0.905 ± 0.235
	100–150	0.013 ± 0.150	0.008 ± 0.194	0.409 ± 0.283	0.349 ± 0.161	0.149 ± 0.112	0.929 ± 0.692
	150–200	−0.098 ± 0.094	−0.039 ± 0.133	0.064 ± 0.131	0.014 ± 0.106	0.204 ± 0.399	0.145 ± 0.532
	200–300	−0.156 ± 0.062	−0.213 ± 0.057	0.006 ± 0.051	−0.081 ± 0.084	0.004 ± 0.054	−0.440 ± 0.228
	300–500	−0.027 ± 0.043	−0.162 ± 0.069	−0.231 ± 0.191	−0.067 ± 0.128	−0.085 ± 0.172	−0.572 ± 0.513
	500–700	0.004 ± 0.018	−0.057 ± 0.044	−0.290 ± 0.102	−0.306 ± 0.098	−0.203 ± 0.169	−0.852 ± 0.234
	700–1000	−0.001 ± 0.003	0.011 ± 0.008	0.010 ± 0.027	−0.014 ± 0.043	−0.009 ± 0.108	−0.003 ± 0.084
	1000–1500	0.001 ± 0.003	0.001 ± 0.005	0.003 ± 0.012	0.004 ± 0.010	0.001 ± 0.059	0.009 ± 0.056
Spring	0–100	0.043 ± 0.524	0.242 ± 0.759	0.388 ± 1.177	0.637 ± 0.958	0.299 ± 0.771	1.609 ± 3.856
	100–150	0.104 ± 0.126	−0.065 ± 0.171	0.270 ± 0.475	0.153 ± 0.500	0.250 ± 0.187	0.712 ± 0.973
	150–200	−0.062 ± 0.110	0.028 ± 0.072	0.087 ± 0.123	0.553 ± 0.288	0.571 ± 0.513	1.178 ± 0.512
	200–300	−0.201 ± 0.095	−0.160 ± 0.062	−0.001 ± 0.024	0.012 ± 0.082	0.833 ± 0.069	0.484 ± 0.190
	300–500	−0.009 ± 0.017	−0.071 ± 0.027	−0.231 ± 0.014	−0.139 ± 0.050	0.226 ± 0.116	−0.225 ± 0.175
	500–700	−0.004 ± 0.032	0.013 ± 0.016	−0.156 ± 0.045	−0.128 ± 0.053	−0.214 ± 0.106	−0.488 ± 0.027
	700–1000	−0.005 ± 0.014	−0.004 ± 0.011	0.000 ± 0.010	−0.018 ± 0.012	−0.230 ± 0.343	−0.257 ± 0.357
	1000–1500	0.000 ± 0.004	−0.001 ± 0.004	0.002 ± 0.010	0.004 ± 0.007	−0.013 ± 0.032	−0.007 ± 0.016
Summer	0–50	−0.116 ± 0.668	0.153 ± 0.728	1.065 ± 0.873*	1.216 ± 0.898	0.369 ± 0.686	2.686 ± 3.472
	50–100	0.104 ± 0.377	0.651 ± 0.435*	1.098 ± 0.616	0.480 ± 0.665	0.263 ± 0.367	2.596 ± 1.088*
	100–150	−0.070 ± 0.104	−0.039 ± 0.223	−0.055 ± 1.389	0.332 ± 0.475	0.440 ± 0.609	0.608 ± 2.464
	150–200	0.016 ± 0.070	−0.121 ± 0.146	0.278 ± 0.155*	−0.023 ± 0.053	0.322 ± 0.199*	0.474 ± 0.363
	200–300	−0.138 ± 0.125*	−0.166 ± 0.073*	0.003 ± 0.083	0.087 ± 0.094	0.084 ± 0.117	−0.130 ± 0.398
	300–500	−0.018 ± 0.058	−0.095 ± 0.091	−0.278 ± 0.134*	−0.289 ± 0.203	−0.059 ± 0.401	−0.739 ± 0.498
	500–700	0.002 ± 0.036	−0.069 ± 0.134	−0.362 ± 0.264	−0.528 ± 0.316*	−0.914 ± 0.570	−1.871 ± 1.076*
	700–1000	0.015 ± 0.014	0.001 ± 0.019	−0.005 ± 0.024	−0.020 ± 0.042	−0.239 ± 0.142*	−0.247 ± 0.161*
	1000–1500	−0.004 ± 0.006	−0.002 ± 0.006	−0.005 ± 0.014	−0.012 ± 0.020	−0.014 ± 0.061	−0.038 ± 0.097

3.3. Source amino acid stable isotope composition

To assess how baseline resources for NPSG zooplankton food webs changed with season, we evaluated source $\delta^{15}N_{AA}$ values in winter and summer. Because source AA $\delta^{15}N$ values change very little with each trophic transfer (Fig. 1), $\delta^{15}N_{Src\text{-}AA}$ values measured in zooplankton are solely a measure of $\delta^{15}N_{Src\text{-}AA}$ values at the base of their food web. In the euphotic zone (0–150 m) source $\delta^{15}N_{AA}$ values were low in winter and summer (Fig. 6; data available at BCO-DMO: https://www.bco-dmo.org/project/537123). In winter, across all size fractions and times of day, $\delta^{15}N_{Src\text{-}AA}$ values ranged from −0.9 to 0.5‰ with an overall weighted average (weighted by SD) of −0.4 ± 0.05‰ for 0–50 m and 0.0 ± 0.06‰ for 100–150 m. In summer, $\delta^{15}N_{Src\text{-}AA}$ values ranged from −0.3 to 1.0‰ with an overall weighted average of 0.2 ± 0.03‰

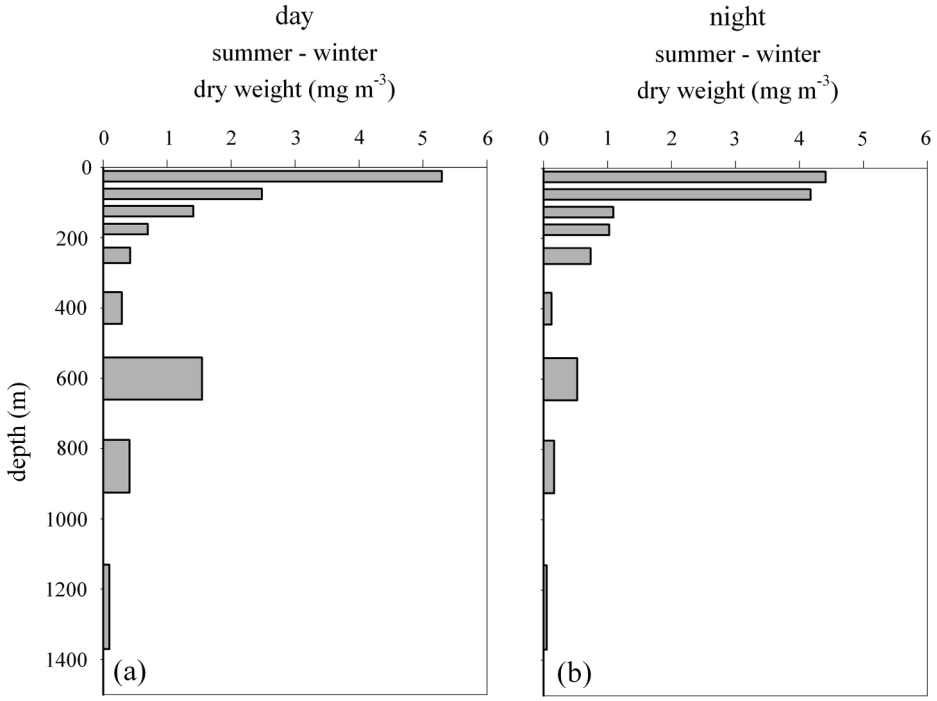

Fig. 4. Difference between total summer – winter size-fractioned zooplankton biomass (mg m^{-3}) at Sta. ALOHA during the (a) day and (b) night. Positive values indicate summer > winter zooplankton biomass.

Table 2
Difference between summer – winter zooplankton biomass (mg m^{-3}) for both total zooplankton and zooplankton size fractions at Sta. ALOHA during the day and night. Positive values indicate summer > winter biomass, and negative values indicate winter > summer zooplankton biomass. Error is the standard deviation.

Season	Depth (m)	0.2 mm	0.5 mm	1 mm	2 mm	5 mm	Total
Day	0–50	1.224 ± 0.584	1.302 ± 0.503	1.175 ± 0.766	0.800 ± 0.699	0.797 ± 0.363	5.298 ± 2.464
	50–100	0.316 ± 0.197	0.539 ± 0.368	0.755 ± 0.343	0.634 ± 0.446	0.239 ± 0.208	2.483 ± 0.448
	100–150	0.022 ± 0.099	0.108 ± 0.205	0.883 ± 1.369	0.254 ± 0.451	0.141 ± 0.257	1.408 ± 2.308
	150–200	0.073 ± 0.073	0.208 ± 0.153	0.150 ± 0.053	0.216 ± 0.068	0.047 ± 0.086	0.695 ± 0.279
	200–300	0.094 ± 0.124	0.045 ± 0.078	0.122 ± 0.074	0.003 ± 0.109	0.157 ± 0.097	0.423 ± 0.401
	300–500	0.020 ± 0.051	−0.111 ± 0.090	0.027 ± 0.223	0.190 ± 0.204	0.164 ± 0.369	0.290 ± 0.592
	500–700	0.059 ± 0.037	0.052 ± 0.139	0.184 ± 0.279	0.295 ± 0.322	0.953 ± 0.517	1.543 ± 1.058
	700–1000	0.023 ± 0.007	0.021 ± 0.019	0.044 ± 0.025	0.019 ± 0.055	0.302 ± 0.091	0.409 ± 0.097
	1000–1500	0.016 ± 0.005	0.008 ± 0.006	0.014 ± 0.013	0.014 ± 0.015	0.044 ± 0.045	0.095 ± 0.062
Night	0–50	0.859 ± 0.427	1.179 ± 0.626	2.151 ± 0.850	0.800 ± 0.683	−0.579 ± 0.830	4.411 ± 2.594
	50–100	0.370 ± 0.346	1.112 ± 0.296	1.550 ± 0.553	0.920 ± 0.527	0.223 ± 0.558	4.175 ± 1.020
	100–150	−0.062 ± 0.154	0.061 ± 0.213	0.419 ± 0.367	0.236 ± 0.220	0.432 ± 0.564	1.087 ± 1.105
	150–200	0.187 ± 0.092	0.127 ± 0.125	0.365 ± 0.196	0.179 ± 0.097	0.165 ± 0.437	1.024 ± 0.581
	200–300	0.111 ± 0.063	0.093 ± 0.051	0.119 ± 0.063	0.172 ± 0.062	0.237 ± 0.085	0.732 ± 0.221
	300–500	0.029 ± 0.051	−0.044 ± 0.069	−0.020 ± 0.069	−0.032 ± 0.126	0.190 ± 0.232	0.123 ± 0.400
	500–700	0.057 ± 0.018	0.040 ± 0.020	0.113 ± 0.051	0.073 ± 0.075	0.242 ± 0.293	0.525 ± 0.304
	700–1000	0.039 ± 0.012	0.011 ± 0.008	0.029 ± 0.026	0.013 ± 0.024	0.072 ± 0.153	0.165 ± 0.154
	1000–1500	0.011 ± 0.004	0.005 ± 0.005	0.006 ± 0.013	−0.002 ± 0.016	0.029 ± 0.071	0.049 ± 0.093

for 0–50 m and 0.6 ± 0.06‰ for 100–150 m. Thus $\delta^{15}N_{Src\text{-}AA}$ values were generally lower in the upper euphotic zone (0–50 m) relative to the deeper euphotic zone (100–150 m; Fig. 6). This difference was significant for both size fractions (0.2 and 1 mm) collected during the night in winter and summer, and for 0.2 mm zooplankton collected during the day in summer (Wilcoxon test, W = 0.0–1.0, df = 10–13, $p < 0.01$). We further compared our results with CSIA of zooplankton previously collected in the euphotic zone at Sta. ALOHA in 1995, 2000, and 2005 (Hannides et al., 2009). In winter, our $\delta^{15}N_{Src\text{-}AA}$ values were significantly lower than those for the 1995–2005 time period (Wilcoxon test, W = 0.0, df = 22, $p < 0.001$), while in summer, our $\delta^{15}N_{Src\text{-}AA}$ values were significantly higher (Wilcoxon test, W = 36.0, df = 14, $p < 0.05$).

Depth changes in stable isotope composition were significant for all individual source AAs and combined $\delta^{15}N_{Src\text{-}AA}$ values (data available at BCO-DMO: https://www.bco-dmo.org/project/537123). For example, values of $\delta^{15}N_{Src\text{-}AA}$ increased from surface waters through the upper bathypelagic zone (1000–1500 m) for all size fractions measured (0.2 and 1 mm) during both the day and night (Fig. 6; linear regression, $F_{1,28\text{-}42}$ = 61.0–993.7, $p < 0.001$). The depth regression differed with size for $\delta^{15}N_{Src\text{-}AA}$ in both seasons (ANCOVA, $F_{1,64\text{-}79}$ = 20.7–31.3, $p < 0.001$). Here slopes were significantly higher for 0.2 mm as compared to 1 mm zooplankton, indicating overall greater changes between 0 and 50 m and 1000–1500 m for the smaller animals (Δ = 4.9–7.2‰ across all seasons and times of day) versus the larger size fraction (Δ = 3.2–5.0‰). Size differences in $\delta^{15}N_{Src\text{-}AA}$ values were particularly apparent in the lower mesopelagic and upper bathypelagic zones (700–1500 m), where the 0.2 mm zooplankton tended to have higher $\delta^{15}N_{Src\text{-}AA}$ values (weighted average of 4.5–6.0‰) than 1 mm zooplankton (Fig. 6; weighted average of 3.1–4.4‰; Wilcoxon test, W = 28–72, df = 10–16, $p < 0.01$; except in winter during the day at 700–1000 m, Wilcoxon test, $p > 0.05$). Size differences were also apparent in winter for the very small zooplankton size fraction (0.06 mm) collected at 300–500 m, which had high $\delta^{15}N_{Src\text{-}AA}$ values (4.9–5.4‰ during the day and night) relative to 0.2 mm and 1 mm zooplankton at that same depth (Fig. 6). In contrast, in summer $\delta^{15}N_{Src\text{-}AA}$ values for 0.06 mm zooplankton collected at 1000–1500 m (4.0‰) were similar to those for the 0.2 mm and 1 mm size fractions (3.1–4.8‰).

Significant differences in $\delta^{15}N_{Src\text{-}AA}$ values were found between

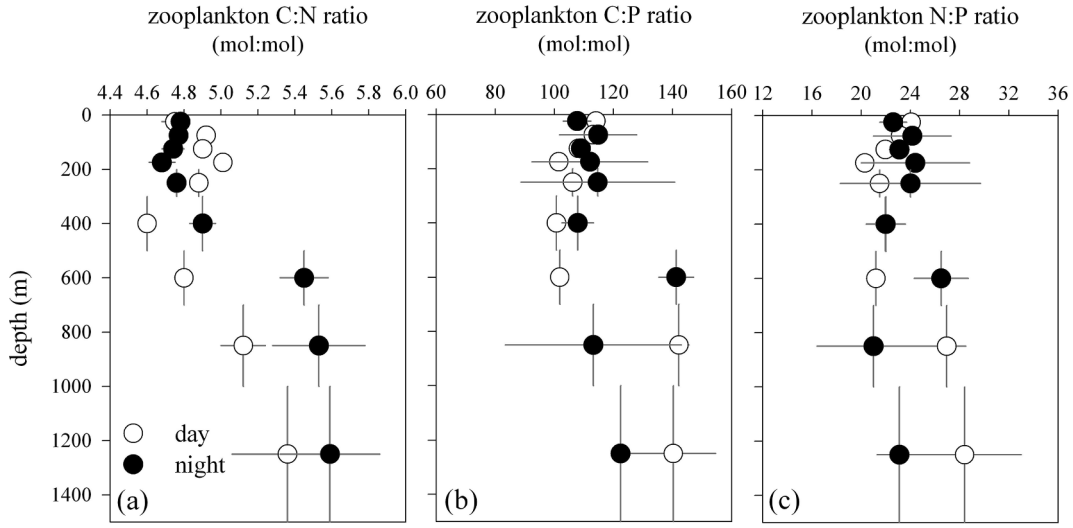

Fig. 5. Biomass-weighted average zooplankton (a) carbon (C): nitrogen (N) ratios, (b) C: total particulate phosphorus (TPP) ratios, and (c) N:TPP ratios. Biomass-weighted averages are calculated using data from summer, spring, and winter cruises (C:N ratios) or from winter and spring cruises (C:TPP and N:TPP ratios). Horizontal bars are the standard error of the mean. Vertical bars indicate the depth range over which the MOCNESS sampled.

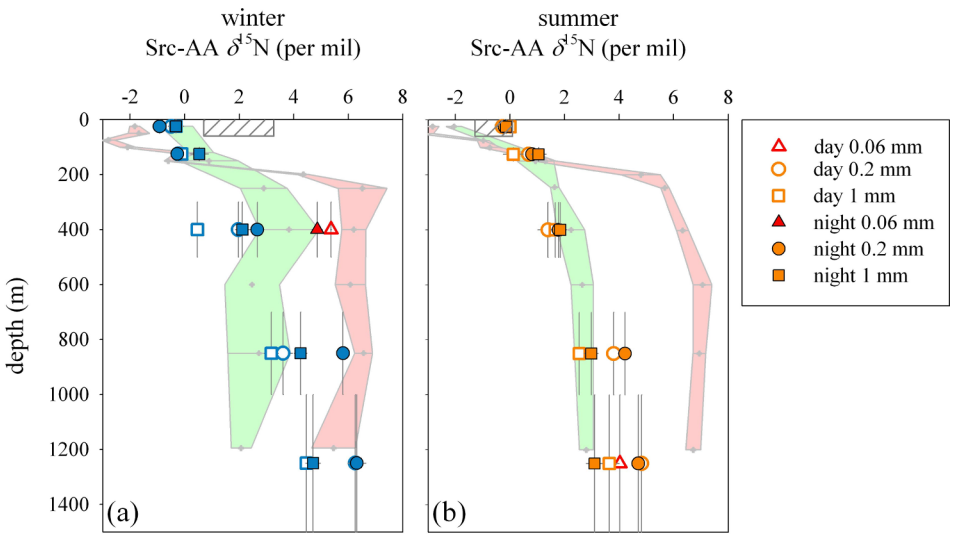

Fig. 6. Average source amino acid (AA) $\delta^{15}N$ values ($\delta^{15}N_{Src\text{-}AA}$) for zooplankton size fractions at Sta. ALOHA during (a) winter (n = 2) and (b) summer (n = 2). Horizontal error bars (often smaller than the symbol) are the SD and vertical bars indicate the depth range over which the MOCNESS sampled. Particle $\delta^{15}N_{Src\text{-}AA}$ values ± SD are shown for comparison, with green shading indicating large (> 53 μm) particles and pink shading indicating small (0.7–53 μm) particles. SD for depths with a single datum is set to a conservative 1.0‰. Hatched boxes are the range in $\delta^{15}N_{Src\text{-}AA}$ values for zooplankton collected in the euphotic zone (0–150 m) at Sta. ALOHA from 1995 to 2005 in winter and summer (Hannides et al., 2009). (For interpretation of the references to colour in this figure legend, the reader is referred to the web version of this article.)

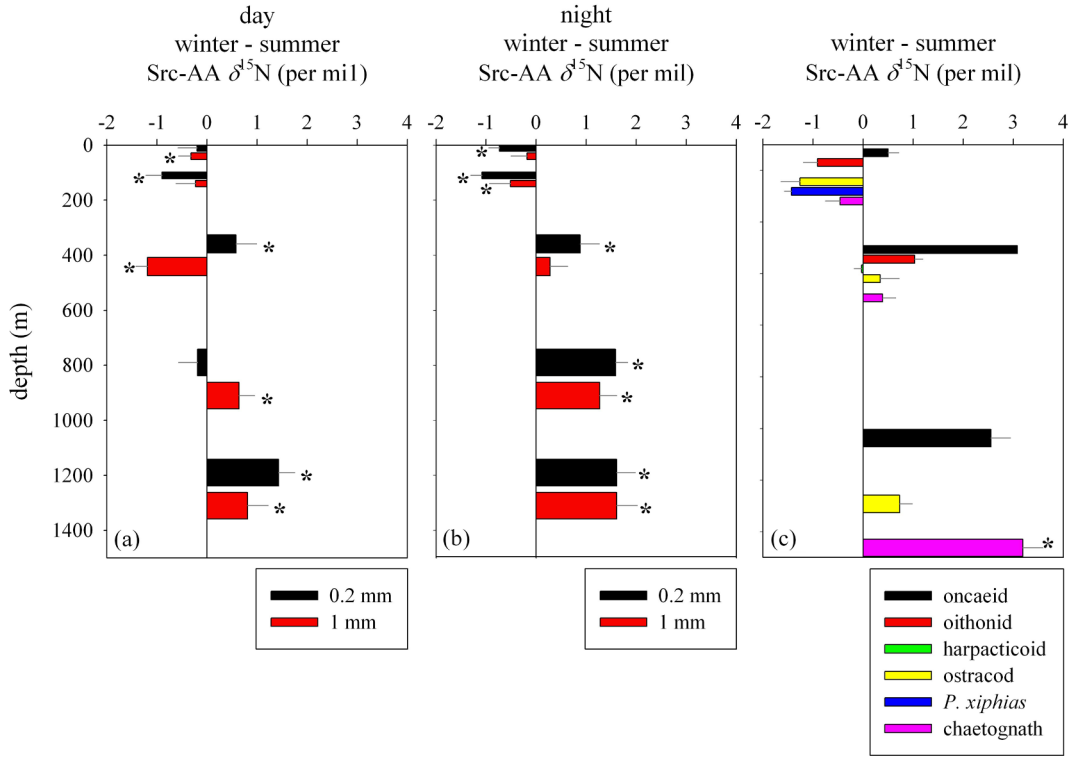

Fig. 7. Seasonal differences in source AA $\delta^{15}N$ value for zooplankton size fractions in day (a) and night (b), and target taxa (c). Differences are expressed as winter – summer $\delta^{15}N_{Src\text{-}AA}$ values and are centered within each depth interval (0–50 m, 100–150 m, 300–500 m, 700–1000 m, 1000–1500 m). Negative values indicate summer > winter $\delta^{15}N_{Src\text{-}AA}$ values, while the opposite is true for positive values. Asterisks (*) indicate significant differences (Wilcoxon test, $p < 0.05$) between winter and summer values.

seasons. In the euphotic zone lower $\delta^{15}N_{Src\text{-}AA}$ values were found in winter as compared to summer for most size fractions (Fig. 7; Wilcoxon test, $0 \leq W \leq 8.5$, df = 12–13, $p < 0.05$), with the exception of 0.2 mm during the day and 1 mm at night at 0–50 m, and 1 mm during the day at 100–150 m (Wilcoxon test, $p > 0.05$). Mixed seasonality was observed at 300–500 m. For 0.2 mm zooplankton, winter $\delta^{15}N_{Src\text{-}AA}$ values were higher than summer values during the day and night (Fig. 7; Wilcoxon test, W = 44–53, df = 13–14, $p < 0.05$). However for 1 mm zooplankton, winter $\delta^{15}N_{Src\text{-}AA}$ values were significantly lower than summer values (during the day; Wilcoxon test, $W = 0$, df = 14, $p < 0.001$) or no significant seasonal difference was found (at night; Wilcoxon test, $p > 0.05$). In contrast, a distinct seasonality was observed for zooplankton in the lower mesopelagic zone and the upper bathypelagic zone (Fig. 7). In all cases winter $\delta^{15}N_{Src\text{-}AA}$ values were significantly greater than summer values (Wilcoxon test, W = 32–64, df = 12–15, $p < 0.01$), except for 0.2 mm zooplankton collected during the day at 700–1000 m (winter = summer; Wilcoxon test, $p > 0.05$). Overall, the depth regressions differed in winter as compared to summer (i.e., a significant season × depth interaction was present; ANCOVA, $F_{1,\ 61\text{-}74}$ = 17.4–34.0, $p < 0.001$). This led to greater overall depth changes in $\delta^{15}N_{Src\text{-}AA}$ values between 0 and 50 m and 1000–1500 m in winter (Δ = 4.8–7.2‰ across all sizes and times of day) as compared to summer (Δ = 3.2–5.1‰).

CSIA of individual zooplankton taxa revealed similar trends as those

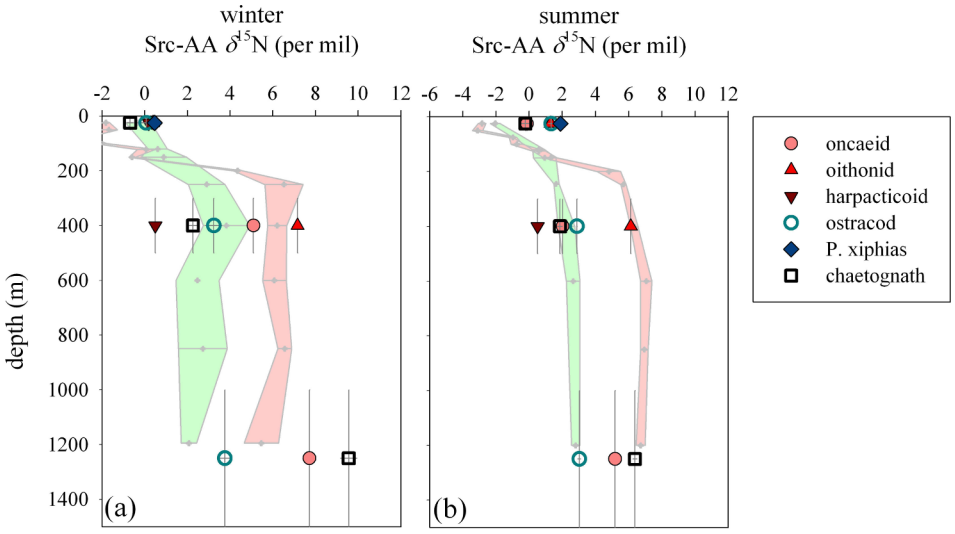

Fig. 8. Source amino acid (AA) $\delta^{15}N$ values ($\delta^{15}N_{Src\text{-}AA}$) for target zooplankton taxa at Sta. ALOHA during (a) winter (n = 1) and (b) summer (n = 1). Horizontal error bars are the SD (often smaller than the size of the symbol) and vertical bars indicate the depth range over which the MOCNESS sampled. Particle $\delta^{15}N_{Src\text{-}AA}$ values ± SD are shown for comparison, with green shading indicating large (> 53 μm) particles and pink shading indicating small (0.7–53 μm) particles. (For interpretation of the references to colour in this figure legend, the reader is referred to the web version of this article.)

found for size fractioned zooplankton and distinct seasonal trends were observed for most taxa. In surface waters, $\delta^{15}N_{Src\text{-}AA}$ values were low with an overall SD-weighted average of 0.2‰ in winter and 1.3‰ in summer (Fig. 8). Values of $\delta^{15}N_{Src\text{-}AA}$ increased significantly with depth (< 50 to > 1000 m), e.g., for oncaeid and oithonid copepods, chaetognaths (Δ = 4.8–10.3‰) and ostracods (Δ = 1.7–3.7‰) in the summer and winter (Fig. 8; linear regression, $F_{1,4\text{-}9}$ = 10.7–3904.1, $p < 0.05$). In contrast, only harpacticoid copepod $\delta^{15}N_{Src\text{-}AA}$ values in winter did not change significantly with depth (linear regression, $p > 0.05$). This latter taxa also increased the least in $\delta^{15}N_{Src\text{-}AA}$ value with depth between 0 and 50 m and 300–500 m (Δ = 0.3‰).

When depth changes in stable isotope composition was taken into account, winter $\delta^{15}N_{Src\text{-}AA}$ values were significantly higher than summer values for oncaeid copepods (ANCOVA, $F_{1,17}$ = 17.3, $p < 0.001$). A significant interaction between depth and season was present for oithonid copepods and chaetognaths (ANCOVA, $F_{1,10\text{-}18}$ = 127.2–233.4, $p < 0.001$), with a greater increase in $\delta^{15}N_{Src\text{-}AA}$ value with depth in winter as compared to summer. Ostracods exhibited no seasonal effect for $\delta^{15}N_{Src\text{-}AA}$ values (ANCOVA, $p > 0.05$). Thus our finding of significantly higher $\delta^{15}N_{Src\text{-}AA}$ values in winter versus summer in deep waters (700–1500 m) holds true for size fractioned zooplankton and most of the individual zooplankton taxa.

3.4. Zooplankton trophic position

Zooplankton trophic position in winter and summer over depth was calculated based on the difference between source AA $\delta^{15}N$ values and trophic AA $\delta^{15}N$ values (Fig. 1; Section 2.7). Thus trophic position estimates are independent of basal resource $\delta^{15}N_{Src\text{-}AA}$ values. Zooplankton trophic position varied with size in surface waters (Fig. 9; data available at BCO-DMO: https://www.bco-dmo.org/project/537123). In the euphotic zone (0–150 m), $TP_{Tr\text{-}Src}$ was lower for 0.2 mm (weighted average of 2.4) versus 1 mm zooplankton (weighted averages of 2.8–2.9), although this size difference was not significant when considering propagation of error (i.e., TP were within 2 SD of each other). Trophic position further increased with depth at all times (Fig. 9; linear regression, $F_{1,28\text{-}42}$ = 66.7–209.0, $p < 0.001$), with $TP_{Tr\text{-}Src}$ increasing by 0.8–1.1 for 0.2 mm zooplankton and 0.5–0.8 for 1 mm zooplankton between the surface waters and 1500 m. Seasonally, in winter at 700–1500 m, weighted average $TP_{Tr\text{-}Src}$ was 3.3 for 0.2 mm zooplankton and 3.3–3.4 for 1 mm zooplankton during the day and night. In summer, weighted average $TP_{Tr\text{-}Src}$ for lower mesopelagic and upper bathypelagic depths (700–1500 m) were significantly lower at 3.0 for the 0.2 mm zooplankton and the same, 3.4, for the 1 mm zooplankton during the day and night. Overall, the winter increase in $TP_{Tr\text{-}Src}$ values for 0.2 mm zooplankton in the lower mesopelagic and upper bathypelagic zone led to a convergence of $TP_{Tr\text{-}Src}$ values for 0.2 and 1 mm zooplankton at depth during this season (Fig. 9).

Seasonal changes in zooplankton TP were significant over all depths, especially for 0.2 mm zooplankton. $TP_{Tr\text{-}Src}$ depth trends were significantly greater in winter compared to summer for both the day and night tows (ANCOVA, $F_{1,72}$ = 17.5, $p < 0.001$ and $F_{1,61}$ = 4.1, $p < 0.05$, respectively). Seasonal changes for 1 mm zooplankton were more varied, and only observed for those collected during the day, where the slope of the depth regression was greater in summer versus winter (ANCOVA, $F_{1,68}$ = 9.0, $p < 0.005$).

Trends in zooplankton TP for individual taxa were in most cases similar to those observed for size fractioned zooplankton (Fig. 10). As with size fractioned zooplankton, significant depth increases in $TP_{Tr\text{-}Src}$ were observed for all taxa in winter and summer (Fig. 10; linear regression, $F_{1,4\text{-}9}$ = 24.2–2480.0, $p < 0.001$). The increase in $TP_{Tr\text{-}Src}$ with increasing depth (Δ over 300–500 m or 1000–1500 m) was high for oncaeid and oithonid copepods (Δ = 1.5–1.8) and relatively low for harpacticoid copepods (Δ = 0.5), ostracods (Δ = 0.6), and chaetognaths (Δ = 0.6–0.8). In the upper bathypelagic zone at 1000–1500 m, $TP_{Tr\text{-}Src}$ for oncaeid copepods reached 3.6–3.9, ostracod $TP_{Tr\text{-}Src}$ was 3.2, and chaetognath $TP_{Tr\text{-}Src}$ was 3.7–3.9. Seasonal variation in TP was observed for some taxa but not others. Overall, winter $TP_{Tr\text{-}Src}$ was greater than summer $TP_{Tr\text{-}Src}$ for oithonid copepods (ANCOVA, $F_{1,9}$ = 12.8, $p < 0.01$). Also, a significant interaction between depth and season was present for chaetognaths (ANCOVA, $F_{1,17}$ = 12.3, $p < 0.005$), with the change in $TP_{Tr\text{-}Src}$ with depth greater in summer than in winter. No significant seasonal effects on $TP_{Tr\text{-}Src}$ were found for oncaeid copepods and ostracods (ANCOVA, $p > 0.05$).

3.5. Comparison of zooplankton and particle source AA $\delta^{15}N$ values

Zooplankton rely on a food web base comprised of large and small particles in midwaters, with zooplankton stable isotope composition tightly coupled to the stable isotope composition of their basal food resources (Hannides et al., 2013). In other words, $\delta^{15}N_{Src\text{-}AA}$ values change very little with trophic transfer, so zooplankton $\delta^{15}N_{Src\text{-}AA}$ values directly reflect the mixture of small (0.7–53 μm) and large (> 53 μm) particle resources at the base of their food web (Figs. 6, 8). Moreover, because only trophic AA $\delta^{15}N$ values change significantly with trophic position (Fig. 1), zooplankton source AA $\delta^{15}N$ values reflect baseline resource $\delta^{15}N$ values independent of zooplankton trophic level. Closer examination of small and large particle $\delta^{15}N_{Src\text{-}AA}$ values at Sta. ALOHA reveals a continuum, with surface water (0–75 m) particles having the lowest $\delta^{15}N_{Src\text{-}AA}$ values, large midwater (≥250 m) particles

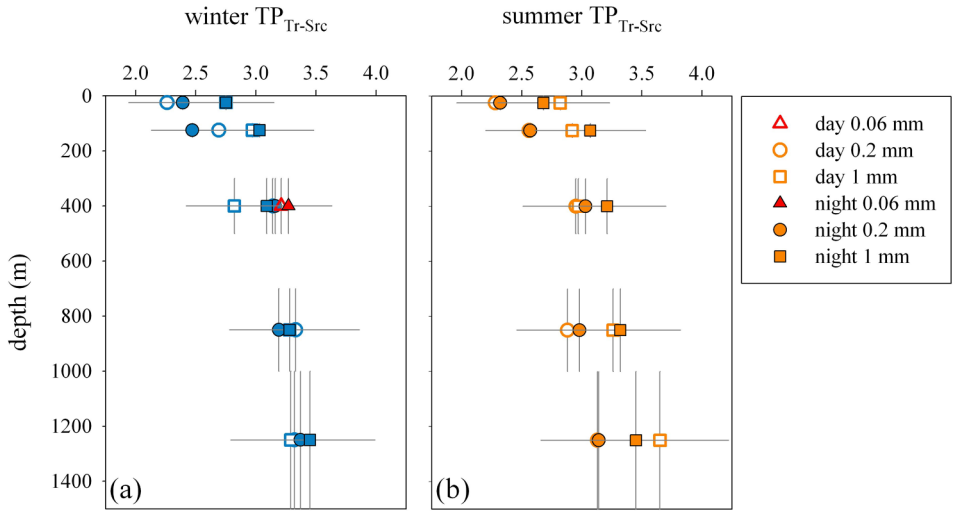

Fig. 9. Trophic position ($TP_{Tr\text{-}Src}$) for zooplankton size fractions at Sta. ALOHA during (a) winter (n = 2) and (b) summer (n = 2). Horizontal error bars are the SD and vertical bars indicate the depth range over which the MOCNESS sampled.

having higher $\delta^{15}N_{Src\text{-}AA}$ values, and small midwater (≥250 m) particles having the highest $\delta^{15}N_{Src\text{-}AA}$ values (Fig. 11). Source AA $\delta^{15}N$ values for these three particle types in the NPSG are distinct and consistent across seasons, thus we can compare them with zooplankton $\delta^{15}N_{Src\text{-}AA}$ values and link midwater zooplankton nutrition with particle cycling. Comparison with zooplankton size fractions (Fig. 6) and taxa (Fig. 8) shows that midwater zooplankton $\delta^{15}N_{Src\text{-}AA}$ values are distributed widely across this particle continuum (Fig. 11). In three cases zooplankton $\delta^{15}N_{Src\text{-}AA}$ values are even higher than small midwater particle $\delta^{15}N_{Src\text{-}AA}$ values (Fig. 11), likely indicating baseline resources for these zooplankton are a high $\delta^{15}N$ value subset of the small particle pool (see below). In general, our results strongly indicate that both small and large particles, from surface to midwater depths, contribute to the food web base for midwater zooplankton, with the relative mixture of components differing by season, depth, zooplankton size, and zooplankton taxa.

Here we take the first steps in quantitatively evaluating the contribution of different particle types to the food web base for zooplankton in midwaters at Sta. ALOHA. Zooplankton source $\delta^{15}N_{AA}$ values reflect a mixture of basal particle resources, and again these $\delta^{15}N_{Src\text{-}AA}$ values are independent of trophic position or the mode of acquisition. To better constrain our initial results we focus on two particle sources and, following Hannides et al. (2013), apply a two-source isotope mass balance mixing model to zooplankton $\delta^{15}N_{Src\text{-}AA}$ values. The majority of midwater zooplankton $\delta^{15}N_{Src\text{-}AA}$ values fall in between those for small and large particles (Fig. 11). We therefore first apply a mass balance mixing model that calculates f_{SMALL}, the fraction of deep small particle-derived N entering midwater zooplankton food webs, as $\delta^{15}N_{Src\text{-}ZP} = \delta^{15}N_{Src\text{-}small} \times f_{SMALL} + \delta^{15}N_{Src\text{-}large} \times (1 - f_{SMALL})$. Here our two endmembers are (1) deep small particles (sampled from 250 to 1200 m) and (2) deep large particles (sampled from 250 to 1200 m). This model necessarily assumes that the fresh surface material contribution is zero, although in reality all three source materials could contribute to zooplankton food web resources at any given depth. If there were additional fresh surface particle contributions (0–200 m) to the mixture of deep large and small particle resources supporting the food web of a specific zooplankton taxa or size fraction, f_{SMALL} would be even larger than calculated. We also note that a few deep zooplankton taxa and size fractions have $\delta^{15}N_{Src\text{-}AA}$ values that are higher than that of deep small particles (small particles collected deeper than 250 m; Fig. 11). Since "small" particles range in size from 0.7 to < 53 μm, we speculate that some zooplankton consume a subfraction of the "small" particle pool with $\delta^{15}N_{Src\text{-}AA}$ values higher than the 0.7–53 μm average.

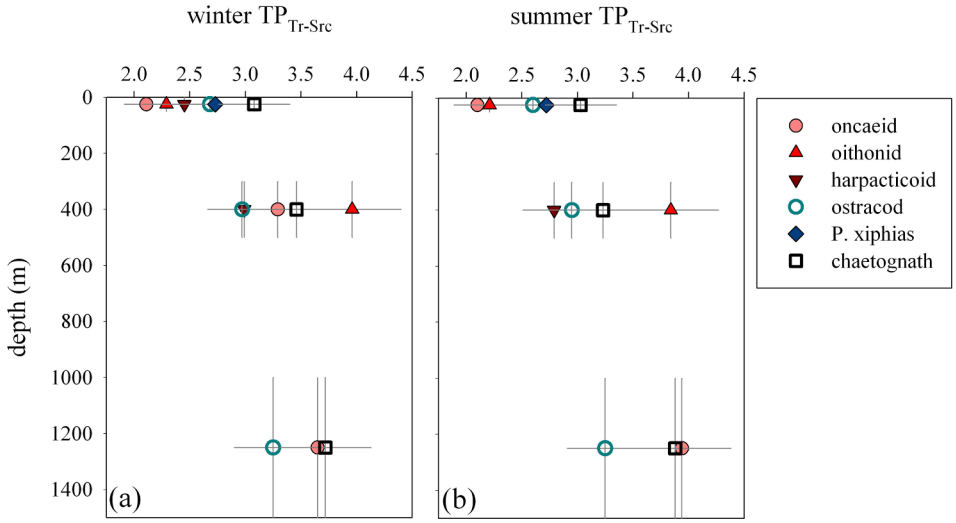

Fig. 10. Trophic position ($TP_{Tr\text{-}Src}$) of target zooplankton taxa at Sta. ALOHA during (a) winter (n = 1) and (b) summer (n = 1). Horizontal error bars are the SD and vertical bars indicate the depth range over which the MOCNESS sampled.

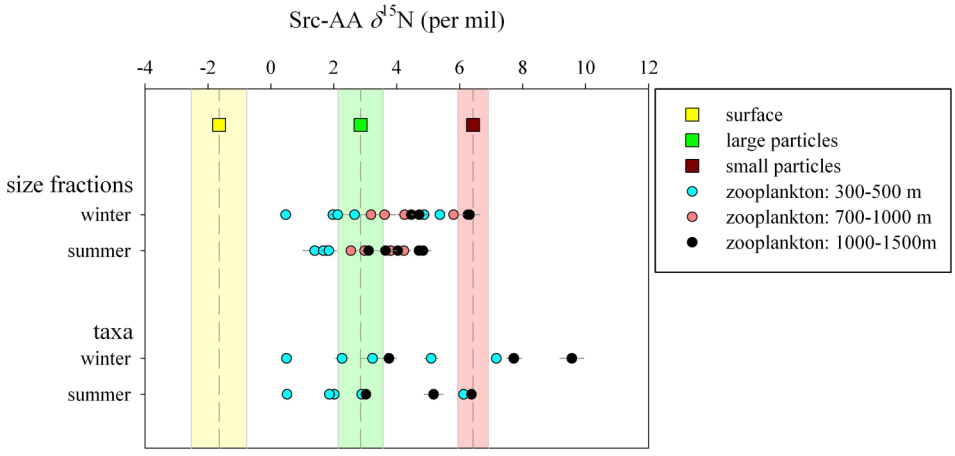

Fig. 11. Source amino acid (AA) δ^{15}N values ($\delta^{15}N_{Src\text{-}AA}$) for zooplankton size fractions and taxa in midwaters at Sta. ALOHA compared to $\delta^{15}N_{Src\text{-}AA}$ values for surface water (0–75 m) particles (0.7 – > 53 μm), large particles (> 53 μm) collected in midwaters (250–1200 m), and small particles (0.7–53 μm) collected in midwaters (250–1200 m). All particle data was averaged across two seasons (summer and winter), and midwater data was additionally averaged across 4–6 samples collected at discrete depths from 250 to 1200 m. For zooplankton, error bars are the SD (often smaller than the size of the symbol), and for particles, shading indicates overall SD with propagated uncertainty.

We note that source $\delta^{15}N_{AA}$ values for some zooplankton size fractions and taxa collected at 300–500 m do not fall in between deep large and small particles, but rather fall in between those for surface material and deep large particles (Fig. 11). We therefore apply a second, alternative mass balance mixing model to these zooplankton. Here we calculate $f_{SURFACE}$, the fraction of fresh surface N entering midwater zooplankton food webs, as $\delta^{15}N_{Src\text{-}ZP} = \delta^{15}N_{Src\text{-}surface} \times f_{SURFACE} + \delta^{15}N_{Src\text{-}large} \times (1 - f_{SURFACE})$. Our two endmembers in this case are (1) fresh surface material (sampled from 0 to 75 m) and (2) deep large particles (sampled from 250 to 1200 m). For surface material we use $\delta^{15}N_{Src\text{-}AA}$ values for presumed "fresh" large and small particles collected in the euphotic zone at Sta. ALOHA, and thus set our depth interval from 0 to 75 m. High $f_{SURFACE}$ for zooplankton could result from feeding on fresh particles sinking rapidly from surface waters, or could result from migrant zooplankton feeding directly at the surface. Similar to our first mixing model, our calculation of $f_{SURFACE}$ assumes that the deep small particle contribution is zero, although in reality all three source materials could contribute to zooplankton food web resources at any given depth. If there were additional deep small particle contributions to the mixture of basal resources supporting the food web of zooplankton at 300–500 m, $f_{SURFACE}$ would be even larger than calculated. Thus, when applied to zooplankton $\delta^{15}N_{Src\text{-}AA}$ values that fall in between those of surface water particles and deep large particles, our model gives minimum values for $f_{SURFACE}$. We consider our modeling approaches conservative and the most appropriate use of information from a one biotracer system.

As we have discussed, for zooplankton in the mid-mesopelagic zone at 300–500 m, we first applied our mixing model, f_{SMALL}, if zooplankton $\delta^{15}N_{Src\text{-}AA}$ values were between those of deep large and small particles, and applied our second mixing model, $f_{SURFACE}$, if zooplankton $\delta^{15}N_{Src\text{-}AA}$ values were between those of surface material and deep large particles. Model results indicate a wide range in source contribution to zooplankton food webs in the mid-mesopelagic zone. For example, $f_{SURFACE}$ ranged from 0.06 to 0.57 and f_{SMALL} ranged from 0.01 to 1.0 (Fig. 12). Again, our models are conservative and we consider these minimum values of $f_{SURFACE}$ and f_{SMALL}. For example, relatively high $f_{SURFACE}$ (0.57 ± 0.18) were found in winter for both 1 mm zooplankton collected during the day and for harpacticoid copepods. Thus 1 mm day-collected zooplankton and harpacticoid copepods have at minimum an $f_{SURFACE} \sim 60\%$, and this value could be higher if deep small particles also contributed to their food webs. Relatively small $f_{SURFACE}$ (0.12–0.23) were found for 0.2 mm zooplankton and 1.0 mm zooplankton collected during the night at 300–500 m. Again, these are minimum values for $f_{SURFACE}$, and could be larger if deep small particles also contributed to the basal resources underlying these zooplankton food webs. In contrast, high f_{SMALL} was found for oithonid copepods (1.0 in winter and 0.90 ± 0.20 in summer). Because our models are conservative, this f_{SMALL} is a minimum value, and could be higher if there was an additional fresh surface material contribution to oithonid copepod food webs.

Overall, we observed consistent diel and seasonal differences in source material contributions at 300–500 m (Fig. 12), although given model uncertainties these differences were not significant. The largest diel difference (Δ day – night = 0.34 ± 0.23) was for 1 mm zooplankton in winter, compared to negligible diel differences for both 0.2 and 1 mm zooplankton in summer. The largest seasonal difference in $f_{SURFACE}$ was found for 1 mm zooplankton collected during the day (Δ winter – summer = 0.44 ± 0.18) and the largest seasonal difference in f_{SMALL} was found for oncaeid copepods (Δ winter – summer = 0.67 ± 0.31).

For zooplankton in the deep mesopelagic zone at 700–1000 m, $\delta^{15}N_{Src\text{-}AA}$ values were generally between those of deep large and small particles, therefore we applied our mixing model for f_{SMALL}. At these depths f_{SMALL} ranged from 0.0 to 0.92 (Fig. 12). The lowest value of f_{SMALL} (0.0) was for 1 mm zooplankton collected during the day in winter. $\delta^{15}N_{Src\text{-}AA}$ values for these zooplankton fell in between deep large particles and surface material (Fig. 11), indicating our alternate $f_{SURFACE}$ model could also be applied. This latter model gives $f_{SURFACE}$ = 0.01, thus both models indicate that deep large particles support daytime 1 mm zooplankton food webs in winter. In contrast, the highest value of f_{SMALL} at 700–1000 m (0.92) was for 0.2 mm zooplankton collected in winter at night. Again, our model is conservative and gives minimum values of f_{SMALL}. Thus if there was a surface particle contribution to nighttime 0.2 mm zooplankton food webs, f_{SMALL} would be even higher. Diel and seasonal differences in f_{SMALL} were found for 0.2 mm and 1 mm zooplankton (Fig. 12), but again given model uncertainties these differences were not significant. Large diel differences were found for both 0.2 and 1 mm zooplankton in winter (0.2 mm: Δ night – day = 0.78 ± 0.44; 1 mm: Δ night – day = 0.37 ± 0.35). The largest seasonal difference at 700–1000 m was found for 0.2 mm zooplankton collected at night (Δ winter – summer = 0.47 ± 0.39). Overall, f_{SMALL} for most zooplankton size fractions at 700–1000 m ranged from 0.14 to 0.45, indicating a mostly large particle-based food web with a modest deep small particle contribution.

For zooplankton in the upper bathypelagic zone at 1000–1500 m, $\delta^{15}N_{Src\text{-}AA}$ values were between those of deep large and small particles and we applied our mixing model for f_{SMALL}. At these depths, f_{SMALL} ranged from 0.17 to 1.0 (Fig. 12). Our model indicates that f_{SMALL} is particularly high (f_{SMALL} = 1.0) for 0.2 mm zooplankton, oncaeid copepods, and chaetognaths in winter, due to their very high $\delta^{15}N_{Src\text{-}AA}$ values (Figs. 8, 11). Again, these high source AA δ^{15}N values are not influenced by trophic position, and instead most likely indicate that a subset of material within the small particle pool with very high $\delta^{15}N_{Src\text{-}}$

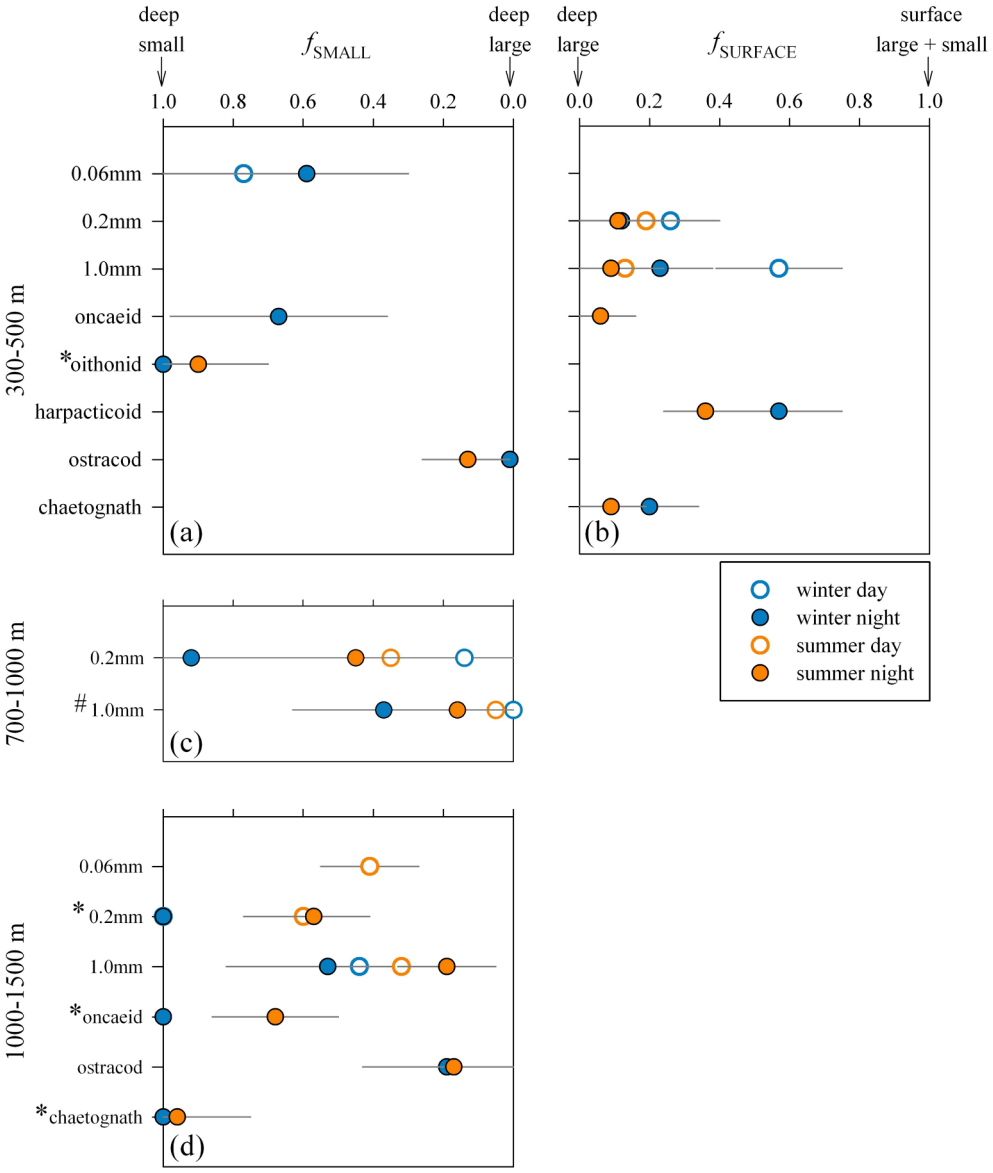

Fig. 12. Average fraction of deep small particles (f_{SMALL}: a, c, d) and average fraction of fresh surface material ($f_{SURFACE}$: b) forming the food web base for zooplankton taxa in the mesopelagic and upper bathypelagic zone at Sta. ALOHA during winter and summer. For f_{SMALL}, an $f = 1.0$ indicates deep small particles (250–1200 m) form 100% of the zooplankton food web base while $f = 0.0$ indicates the food web base is comprised of all deep large particles (250–1200 m). For $f_{SURFACE}$, an $f = 1.0$ indicates fresh surface material (large and small particles sampled from 0 to 75 m) forms 100% of the zooplankton food web base while $f = 0.0$ indicates the food web base is comprised of all deep large particles (250–1200 m). Note the reversal in direction of the x-axis for f_{SMALL}. (a) f_{SMALL} for zooplankton collected at 300–500 m. (b) $f_{SURFACE}$ for zooplankton collected at 300–500 m. (c) f_{SMALL} for zooplankton collected at 700–1000 m. (c) f_{SMALL} for zooplankton collected at 1000–1500 m. Zooplankton labels with asterisks (*) indicates very high $\delta^{15}N_{Src\text{-}AA}$ values for oithonid copepods collected in winter at 300–500 m and 0.2 mm zooplankton, oncaeid copepods, and chaetognaths collected in winter at 1000–1500 m. Here we set $f_{SMALL} = 1.0$. Zooplankton labels with hashtags (#) indicates relatively low $\delta^{15}N_{Src\text{-}AA}$ values for 1 mm zooplankton collected in winter during the day, and here we set $f_{SMALL} = 0.0$. Horizontal error bars reflect the uncertainty in $f_{SURFACE}$ and f_{SMALL} propagated through the model calculations.

$_{AA}$ values is the basal resource for these zooplankton food webs. In summer, f_{SMALL} is again large for chaetognaths (0.96 ± 0.21). Because our model is conservative these values of f_{SMALL} can be considered minimum values, and thus indicate an overall large contribution of deep small particles to basal resources for many zooplankton taxa at 1000–1500 m. The contribution of deep small particles to zooplankton food webs at 1000–1500 m is lowest for ostracods (f_{SMALL} = 0.17–0.19) and 1 mm zooplankton in summer (f_{SMALL} = 0.19–0.32). Overall the difference between night and day basal food sources were small (Δ night – day f_{SMALL} = −0.13–0.09), indicating negligible diel changes in the contribution of source materials to zooplankton food webs at 1000–1500 m. However consistent seasonal changes were observed (Fig. 12), although given model uncertainties these changes were not significant. Generally winter f_{SMALL} was greater than summer f_{SMALL}, with the largest seasonal differences observed for 0.2 mm zooplankton collected during the day and night (Δ winter – summer = 0.40–0.43) and for 1 mm zooplankton collected during the night (Δ winter – summer = 0.34 ± 0.32). In summary, our conservative model indicates that the contribution of small particle resources to the base of zooplankton food webs in the upper bathypelagic zones is at least 0.19–0.60, and in the case of many small zooplankton and chaetognaths much higher (up to 1.0), particularly during winter.

4. Discussion

4.1. Zooplankton in the surface ocean of the North Pacific Subtropical Gyre

Early studies in the NPSG emphasized the 'monotonous' nature of the environment and constancy in zooplankton community dynamics, even over multiyear periods (McGowan and Walker, 1985). In contrast to this historical perspective, more recent time-series work has revealed a distinct seasonality and long-term temporal change in the NPSG based on rigorous monthly cruises to Sta. ALOHA over the past two and a half decades. The emerging climatology indicates that primary production varies two-fold over the year at Sta. ALOHA, with highest rates uniquely observed in summer when the water column is highly stratified and the euphotic zone is nutrient-starved (Church et al., 2013). This cycle is linked to maximal irradiance values during the summer months (Karl and Church, 2014) that facilitates a nitrogen fixation-mediated diatom bloom (Dore et al., 2002).

Zooplankton in the surface ocean respond to observed NPSG seasonal phytoplankton dynamics, by increasing euphotic zone biomass in summer (Landry et al., 2001). This is consistent with an approximate doubling of summertime zooplankton biomass (Valencia et al., 2016) and has associated top-down effects on lower trophic levels such as

eukaryotic autotrophs (Pasulka et al., 2013).

Here modest increases in euphotic zone zooplankton biomass were also observed in summer. Biomass in the upper 150 m was 1.7–2 times higher in summer versus winter for day and night tows. We further evaluated zooplankton dynamics in the upper (0–50 m) and lower euphotic zone (100–150 m). Day, night, and migrant biomass were generally higher in the upper versus lower euphotic zone, in concert with primary productivity levels that are also highest in the upper 75 m (Karl, 1999; Karl et al., 1996).

Summertime source $\delta^{15}N_{AA}$ values were higher than previous measurements by Hannides et al. (2009), who measured zooplankton source $\delta^{15}N_{AA}$ values during the summer months over a ten-year period at Sta. ALOHA of −2 to −4‰ and attributed this signature to summer N_2 fixation. This study further hypothesized that winter zooplankton $\delta^{15}N_{Src\text{-}AA}$ values would be higher due to increased injection of nitrate with high $\delta^{15}N$ values. Here, $\delta^{15}N_{Src\text{-}AA}$ values are still low during the summer (< 2‰), which suggests that sampling may have missed the peak in nitrogen fixation. Zooplankton $\delta^{15}N_{Src\text{-}AA}$ values were also significantly lower in the upper versus lower euphotic zone in most cases. Pasulka et al. (2013) found biomass of the diazotrophs *Trichodesmium* spp. and *Crocosphaera* spp. to be concentrated in the upper 50 m and Church et al. (2009) found N_2 fixation activity in both whole seawater and < 10-μm size fractionated seawater to be greatest at depths < 50 m. Thus lower zooplankton $\delta^{15}N_{Src\text{-}AA}$ values in the upper euphotic zone are likely driven in part by the introduction of ^{15}N-depleted N into zooplankton food webs through diazotroph activity. At the same time plankton dynamics in the upper 50 m are separated from deep water nutrient sources, with the nitracline at Sta. ALOHA typically starting at 90–120 m (Letelier et al., 2004). Intense plankton food web recycling of N thus also likely contributes to low $\delta^{15}N_{Src\text{-}AA}$ values in the upper euphotic zone (Checkley and Miller, 1989). In contrast, plankton in the lower euphotic zone grow within the nitracline (Letelier et al., 2004). Higher $\delta^{15}N_{Src\text{-}AA}$ values at 100–150 m therefore reflect the ^{15}N enrichment of deep-water nitrate (NO_3^-) sources supporting zooplankton food webs at these depths.

The $\delta^{15}N_{Src\text{-}AA}$ values measured during the winter were unexpectedly lower than that measured during the summer suggesting additional diazotroph activity contributing to zooplankton community food webs prior to our winter cruise. N_2 fixation does occur in the winter and *nifH* gene abundances for bloom-forming filamentous cyanobacteria can be significant during these months (Church et al., 2009). While a bloom was not detected in particles sampled on our winter cruise, subtropical zooplankton generation times are on the order of several weeks. However, winter N_2 fixation did not result in enhanced particle export. As mentioned earlier, low particle $\delta^{15}N_{Src\text{-}AA}$ values were apparent only in surface waters and did not translate to deeper depth (Fig. 6). Low $\delta^{15}N$ values were also not found in the Hawaiian Ocean Time series particulate nitrogen fluxes captured in particle interceptor sediment traps at 150 m. During December 2013, January 2014 and February 2014 $\delta^{15}N$ values averaged 3.4‰, within the range of historical nitrogen isotopic compositions measured at ALOHA (3.4–3.7‰, http://hahana.soest.hawaii.edu/hot/hot-dogs/interface.html) and lower than the average measured in May, June and July 2014 (2.8‰).

In summary, our findings suggest variability in zooplankton community biomass and $\delta^{15}N_{Src\text{-}AA}$ values within the euphotic zone in the NPSG are driven by bottom-up processes, such as changes in primary productivity, diazotroph activity, and nutrient delivery.

4.2. Midwater zooplankton in the North Pacific Subtropical Gyre

The vertical structure of the NPSG zooplankton community in the upper 500–600 m in the 1970s and 1980s has been described in detail. Our finding of a decrease in zooplankton biomass with depth matches these early observations (e.g., McGowan and Walker, 1979). Particle concentrations also decrease rapidly with increasing depth (Benitez-Nelson et al., 2001; Casciotti et al., 2008; Hebel and Karl, 2001) as do particle fluxes (Buesseler et al., 2007; Christian et al., 1997; Karl et al., 1996, Umhau et al., 2019). Thus the exponential decrease in zooplankton biomass we observed over 1500 m is likely related to a reduction in particulate food resources available to mesopelagic and bathypelagic populations.

An important aspect of zooplankton structure in early studies and in our data is vertical migration. McGowan and Walker (1979) found two multi-species copepod groups that engaged in diel vertical migration. The first group was found in the upper 160 m at night versus the mesopelagic zone during the day, and the second group migrated between the upper- to mid-mesopelagic zone (100–350 m) at night and to below 600 m during the day. Some species also engage in smaller amplitude diel migrations entirely within the euphotic zone or only between the euphotic zone and upper mesopelagic zone (McGowan and Walker, 1979). For example, some cyclopoid and oncaeid copepod species migrate only within the upper 150–200 m or the upper 300 m (Zalkina, 1970). Based on day-night differences in biomass, we identify similar diel vertical migration in our samples between the surface and 200–300 m for smaller zooplankton (0.2 and 0.5 mm) and between the surface and 300–1000 m for larger zooplankton (1 mm, 2 mm, and 5 mm). The day-night differences were significant in summer when the largest number of replicate net tows were collected, and indicate progressively deeper migration of larger zooplankton size fractions into midwaters during the day. That is, 1 mm zooplankton migrated down to 300–500 m, 2 mm zooplankton migrated down to 500–700 m, and 5 mm zooplankton migrated down to 700–1000 m. Migration of the smaller size fractions to 200–300 m could be due to both the movement of small species (as found by Zalkina, 1970) or migration of the juvenile stages of larger species, as ontogenetic migration patterns were previously noted in the NPSG (Ambler and Miller, 1987).

Zooplankton bulk $\delta^{15}N$ values in many regions of the world's oceans increase with depth from surface waters into the mesopelagic and bathypelagic zones (Koppelmann et al., 2009; Laakmann and Auel, 2010). Our CSIA-AA enables us to distinguish between two possible mechanisms driving this depth increase: differences in $\delta^{15}N$ values of food resources at the base of the midwater zooplankton food web, or changes in zooplankton TP (e.g., Hannides et al., 2013). We find both mechanisms to be important. Zooplankton $\delta^{15}N_{Src\text{-}AA}$ values increase significantly with depth, indicating resources at the base of the zooplankton food web are more ^{15}N-enriched in the mesopelagic and upper bathypelagic zone as compared to surface waters. At the same time, small particle $\delta^{15}N_{Src\text{-}AA}$ values increased by ~8.7‰, and large particle $\delta^{15}N_{Src\text{-}AA}$ values increase by ~3 to 4‰ with depth. Thus, depth changes in zooplankton bulk $\delta^{15}N$ values are likely due in part to changes in the stable isotope composition of their basal food resources, which includes small and large particles through the midwaters.

Depth related increases in bulk $\delta^{15}N$ values are also the result of increasing TP. Our observed increase in $TP_{Tr\text{-}Src}$ was 0.5–1.1 for all size fractions and 0.5–1.8 for most target taxa through the midwaters in both winter and summer. One mechanism driving higher TP for zooplankton size fractions in midwaters could be an increased contribution of carnivory (Koppelmann et al., 2003) or carnivore layers (Steinberg et al., 2008a). However many individual taxa increased in TP, and it is difficult to understand how feeding habits for all taxa could change drastically to become more carnivorous in midwaters. For example, ostracod $TP_{Tr\text{-}Src}$ at depth was 3.2. While gut content evidence does indicate some scavenging or carnivorous feeding on crustaceans, cyanobacteria and eukaryotic phytoplankton were also prevalent in ostracod guts from 200 to 1000 m, likely ingested as part of marine snow particles (Wilson and Steinberg, 2010). Thus a completely carnivorous existence for ostracods at depth seems unlikely. Similarly, chaetognath $TP_{Tr\text{-}Src}$ at 1000–1500 m was 3.7–3.9, but these known primary carnivores are not likely to act as secondary carnivores in midwaters. Instead, we explore a second mechanism that could result in increased zooplankton TP with depth, specifically a depth increase in the TP of

particles at the base of their food web. In fact, $TP_{Tr\text{-}Src}$ of small and large particles also increases with depth, and the magnitude of this change ($\Delta \sim 0.3$–0.9; Hilary Close, personal communication) is similar to the changes observed for zooplankton size fractions and larger taxa ($\Delta \sim 0.5$–1.1). Thus while increased carnivory is likely with depth, our results indicate that a second mechanism, changes in the composition of particles at the base of the food web, partially drive our observed depth variation in zooplankton $TP_{Tr\text{-}Src}$. One exception may be small zooplankton taxa (see Section 4.5); the very large depth changes in $TP_{Tr\text{-}Src}$ observed for some small taxa ($\Delta \sim 1.6$–1.8) may be due to foraging strategies such as coprophagy and semi-parasitism. Such strategies could allow the incorporation of material from higher trophic levels into zooplankton tissues, and result in relatively high $TP_{Tr\text{-}Src}$.

4.3. Seasonal change in midwaters of the North Pacific Subtropical Gyre

We have limited information on how seasonal cycles impact NPSG zooplankton in the mesopelagic zone. Evidence for biogeochemical seasonality in midwaters at Sta. ALOHA has come primarily from time-series research on sediment trap measurements of particle fluxes to the deep ocean. Recent seasonal climatologies indicate euphotic zone export increases $<$ 2-fold over the more productive spring and summer months (Church et al., 2013). This export, especially in late summer, has been linked to blooms of diatoms including *Hemiaulus* spp., which contain N_2-fixing endosymbionts (Scharek et al., 1999a,b). Records from deep-sea sediment traps further identify a late 'summer export pulse' which is both predictable, occurring each year typically in late July – early August, and efficient, with less vertical attenuation of particle fluxes during this period (Karl et al., 2012). N_2-fixation is likely an important driver of this 'pulse', based not only on the earlier work of Scharek et al. (1999b), but also on low $\delta^{15}N$ values of sinking particulate material in summer and the significant presence of Het 1–3 phylotypes in material from sediment traps deployed at 4000 m (Karl et al., 2012). The larger flux of organic-rich material in summer may impact midwater zooplankton communities through preferential consumption of labile particles exported from the euphotic zone.

Seasonality in particle flux at the time of our cruises and available from the Hawaiian Ocean Time series agrees with these long term observations. Average particulate nitrogen fluxes in winter at 150 m from both *in situ* traps and tracer based studies are two-fold lower (ANOVA, $p = 0.019$) than that measured in summer (Umhau et al., 2019). Flux profiles measured during our cruises further suggest seasonal linkages between export, particle size, and zooplankton and microbial reworking at depth. In winter, particulate carbon (PC) flux profiles for both large and small particles indicated negligible export below 200 m, suggesting that zooplankton and microbes efficiently reduced fluxes of both particle size classes below the euphotic zone (Umhau et al., 2019). In summer by contrast, small and large particle fluxes remained high throughout the water column to 400 m (Umhau et al., 2019). Umhau et al. (2019) attribute this to inefficient zooplankton grazing. That is, production of phytodetrital material during the summer export pulse is greater than zooplankton grazing in the upper mesopelagic zone, with a significant fraction of the summer pulse escaping zooplankton consumption at depth. This hypothesis is supported by CSIA-AA of large and small particles. Specifically, small particle $\delta^{15}N_{AA}$ values in summer indicated more microbial as compared to metazoan reworking, versus $\delta^{15}N_{AA}$ values of small particles collected in winter (Close et al., 2015). In general, CSIA-AA patterns for small particles indicate a stronger signature of microbial degradation, as compared to large particles, which exhibit CSIA-AA patterns more consistent with metazoan reworking (Close et al., 2015; Ohkouchi et al., 2017). PC to thorium ratios (PC/Th) also indicate that small particles contained fundamentally different material than large particles (Umhau et al., 2019). In winter and spring, PC/Th ratios in both particle sizes were nearly identical, suggesting similar processes of formation and degradation. In summer, small and large particle PC/Th ratios significantly differed, arguing that processes other than aggregation and disaggregation were influencing particle composition, such as size-selective zooplankton grazing. Taken together with the time series observations, combined results confirm a distinct seasonal cycle in particle dynamics in the NPSG. In winter export is relatively low and particles sinking to depth are efficiently grazed by zooplankton in midwaters. However in summer, during the export pulse, zooplankton are unable to efficiently rework the large amount of phytodetritus produced during this time period, and thus particles in summer mainly exhibit a microbial reworking signature.

Our CSIA-AA of the midwater zooplankton community at Sta. ALOHA indicates a strong functional response to seasonal changes in production and export in the NPSG. For size fractionated zooplankton, there was a greater increase with depth of $\delta^{15}N_{Src\text{-}AA}$ values in winter ($\Delta \sim 5$–7‰) as compared to summer ($\Delta \sim 3$–5‰). This trend was defined by higher winter $\delta^{15}N_{Src\text{-}AA}$ values as compared to summer values for all size fractions at depths of 700–1500 m (with one exception). Moreover, similar trends with season were observed for most individual zooplankton taxa. We can evaluate two mechanisms potentially driving higher zooplankton $\delta^{15}N_{Src\text{-}AA}$ values at depth in winter as compared to summer. First, particulate source contributions at the base of the zooplankton food web could remain constant, but $\delta^{15}N_{Src\text{-}AA}$ values for these food web basal resources vary seasonally. However CSIA-AA of particles collected on each cruise indicated no significant seasonal difference in $\delta^{15}N_{Src\text{-}AA}$ value for all particle size fractions at depths $>$ 400 m (Fig. 6). Alternatively, if midwater zooplankton altered their feeding in winter and summer on food resources with distinct $\delta^{15}N_{Src\text{-}AA}$ values, we might also observe a seasonal effect. Source $\delta^{15}N_{AA}$ values were significantly different for large ($>$ 53 μm) versus small (0.7–53 μm) particles in midwaters, with small particle $\delta^{15}N_{Src\text{-}AA}$ values approximately 3–4‰ greater than large particle $\delta^{15}N_{Src\text{-}AA}$ values in all seasons (Figs. 6, 8). We posit that the food web base of midwater zooplankton was primarily large particles with lower $\delta^{15}N_{Src\text{-}AA}$ values at depth in summer, when export from the euphotic zone was elevated (Church et al., 2013; Umhau et al., 2019) and this relatively labile 'pulse' material was transported rapidly to mesopelagic depths (Karl et al., 2012). In contrast, in winter, export of particulate material from the euphotic zone was lower, thus zooplankton deep in the mesopelagic and upper bathypelagic zone switched to include more small particles with higher $\delta^{15}N_{Src\text{-}AA}$ values in their food web base derived from deeper in the water column.

4.3.1. Zooplankton in the mid-mesopelagic zone

Our stable isotope-based mixing model indicates a nuanced seasonal response for zooplankton at 300–500 m. The food web base for many taxa and size fractions in the mid-mesopelagic zone appears to be deep large particles. That is, in both seasons large particles sinking from the euphotic zone appear to be generally available and utilized by most zooplankton. One exception was large day-collected zooplankton (1 mm size fraction), which had a strong 'fresh surface particle' contribution (57%) in winter. This is reasonable considering that zooplankton at 300–500 m include migrants that forage in the upper euphotic zone at night. In contrast, in summer the surface particle contribution for 1 mm day-collected zooplankton was small (13%). This finding is unexpected, given that large migrants foraging in the euphotic zone at night contributed significantly to midwater zooplankton biomass in all seasons. Moreover, day-night biomass differences indicate diel vertical migration of 1 mm zooplankton to 300–500 m in summer.

Given our observed vertical migration of large zooplankton into the mid-mesopelagic zone, why do we not observe a greater 'fresh surface particle' contribution to zooplankton food webs in summer? One explanation could be foraging depth in the euphotic zone. That is, migrant biomass at Sta. ALOHA was distributed more evenly throughout the upper 100 m at night in summer. In summer, 1 mm migrants also appear to feed directly beneath the euphotic zone at night, at 150–200 m. Large and small particle $\delta^{15}N_{Src\text{-}AA}$ values were somewhat higher at the

base of the euphotic zone, as compared to those found in the mixed layer (Fig. 6), with this difference being somewhat greater in winter, possibly due to increased remineralization (e.g., Hannides et al., 2013). Thus, one mechanism likely driving higher $\delta^{15}N_{Src\text{-}AA}$ values for mid-mesopelagic migrant zooplankton in summer was more evenly distributed foraging throughout the euphotic zone and even into the shallow upper mesopelagic zone during this season. We also consider migrant zooplankton consumption of deep large particles during the day in summer. For example, the summer pulse event drives significant large particle contributions to resident zooplankton food webs, and large migrant zooplankton could also benefit from the same resources. Numerous studies have shown empty gut contents and negligible migrator feeding below the euphotic zone during the day (Hayward, 1980; Longhurst et al., 1989). In addition, oxygen consumption rates are higher for vertical migrants at night (Ikeda et al., 2000), and the significant energy requirements of these large, muscular zooplankton are not likely to be met by deep large particle fields, even in summer. Thus our low 'fresh surface particle' contribution for large mid-mesopelagic migrators in summer appears to be driven by more evenly distributed nocturnal grazing through the euphotic zone and into the shallow upper mesopelagic zone. Migrant zooplankton feeding below the DCM in summer indicates that they could act as 'gatekeepers' for transfer of summer export pulse material into the mesopelagic zone *sensu* Jackson and Checkley (2011), although Umhau et al. (2019) also hypothesize that a significant portion of the summer export pulse material reaches midwater depths via direct sinking past these 'gatekeepers'.

We find limited support for a significant role of carnivory on vertical migrants in the mid-mesopelagic zone. Zooplankton migrating to feed in surface waters at night would have relatively low $\delta^{15}N_{Src\text{-}AA}$ values and high $f_{SURFACE}$, and the carnivorous zooplankton feeding on those migrants would have the same low $\delta^{15}N_{Src\text{-}AA}$ values and high $f_{SURFACE}$. However, as discussed above, the food web base for many taxa and size fractions in the mid-mesopelagic zone appears to be deep large particles rather than material from the surface ocean. Relatively high $f_{SURFACE}$ for 1 mm day-collected zooplankton in winter was likely due the vertical migrants themselves as discussed, rather than carnivores on migrants. Other size fractions and even zooplankton predators such as chaetognaths have high $\delta^{15}N_{Src\text{-}AA}$ values that indicate a low input from surface ocean basal resources. Thus, our results do not support a large contribution from migrant carnivores to the zooplankton community at Sta. ALOHA, although we caution that we did not perform CSIA-AA on the larger zooplankton size fractions (2 mm and 5 mm) that could have a significant carnivore contribution.

Another exception to the rule that deep large particles fuel zooplankton food webs at 300–500 m was found primarily for specific small zooplankton taxa, whose basal resources appear to be small particles. For example, cyclopoid copepods specialized on a small particle-based food web in both winter and summer. In winter cyclopoid copepod $\delta^{15}N_{Src\text{-}AA}$ values were higher than those for 'deep small particles', suggesting that their food webs in winter are based on a subset of the 'small particle' size fraction with even higher $\delta^{15}N_{Src\text{-}AA}$ values. Our 'small particles' are operationally defined by filter collection, and include a mixture of organic material with different sources and degradation states within a size range of 0.7–53 μm. We postulate that, in winter, cyclopoid copepods ultimately derive their N from a subset of organic material within this 'small particle' mixture. Another small taxon, oncaeid copepods, switch from a food web base dominated by large particles in summer to one comprised of more small particles in winter. Our smallest zooplankton size fraction, 0.06 mm, also had significant small particle contributions to their food web in winter. Thus, while most zooplankton at 300–500 m rely on basal resources dominated by large particles, the winter reduction in export flux apparently results in an increased small particle contribution to the food webs of select small taxa and, perhaps, juvenile zooplankton.

4.3.2. Zooplankton in the lower mesopelagic and upper bathypelagic zones

Small particles continued to contribute significantly to zooplankton food webs at depths deeper than 700 m, particularly in winter. In the lower mesopelagic zone the seasonal switch to a small particle-based food web was largest for residents, with small particles contributing up to 47% more to resident zooplankton food webs in winter as compared to summer. At greater depths, in the upper bathypelagic zone, the small particle contribution also increased by up to 43% in winter as compared to summer for 0.2 mm zooplankton, oncaeid copepods, and zooplanktivorous chaetognaths. These animals had $\delta^{15}N_{Src\text{-}AA}$ values higher than those found for our deep small particles, again suggesting that small zooplankton food webs in winter were based on a subset of the 'small particle' size fraction with very high $\delta^{15}N_{Src\text{-}AA}$ values. Thus although food webs for some large zooplankton (1 mm size fraction and ostracods) consistently included some large particles, the basal resources for many deep small resident zooplankton and zooplankton predators switched to small particles in winter.

In the lower mesopelagic and bathypelagic zones 'fresh surface material' was not an important basal resource for zooplankton. This indicates that both feeding on fresh surface-derived aggregates and carnivory on vertical migrants were not significant contributors to baseline zooplankton resources at these depths.

Seasonality in export flux not only impacts migrant zooplankton at 300–500 m, but also appears to drive migration for deep mesopelagic zooplankton. In winter, f_{small} was higher by 37–78% at night as compared to the day for both size fractions at 700–1000 m. Thus while small particles fuel a significant proportion of deep resident food webs in winter, our findings suggest some small and large zooplankton migrate into shallower mesopelagic depths at night to feed on the presumably greater abundance of large particles. This is not unreasonable given that McGowan and Walker (1979) found a group of NPSG zooplankton species that migrate between depths of 100–350 m at night to below 600 m (their deepest sampling depth) during the day. Our study suggest this 'deep migration' within the mesopelagic zone was present in winter, and resulted in lower $\delta^{15}N_{Src\text{-}AA}$ values for day-collected zooplankton as compared to those for deep mesopelagic residents in the same season. However in summer, we observed little diel change in f_{small} at 700–1000 m, indicating a reduction in this 'deep migration' with the advent of the summer export pulse and increase in availability of organic-rich material at depth.

The end result of our observed seasonal changes in NPSG zooplankton community function was a modest increase in midwater biomass in the spring and summer as compared to winter. Our findings indicate that the larger contribution of more labile large particle resources from the 'pulse' in summer spurred growth in zooplankton populations at depth, a mechanism similar to that previously observed for zooplankton in surface waters (Landry et al., 2001). When evaluated at each depth interval, the seasonal differences were only marginally significant, most likely a function of the relatively small number of replicate tows (n = 2–4) compared to the large variability in biomass we typically observe for net tow collections (standard deviations were 28–48% of mean biomass estimates, on average, for the different size fractions). Nonetheless, the results highlight the importance of small zooplankton size fractions in driving seasonal biomass changes both in surface waters and at depth. Specifically, 0.2–1 mm zooplankton contributed to the marginal summer increase in biomass at depths of 500–700 m at night and 700–1000 m during the day. The increased contribution of large particles to deep zooplankton food webs in summer thus appears to drive modest growth in small zooplankton populations in the lower mesopelagic zone and upper bathypelagic zone. To further evaluate seasonal change we suggest a time-series approach, evaluating midwater zooplankton biomass over multiple years.

4.4. Depths trends and seasonal constancy in zooplankton elemental composition

We observed seasonal change in midwater zooplankton biomass and stable isotope composition at Sta. ALOHA, but we did not find a corresponding seasonality in zooplankton elemental ratios. Zooplankton elemental composition did not change with season during our observations in the winter, spring, and summer. This indicates that the seasonal plasticity we observed in zooplankton trophic function does not impact overall community elemental compositions. Zooplankton communities in the NPSG are dominated by copepods in surface waters and at depth (Steinberg et al., 2008a), and correspondingly our average biomass-weighted zooplankton C:N molar ratios are within the range found by Mauchline (1998) for tropical and subtropical copepods. Moreover, constancy in zooplankton elemental composition at Sta. ALOHA is also likely maintained through stoichiometric homeostasis (Hessen et al., 2013). In other words, regardless of seasonal or depth changes in the stoichiometry of food resources, zooplankton will maintain homeostasis of body elemental content through post assimilative metabolism and nutrient release (e.g., Liu et al., 2006), or other mechanisms of elemental adjustment.

Despite seasonal constancy, when data from all seasons were combined we observed changes in elemental composition with depth. C:N ratios clearly increased with depth over the 1500 m water column during the day and night, while C:TPP and N:TPP ratios increased with depth during the day. The increase in zooplankton C content, but decrease in N and P content, with depth suggests a change either in community composition or biochemical composition, or both. With regards to community composition, Steinberg et al. (2008a) found zooplankton collected to depths of 1000 m at Sta. ALOHA to be dominated by copepods, consistent with our overall elemental composition reflecting this dominance. It is possible that other community members drive our observed depth changes. Higher crustacea such as euphausiids are relatively rich in P (Postel et al., 2000) as compared to chaetognaths and gelatinous zooplankton (Beers, 1966). However numbers of chaetognaths, siphonophores, and euphausiids are similar in surface and midwaters at Sta. ALOHA, especially during the day when changes in C:TPP ratios were observed (Steinberg et al., 2008a). Ostracods increase in abundance with depth (Steinberg et al., 2008a), and were also found to be important contributors to species composition in midwaters at Sta. ALOHA (Sommer et al., 2017), but it is unclear how this might impact elemental composition. Thus while work to date does not support a strong effect of community structure on midwater elemental ratios, we suggest further investigation of plankton abundance and especially of ostracods in this regard.

Changes in the biochemical composition of specific zooplankton assemblages could also play a major role. Båmstedt (1986), for example, highlighted the low protein content of deep sea copepods at low latitudes, and Ikeda et al. (2006b) also found that a decline in body musculature drove high C:N ratios for deep-sea copepods at high latitudes. Our observed increase in C:N ratios thus is likely influenced by a loss in proteinaceous structures with depth, perhaps due to 'predation-mediated selection' for less musculature in deep waters (Ikeda et al., 2006a). In the mid- to lower mesopelagic zone (300–700 m) C:N ratios were higher at night than during the day, a diel difference likely driven by the contribution of muscular migrators to day-collected zooplankton size fractions. Lipids can also contribute significantly to variation in the C:N ratio. Deep-sea zooplankton often have significant lipid stores, which serve as long-term energy deposits and help regulate buoyancy at depth (Lee et al., 2006). These storage lipids are often wax esters, simple esters of long-chain primary alcohols and long-chain fatty acids that are highly enriched in C. Lipid reserves likely contribute to the higher C:N and C:TPP ratios found for midwater zooplankton in our study. P content in several zooplankton size fractions decreased at depth (see Appendix C), with the differences most apparent for zooplankton in midwaters (300–700 m) versus zooplankton in the deep mesopelagic to upper bathypelagic zone (700–1500 m). The changes appear to be driven by depth trends in POP rather than PIP (Appendix C), indicating a relative loss of organic P compounds in deep waters. Ikeda et al. (2007) have shown that RNA:DNA ratios in copepods decrease with depth, likely due to the 'slower life modes' and lower protein synthetic activity of deep living zooplankton. A reduction in the contribution of organic P compounds such as RNA could thus drive the changes in P content and higher C:TPP ratios for many zooplankton size fractions in the deep sea.

4.5. The importance of small zooplankton taxa at Sta. ALOHA

The role of small zooplankton as drivers of change in the NPSG has been previously recognized through time-series work in the surface ocean. Seasonal change in euphotic zone biomass was found by Landry et al. (2001) primarily for < 2 mm size fractions collected during the day, that is, small zooplankton that do not migrate on a diel cycle. These same animals also drove a 9-y increase in zooplankton biomass at Sta. ALOHA (Sheridan and Landry, 2004), with both the seasonal and long-term changes linked to the effect of N_2 fixation on ecosystem productivity. Our work further highlights the role of small zooplankton in the mesopelagic and upper bathypelagic zones. Small size fractions, (< 0.2 mm) appear particularly responsive to seasonal export cycles and are able to access small particle resources in winter when sinking fluxes are low.

Our study also focused on small zooplankton taxa. We specifically targeted oncaeid, oithonid, and harpacticoid copepods in an attempt to understand the range of responses of these small animals to seasonal change in midwaters. Oncaeid and oithonid copepods may be the most abundant and most diverse zooplankton in the world's ocean (Gallienne and Robins, 2001; Sommer et al., 2017) and oncaeid copepods have been found to dominate small copepod communities in the deep sea (Böttger-Schnack, 1997, 1996; Yamaguchi et al., 2002). Oncaeid copepods are considered detritivores, although information in the literature indicates semi-parasitic feeding on soft-bodied animals such as chaetognaths (Metz, 1998) as well as feeding on surfaces such as appendicularian houses (Alldredge, 1972; Ohtsuka et al., 1993) or algal and detrital aggregates (Metz, 1998). Oithonid copepods, in contrast, are omnivorous ambush predators that detect food particles as they sink and exhibit a preference for larger cells and motile prey (Paffenhöfer and Mazzocchi, 2002; Wiggert et al., 2005). Coprophagy on sinking fecal pellets has also been recorded for oithonids (Gonzalez and Smetacek, 1994). In contrast harpacticoid copepods are clearly associated with 'pseudo-benthic' structures such as large phytoplankton aggregates in the pelagic realm. Our target in surface waters was the harpacticoid *Macrosetella gracilis*, which uses colonies of the diazotroph *Trichodesmium* spp. as a physical and nutritional substrate (O'Neil, 1998). In deeper waters we focused on *Aegisthus* spp., a common deep sea harpacticoid thought to have evolved from epibenthic-hyperbenthic ancestral stock (Conroy-Dalton and Huys, 1999).

Small zooplankton are tightly coupled to primary production in surface waters. The small target taxa we list above exhibited a $TP_{Tr\text{-}Src}$ of 2.1–2.5 at 0–50 m, which was generally similar to the $TP_{Tr\text{-}Src}$ found for the 0.2 mm zooplankton size fraction (2.3–2.4) at these depths and can be compared to an assumed $TP_{Tr\text{-}Src} \approx 1$ for fresh photosynthate. Moreover $\delta^{15}N_{Src\text{-}AA}$ values for small zooplankton in surface waters were low and similar to $\delta^{15}N_{Src\text{-}AA}$ values for small and large particles at 0–150 m. Thus oncaeids, oithonids, and harpacticoid copepods appear to have tight trophic links with phytoplankton resources in the euphotic zone, although these are likely accessed through different feeding modes. For example oncaeids ($TP_{Tr\text{-}Src}$ of 2.1) may feed on algal aggregates whereas oithonid copepods ($TP_{Tr\text{-}Src}$ of 2.2–2.3) likely ambush motile algal and protozoan cells. *M. gracilis* is a clear associate of the cyanobacteria *Trichodesmium* spp. (O'Neil, 1998), thus it is interesting that the $TP_{Tr\text{-}Src}$ for this species (2.5) indicates more omnivorous feeding. It may be that *M. gracilis* takes advantage of both

Trichodesmium spp. and the microplankton community that associates with *Trichodesmium* colonies (Sheridan et al., 2002).

In midwaters, our study indicates small zooplankton have a unique response to depth trends and seasonal changes. For the 0.2 mm size fraction, depth trends in $\delta^{15}N_{Src\text{-}AA}$ and $TP_{Tr\text{-}Src}$ were largely driven by similar trends in their food web base, i.e., large and small particles. However depth changes for small taxa were more varied. Oncaeid and oithonid copepods increased in $\delta^{15}N_{Src\text{-}AA}$ value by 5–7‰ and $TP_{Tr\text{-}Src}$ by 1.5–1.8. Remarkably for oithonids this change occurred between the surface and only 300–500 m, and they had the highest $\delta^{15}N_{Src\text{-}AA}$ values and TP in the mid-mesopelagic zone. At the same time the food web base for oithonids at 300–500 m appears to consist entirely of deep small particles in winter, and as we have discussed perhaps even a subfraction of the 0.7–53 μm deep small particle pool. One interpretation is that midwater oithonids access detrital small particle food webs through ambush predation on midwater protozoa. In other words, they access small particle resources through a deep pelagic microbial loop. At the same time they likely engage in coprophagy. In fact coprophagous particle recycling, zooplankton consumption, production, and re-consumption of fecal material derived from other zooplankton or higher trophic levels, may result in our observed high oithonid $TP_{Tr\text{-}Src}$. Coprophagy might also alter oithonid $\delta^{15}N_{Src\text{-}AA}$ values, however we have no CSIA-AA information on the relationship between zooplankton fecal matter and original food sources, making this difficult to evaluate. In contrast, oncaeid copepods were the dominant small zooplankton at 1000–1500 m and their $\delta^{15}N_{Src\text{-}AA}$ values and $TP_{Tr\text{-}Src}$ were among the highest found at this depth, particularly in winter. Oncaeids have been observed feeding on detritus such as the clogged inner filters of discarded appendicularian houses (Alldredge, 1972) where particles as small as 0.2 μm may be trapped (Flood, 2003). Thus oncaeids in the upper bathypelagic zone could indirectly access small particle food webs in winter through feeding on appendicularian houses and other detrital aggregates. However in summer, large particles, perhaps large algal aggregates sinking rapidly from surface waters, contributed more significantly to their diet. Semi-parasitic feeding by oncaeids, for example on chaetognaths (Metz, 1998), could also occur in the deep sea and contribute to the observed high TP for these small zooplankton. In complete contrast to the above, harpacticoid copepod stable isotope composition remained stable through the water column and their $\delta^{15}N_{Src\text{-}AA}$ values were the lowest for all studied taxa at 300–500 m. Little is known concerning *Aegisthus* spp. but these results and our modeling efforts indicate they are strongly associated with large, fresh particles sinking from the euphotic zone and use them as a nutritional substrate. This is reasonable considering the 'epibenthic' nature of harpacticoid copepod existence in the pelagic realm.

In summary, our findings for small zooplankton indicate that they have diverse feeding approaches to support their existence in the deep sea. While traditional deep-water pelagic microbial food chains likely exist, many zooplankton may acquire food resources through physical association with large particles, coprophagy, semi-parasitism, or other foraging strategies. Given their dominance (e.g., Böttger-Schnack, 1997; Sommer et al., 2017; Yamaguchi et al., 2002), oncaeid copepods appear particularly well adapted to life in the deep sea. Their ability to access a food web base comprised of small particles, but also include deep large particles as a basal resource when available, could contribute to their success in an environment characterized by scarcity. In contrast, other small zooplankton taxa appear more specialized in midwaters, for example harpacticoids feeding on large, surface-derived particles, or oithonids relying entirely on small particle basal resources at depth. These taxa were less common in the upper bathypelagic zone (based on the limited number of samples we examined) indicating the distinct foraging strategies they use may limit their abundance deep in the water column. Regardless, a large component of small zooplankton at depth (based on our size fraction analysis) appears able to switch between deep large and small particle-based food webs in response to seasonal variation in NPSG export conditions. Future work in the NPSG should continue to target small zooplankton in an effort to understand their role as drivers of change and energy conduits in the deep sea.

5. Conclusions

Our study indicates midwater zooplankton respond strongly to seasonal change in production and export in the NPSG. After the 'summer export pulse' typically observed in late July – early August, large particles contribute significantly to midwater zooplankton food webs. However in winter, when export is lower, zooplankton rely on a more diverse food web base. Large particles dominate food webs for most zooplankton in the mid-mesopelagic zone in winter, but deeper in the water column, below 500 m, basal resources supporting zooplankton food webs are comprised of more small particles, or even a subset of the small particle pool with very high $\delta^{15}N_{Src\text{-}AA}$ values. The switch to a small particle-dominated food web in winter is most prominent for small zooplankton, including oncaeid and oithonid copepods in the mid-mesopelagic zone, and the 0.2 mm zooplankton size fraction and oncaeid copepods in the lower mesopelagic and upper bathypelagic zones. Our modeling results indicate small zooplankton are in turn prey for chaetognaths in the upper bathypelagic zone, which also have basal resources dominated by small particles. Furthermore these small zooplankton residents are likely an important trophic link for other mesopelagic animals, such as those studied by Choy et al. (2015) and Gloeckler et al. (2017). The latter study identified several NPSG micronekton in the lower mesopelagic and upper bathypelagic zones with almost entirely small particle-dominated food webs. Given that the small oncaeid copepods we studied here dominate deep sea zooplankton communities, our observed 'small particle-small zooplankton' food web could form not only the trophic base for these NPSG micronekton, but may also be a globally important mechanism for energy flow from small particles to higher trophic levels in the deep sea.

Change in midwater zooplankton basal resources and migration patterns has important implications for midwater metabolism and the transfer of organic material to the deep sea. We suggest that small particles are a more important source of C fueling midwater communities than has been previously recognized. In particular, small particle C sources must be important in the lower mesopelagic zone where we demonstrate small particle-supported zooplankton food webs in winter and likely much of the year, and where Giering et al. (2014) find a C deficit (respiration $\gg$ C supply). Overall, our findings complement rapidly evolving lines of evidence that indicate small, slow-sinking particles contribute significantly to total C flux (Baker et al., 2017; Close et al., 2013; Durkin et al., 2015; Richardson and Jackson, 2007) and indicate this overlooked source of organic material drives midwater mesopelagic zooplankton production, possibly through a deep microbial loop (e.g., Mayor et al., 2014).

Carnivory is also thought to contribute to reconciliation of midwater C budgets. That is, carnivory on zooplankton migrants that ultimately derive their sustenance from the surface ocean is another C supply mechanism thought to drive a significant fraction of midwater zooplankton energy requirements (Steinberg et al., 2008b). Our biomass data and C:N ratios indicate a significant contribution of vertical migrants to zooplankton communities at 300–700 m. If these migrants were a significant food resource for carnivores at depth, we would expect a strong 'fresh surface' signal in the carnivore's stable isotope ratios. However our mixing models indicate food webs for most zooplankton at 300–500 m were sustained by deep large particles rather than 'fresh surface' material. Thus our results to date do not support a large role for carnivory on zooplankton migrants, but we stress that future studies should also focus on the larger zooplankton size fractions that could include more zooplanktivorous carnivores.

While our findings argue that zooplankton food webs are supported, at least in part, by small particles or zooplankton carnivory, these findings do not obviate the traditional viewpoint of tight trophic linkages between midwater zooplankton and large, sinking particles. As

we have shown, the majority of zooplankton production in mid-mesopelagic zone is supported by large particle-dominated food webs throughout the year. Deeper in the water column, in the lower mesopelagic and upper bathypelagic zones, large particles form 40 to 95% of the basal resources for most zooplankton in summer. Thus the 88–90% reduction in C flux between 150 and 4000 m noted by Karl et al. (2012) for the summer export pulse is driven at least in part by zooplankton trophic processing. Together our results and earlier work support the paradigm that zooplankton contribute to large particle flux attenuation in the NPSG, and likely also drive changes in organic composition and degradation state as has been found for other open ocean ecosystems (Abramson et al., 2010; Sheridan et al., 2002).

In summary, export-driven seasonal variation in the particle field at depth drives a switch in basal resources and particle size supporting midwater zooplankton food webs, and also modifies vertical migration patterns throughout the mesopelagic zone. We suggest that future work explore the quantitative implications of these changes for the passive and active transport of C to the deep sea, particularly given predicted climate-driven increases in ocean stratification and small phytoplankton dominance (Doney et al., 2012; Moran et al., 2010; Taylor et al., 2012). Based on our observed seasonal dynamics, midwater zooplankton will respond to potential associated climate-driven shifts in export flux size spectra, perhaps through an increasing importance of 'small particle-small zooplankton' trophic processing and a shift to small copepod-dominated mesopelagic food webs.

Acknowledgments

We sincerely thank the many people who helped support this work. Many thanks to Erica Goetze, Mike Landry, and Karen Selph, who helped provide equipment used on the cruises. We also thank members of Team MOCNESS, including C. Anela Choy, Astrid Leitner, Lauren Von Woudenberg, Whitney Ko, Tamara Allen, and Jan Reichelderfer, who helped with tows and processing. A big thank you to members of the UH Ocean Technology Group and Meghan Donohue, John Calderwood, and Josh Manger, who ensured smooth tows. Many thanks also to the captain and crew of the R/V Kilo Moana. This work was supported by National Science Foundation, United States (NSF) grants OCE-1333734 (to CCSH, JCD, HGC, and BNP), OCE-1433846 (to CCSH, BNP, and JCD) and OCE-1433313 (to CRBN). This is University of Hawaii School of Ocean and Earth Science and Technology contribution number 10903. There were no conflicts of interest associated with this study.

Disclosure

C.C.S.H., J.C.D., B.N.P. and H.G.C. designed the study. C.C.S.H., B.N.P., J.C.D., H.G.C, and K.G. collected samples and C.C.S.H., C.A.K.L, N.W., H.G.C., and E.P. processed samples in the laboratory. C.C.S.H. wrote the manuscript with J.C.D., B.N.P, C.R.B.N., H.G.C., and K.G., C.A.K.L., N.W. and B.U. commented on the manuscript.

Appendix A. Stable isotope replication and preservation for zooplankton

Variability in stable isotope composition for replicate samples was assessed through analysis of zooplankton taxa and size fractions. Within-taxa differences in bulk stable isotope composition were determined for 10 *P. xiphias* collected from 0 to 50 m. The average (± standard deviation [SD]) absolute difference in δ^{15}N values between replicates was 0.4 ± 0.4‰ in winter and 1.0 ± 0.7‰ in summer. In spring, within-tow variability was assessed through analysis of four 500–700 m net samples collected during one 'yo-yo' tow. Bulk δ^{15}N values across all size fractions in these replicate net samples differed by 0.4 ± 0.3‰, on average. Moreover the average difference in bulk δ^{15}N value at all depths in winter and summer for duplicate tows ranged from 0.4 to 0.8‰, across the different size fractions. These intra-cruise values are similar to the average within-cruise difference in bulk δ^{15}N value (0.4 ± 0.1‰) previously found by Hannides et al. (2009) for zooplankton in the euphotic zone at Station ALOHA. For CSIA, average differences in $\delta^{15}N_{AA}$ value for duplicate samples ranged from 0.5 (Phe) – 1.3‰ (Val) across all depths and size fractions. Differences in $\delta^{15}N_{Src\text{-}AA}$ and $TP_{Tr\text{-}Src}$ were 0.5‰ and 0.1, respectively. Overall, the replicate sample differences were much less than observed depth changes in δ^{15}N value, for example the increase in bulk biomass-weighted average zooplankton δ^{15}N value of 3.4–6.2‰ over 1500 m depth.

To evaluate the effect of formalin preservation on δ^{15}N values, stable isotope composition was determined for the large midwater copepod *Gaussia princeps* that had been frozen versus preserved in formalin for ~1 yr. *G. princeps* was collected at night on the winter cruise using a 10-m^2 MOCNESS equipped with five 3 mm mesh sampling nets. Cod end samples were sorted on ice, and the identified *G. princeps* either frozen immediately in liquid N_2 or individually preserved in 4.5% borate-buffered formalin. Stable isotope analysis was conducted on frozen and formalin-preserved specimens collected from 100 to 500 m. Bulk stable isotope analyses were conducted on the urosome from each individual, with each urosome dried at 60 °C, weighed using a microbalance, and packaged in tin capsules. The remaining biomass was used for CSIA, with each sample comprised of the prosomes of two individuals that were transferred to a combusted hydrolysis vial and lyophilized for 24 h. Both bulk stable isotope analysis and CSIA were conducted in a manner identical to that used for target zooplankton taxa (see *2. Materials and Methods*).

Bulk δ^{15}N values of individual *G. princeps* (n = 12) did not differ between the two treatments (formalin: 9.9 ± 0.8‰, frozen: 9.8 ± 1.0‰; Wilcoxon test, $p \gg 0.05$). Results for CSIA were similar. No significant difference between formalin-preserved and frozen samples was found for $\delta^{15}N_{Phe}$, $\delta^{15}N_{Src\text{-}AA}$, $TP_{Tr\text{-}Src}$ and $TP_{Glx\text{-}Phe}$ (Wilcoxon test, $p > 0.05$). In addition, although variability between treatments was found for $\delta^{15}N_{Glx}$ values (Wilcoxon, $W = 5.0$, df = 12, $p < 0.05$), the differences were small ($\Delta_{frozen\text{-}formalin}$ $\delta^{15}N_{Glx}$ = 0.8‰) and less than the observed environmental variation (i.e., $\Delta\,\delta^{15}N_{Glx}$ = 1.0‰). Our findings thus support those of Hannides et al. (2009) and Heatherington et al. (2019), who found negligible formalin preservation effects for bulk and compound-specific stable N isotope analysis of zooplankton taxa even for zooplankton taxa preserved in formalin for 24–25 years.

Appendix B. Bulk stable isotope analysis of NPSG midwater zooplankton

Bulk (whole animal) stable isotope analysis was conducted on zooplankton size fractions and target zooplankton taxa collected at Sta. ALOHA (see *2.1 Sample collection*). For bulk analysis of size fractions, zooplankton processing (see 2.2 *Sample processing*) involved all size fractions (0.2–5 mm) from all depths on each cruise, with ~0.5 mg of each sample packaged in tin capsules. For bulk analysis of target taxa, numbers of individuals analyzed ranged from 70 (oithonid and oncaeid copepods) – 1 (*P. xiphias*) or 1/2 animal (large chaetognaths), with each sample transferred into tin capsules, dried at 60 °C, weighed using a ultramicrobalance, and packaged for isotope analysis.

Bulk stable N and C isotope composition of zooplankton were determined using a Costech elemental combustion system (Model 4010) coupled to a Thermo-Finnigan Delta Plus XP isotope ratio mass spectrometer (IRMS) through a Conflo IV interface. Isotope values are reported in standard δ-notation relative to the atmospheric N_2 standard (AIR) as δ^{15}N (‰) = $[(^{15}N{:}^{14}N_{sample}/^{15}N{:}^{14}N_{AIR}) - 1] \times 1000$ or relative to Vienna Pee Dee Belemnite (VPDB) as δ^{13}C (‰) = $[(^{13}C{:}^{12}C_{sample}/^{13}C{:}^{12}C_{VPDB}) - 1] \times 1000$. To ensure accuracy, glycine and ground tuna reference samples with well-characterized δ^{15}N values were analyzed every 10 samples. The standard deviation on samples analyzed in duplicate was ≤0.2‰. Calculated

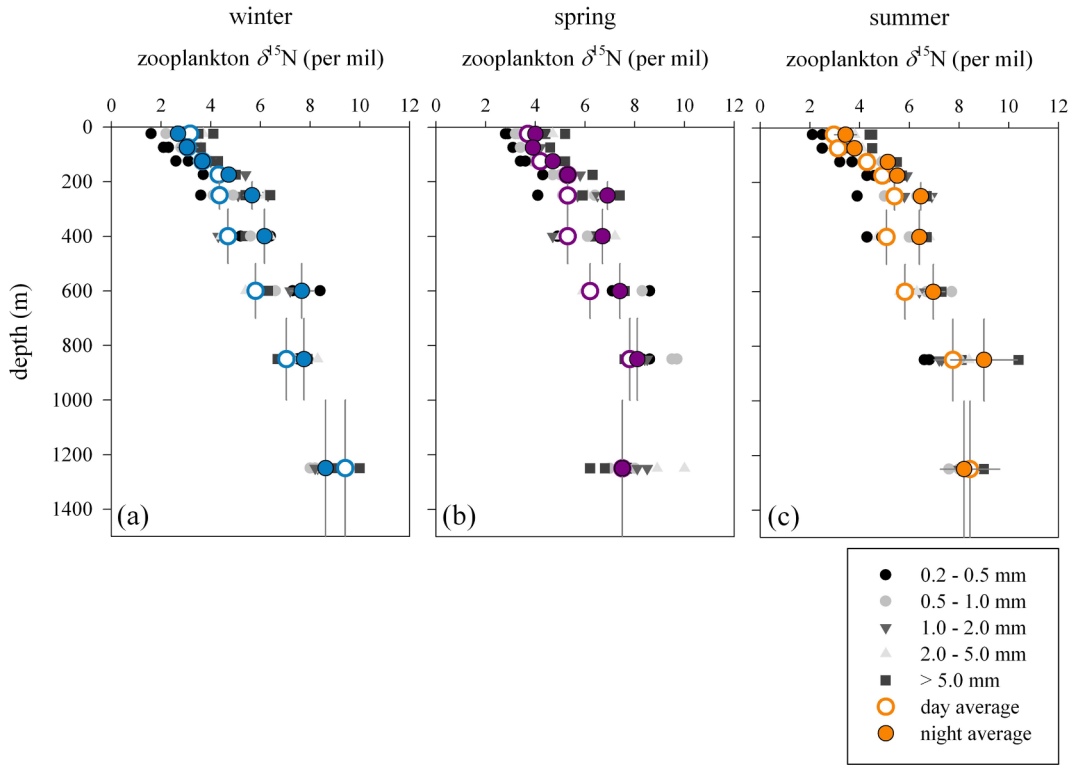

Fig. A.1. Bulk (whole animal) zooplankton δ^{15}N values at Sta. ALOHA during (a) winter (n = 2), (b) spring (n = 1), and (c) summer (n = 2). Bulk δ^{15}N values for the size fractions and biomass weighted averages are shown. Horizontal error bars are the standard deviation (SD) and vertical bars indicate the depth range over which the MOCNESS sampled.

parameters included 'biomass-weighted average δ^{15}N value', which refers to the average zooplankton bulk δ^{15}N value at each depth calculated by applying biomass weights (see *2.3 Biomass analysis*) to the δ^{15}N value of each size fraction.

Bulk stable N isotope analysis indicated that biomass-weighted average zooplankton δ^{15}N value for the whole euphotic zone (0–150 m) at Station ALOHA ranged from 3.0 to 4.1‰ over different seasons, with values for the different size fractions in the euphotic zone ranging from 2.0 to 5.0‰ (Fig. A.1). We compared euphotic zone δ^{15}N values measured for the 1 mm fraction in different seasons in this study (3.2–4.1‰) with those measured by Hannides et al. (2009) for the same size fraction collected from the upper 150 m at Station ALOHA from 1998 to 2005. In winter, zooplankton δ^{15}N values were significantly lower in 2014 as compared to 1998–2005 (Wilcoxon test, $W = 34$, df = 19, $p < 0.05$), while in summer zooplankton δ^{15}N values were not significantly different between the two time periods (Wilcoxon test, $p > 0.05$).

Zooplankton stable isotope composition changed with depth from surface waters through the upper bathypelagic zone. Across the different size fractions, zooplankton δ^{15}N values ranged from 1.6 to 5.2‰ in the 0–50 m depth interval vs. 6.2–10.0‰ in the upper bathypelagic zone, thus increasing by as much as 7.9‰ within a given size fraction over the upper 1500 m (Fig. A.1). For biomass-weighted average zooplankton δ^{15}N value, the increase over 1500 m was 5.9 (night) – 6.2‰ (day) in winter, 3.4 (night) – 3.8‰ (day) in spring, and 4.8 (night) – 5.5‰ (day) in summer (Fig. A.1). This depth increase was significant for all size fractions in all seasons (day: linear regression, $F_{1,10\text{-}16} = 11.4\text{–}724.4$, $p < 0.01$; night: linear regression, $F_{1,7\text{-}21} = 13.7\text{–}111.7$, $p < 0.01$), except for 5 mm zooplankton collected at night in spring (linear regression, $p > 0.05$).

We tested for seasonal variation in bulk δ^{15}N value by comparing depth profiles in winter and summer. Significant interactions between depth and season were found for 0.2 mm zooplankton during the day and night (ANCOVA, $F_{1,32\text{-}37} = 7.3\text{–}7.1$, $p < 0.05$), indicating a larger increase in bulk δ^{15}N value with depth in winter as compared to summer. Additionally, a significant seasonal difference in bulk δ^{15}N value was found for 0.5 mm zooplankton (summer > winter; ANCOVA, $F_{1,38} = 4.4$, $p < 0.05$). However, no seasonal differences were detected for other size fractions of zooplankton and for biomass-weighted average δ^{15}N values (ANCOVA, $p > 0.05$). Thus a seasonal effect on bulk δ^{15}N value was found only for the smallest zooplankton size fractions.

Trends in bulk stable N isotope composition for individual zooplankton taxa were similar to those found for zooplankton size fractions. Low δ^{15}N values were found in surface waters, ranging from 1.8‰ (oncaeid copepods) – 5.1‰ (chaetognaths) in winter and 1.4‰ (oncaeids) – 5.8‰ (large chaetognaths) in summer (Fig. A.2). Summer and winter δ^{15}N values were similar at each depth (Wilcoxon test, $p > 0.05$; except for *P. xiphias* at 0–50 m: summer > winter; Wilcoxon test, $W = 6.0$, df = 19, $p > 0.001$), thus we evaluated depth change in stable isotope composition across all seasons. For most taxa, a significant increase in bulk δ^{15}N value with depth was found (Fig. A.2; linear regression, $F_{1,6\text{-}13} = 7.4\text{–}959.7$, $p < 0.05$). The bulk δ^{15}N value of oncaeid copepods increased by up to 10.8‰ from 0 to 50 m to 1000–1500 m, while values for oithonid copepods increased by up to 8.6‰ between surface waters and 300–400 m. Large and small chaetognath δ^{15}N values increased by 5.3–9.2‰ between 0 and 50 m and the upper bathypelagic zone. A more modest, but still significant increase in δ^{15}N value (up to 3.3‰) was found for ostracods between surface waters and 1000–1500 m. The only zooplankton taxa that did not increase significantly in bulk δ^{15}N value with depth were harpacticoid copepods (linear regression, $p > 0.05$), which only differed by up to 1.1‰ between 0 and 50 m and 300–400 m or 1000–1500 m. Also, a few *P. xiphias* were found at 1000–1500 m in summer, and the δ^{15}N value of these individuals (6.3‰) was not significantly different from that for *P. xiphias* found in surface waters during the same season (5.9‰; Wilcoxon test, $p > 0.05$).

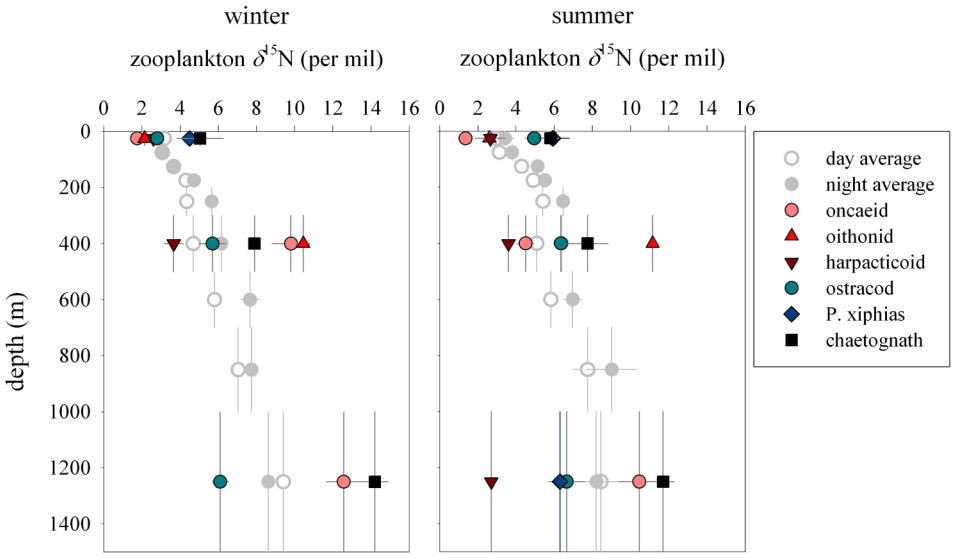

Fig. A.2. Bulk δ^{15}N values at Sta. ALOHA for target zooplankton taxa in the (a) winter (n = 1) and (b) summer (n = 1). Target taxa include oncaeid copepods, oithonid copepods, harpacticoid copepods, ostracods, the copepod *Pleuromamma xiphias*, and chaetognaths. Bulk δ^{15}N values for biomass weighted averages are included for comparison. Horizontal error bars are the SD and vertical bars indicate the depth range over which the MOCNESS sampled.

Appendix C. Zooplankton elemental content at Station ALOHA

Carbon (C), nitrogen (N), and phosphorus (P) content was determined for zooplankton size fractions collected at Sta. ALOHA (see *2.1 Sample collection*). Zooplankton size fractions (0.2–5 mm) were analyzed for C and N content using an EA-IRMS (see *2.4 Carbon, nitrogen and bulk stable isotope analysis*). Zooplankton size fractions (0.2–5 mm) were analyzed for P content using a modification of the Aspila phosphomolybdate method (see *2.5 Phosphorus analysis*).

Zooplankton C and N content was evaluated in the winter, spring, and summer at Sta. ALOHA. Over day and night and all depths and size fractions, biomass-weighted zooplankton C content averaged (± standard error of the mean (SEM)) 362.0 ± 2.8 mg C g dry wt^{-1} and zooplankton N content averaged 86.0 ± 0.9 mg N g dry wt^{-1}. Zooplankton C and N content did not change with season (when split by depth and size fraction: Kruskal-Wallis test, $p > 0.05$; except for one case: C content of 0.2 mm zooplankton during the day at 600 m, Kruskal-Wallis test, $\chi^2 = 6.5$, $p < 0.05$). However considerable variability was apparent when data from all seasons were combined (Table A.1). Biomass-weighted average zooplankton C content ranged from 339.0 to 388.1 mg C g dry wt^{-1} and biomass-weighted average N content ranged from 76.1 to 95.1 mg N g dry wt^{-1} (Fig. A.3).

For many depth intervals zooplankton C content and N content varied with size (Table A.1) and in all cases a significant interaction was present between size and depth (ANCOVA, $F_{4,230\text{-}239} = 3.5\text{–}31.5$, $p < 0.01$). That is, for many zooplankton size fractions depth drove increases in C content (Table A.1; day: 1–2 mm; night: 0.5–2 mm; linear regression, $F_{1,46\text{-}48} = 5.1\text{–}27.1$, $p < 0.05$) and decreases in N content (Table A.1; day: 0.2–0.5 mm; night: 0.2–2 mm; linear regression, $F_{1,46\text{-}48} = 9.2\text{–}51.6$, $p < 0.005$). Biomass-weighted averaged C content, and N content during the day, increased with depth to 500–700 m but then decreased with depth into the upper bathypelagic zone (Fig. A.3), thus no significant increase or decrease over the whole water column was observed for these parameters (linear regression, $p > 0.05$). However biomass-weighted average N content at night decreased significantly with depth (linear regression, $F_{1,25} = 27.4$, $p < 0.001$).

P content for zooplankton was evaluated in the winter and spring at Sta. ALOHA. Over day and night and all depths and size fractions, biomass-weighted zooplankton TPP content averaged (± SEM) 8.6 ± 0.2 mg P g dry wt^{-1}, PIP content averaged 4.7 ± 0.2 mg P g dry wt^{-1} and POP

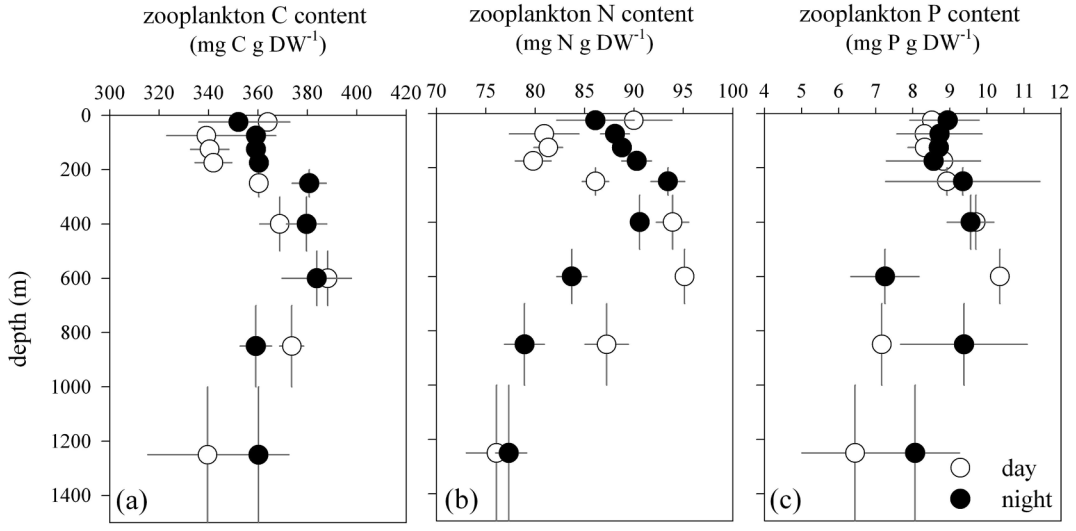

Fig. A.3. Biomass-weighted average zooplankton (a) carbon (C) content, (b) nitrogen (N) content, and (c) total particulate phosphorus (P) content. Horizontal bars are the standard error of the mean. Vertical bars indicate the depth range over which the MOCNESS sampled.

content averaged 4.0 ± 0.1 mg P g dry wt^{-1}, thus POP averaged 47 ± 1% of zooplankton TPP content. Zooplankton P content did not change with season (when split by depth and size fraction: Kruskal-Wallis test, $p > 0.05$). However significant variability in zooplankton P composition was observed when data from all seasons was pooled (Table A.2). Biomass-weighted average TPP content ranged from 6.4 to 10.4 mg P g dry wt^{-1}, PIP content ranged from 3.4 to 6.6 mg P g dry wt^{-1}, and POP content ranged from 2.9 to 4.8 mg P g dry wt^{-1} (Fig. A.3; Table A.2).

Differences in P content with size were rarely observed when evaluated at each depth interval (Table A.2). However depth drove significant change in P content for many size fractions. For example, in several cases depth drove significant decreases in TPP content (Table A.2; day: 0.5–2 mm; night: 2 mm; linear regression, $F_{1,20\text{-}23} = 8.8\text{–}18.5$, $p < 0.01$). When all size fractions were combined into biomass-weighted averages, modest changes with depth were found mostly for zooplankton collected during the day (Fig. A.3). That is, biomass-weighted average TPP content decreased significantly with depth during the day (linear regression, $F_{1,14} = 4.9$, $p < 0.05$) and POP content decreased significantly with depth during the day (linear regression, $F_{1,14} = 25.8$, $p < 0.001$). Interestingly, biomass-weighted average PIP content did not change with depth during the day or night (linear regression, $p > 0.05$), and for size fractions PIP content only increased (day: 0.2 mm; linear regression, $F_{1,16} = 6.4$, $p < 0.05$) or decreased (night: 2 mm; linear regression, $F_{1,23} = 6.3$, $p < 0.05$) significantly in two cases.

Appendix D. Zooplankton elemental composition at Station ALOHA: Tables

See Tables A.1 and A.2.

Table A.1
Zooplankton carbon (C) and nitrogen (N) content and zooplankton C:N molar ratios at Sta. ALOHA. C and N composition is given as the mean ± standard error of the mean for data pooled across the winter, spring, and summer seasons. Asterisks (*) after each size indicate a significant increase or decrease with depth (Linear regression, $p < 0.05$). Letters in superscript indicate significant differences in elemental composition with size (Kruskal-Wallis test, $p < 0.05$) within each depth interval.

Variable	Time	Depth (m)	0.2 mm	0.5 mm	1 mm*	2 mm*	5 mm	Wtd AVG
C (mg C g DW^{-1})	day	0–50	343.4 ± 14.8	376.1 ± 9.9	373.4 ± 9.8	347.2 ± 9.6	352.2 ± 11.3	363.9 ± 9.0
		50–100	329.0 ± 9.6	363.7 ± 18.6	349.1 ± 17.7	326.9 ± 17.3	311.1 ± 11.2	339.0 ± 16.1
		100–150	344.8 ± 14.5	344.8 ± 18.5	346.7 ± 11.5	319.8 ± 14.7	340.1 ± 5.2	340.4 ± 7.7
		150–200	370.5 ± 12.3	356.5 ± 14.1	329.5 ± 6.5	322.4 ± 4.7	324.9 ± 20.3	341.9 ± 7.4
		200–300	375.6 ± 6.3	385.8 ± 7.1	367.6 ± 20.0	328.3 ± 13.2	326.4 ± 25.8	360.3 ± 2.9
		300–500	393.4 ± 17.6	377.1 ± 12.4	386.8 ± 7.1	372.2 ± 14.8	337.9 ± 14.9	368.8 ± 8.1
		500–700	360.0 ± 19.0^{a}	411.5 ± 11.2^{b}	412.9 ± 7.6^{b}	390.3 ± 7.3^{ab}	365.4 ± 10.3^{ab}	388.1 ± 3.2
		700–1000	326.0 ± 26.6^{a}	400.5 ± 10.2^{b}	414.0 ± 2.8^{b}	386.6 ± 14.5^{ab}	361.9 ± 9.2^{ab}	373.6 ± 4.9
		1000–1500	312.8 ± 35.5	321.6 ± 25.3	407.8 ± 13.9	376.3 ± 22.7	322.6 ± 13.0	339.5 ± 24.2
	Time	**Depth (m)**	**0.2 mm**	**0.5 mm***	**1 mm***	**2 mm***	**5 mm**	**Wtd AVG**
	night	0–50	340.1 ± 5.5	365.4 ± 7.6	364.2 ± 8.2	356.7 ± 29.8	317.6 ± 10.5	352.0 ± 16.1
		50–100	354.3 ± 16.8	374.4 ± 4.3	366.0 ± 7.6	354.9 ± 6.3	337.9 ± 7.2	359.2 ± 8
		100–150	341.7 ± 12.8	367.7 ± 8.2	370.9 ± 9.1	369.3 ± 3.4	328.5 ± 17.0	359.2 ± 0.6
		150–200	350.1 ± 8.1	373.6 ± 9.5	381.0 ± 6.2	360.8 ± 9.5	338.5 ± 14.0	360.4 ± 1.4
		200–300	380.4 ± 6.9^{ab}	392.6 ± 6.0^{a}	406.8 ± 3.4^{a}	356.9 ± 11.6^{b}	359.7 ± 11.1^{b}	380.7 ± 6.9
		300–500	405.2 ± 10.4^{a}	400.0 ± 8.1^{a}	414.3 ± 4.9^{a}	369.1 ± 4.1^{b}	364.0 ± 5.0^{b}	379.7 ± 8.1
		500–700	386.7 ± 16.3	427.1 ± 7.8	423.8 ± 6.9	378.1 ± 12.2	364.4 ± 30.1	383.8 ± 14.1
		700–1000	318.0 ± 15.5^{a}	400.9 ± 14.0^{b}	417.1 ± 13.4^{b}	404.6 ± 7.7^{b}	323.8 ± 9.7^{a}	359.1 ± 6.4
		1000–1500	344.7 ± 20.6^{ab}	384.7 ± 16.5^{ab}	408.3 ± 19.2^{a}	392.1 ± 5.6^{a}	330.1 ± 11.5^{b}	360.2 ± 12.3
Variable	**Time**	**Depth (m)**	**0.2 mm***	**0.5 mm***	**1 mm**	**2 mm**	**5 mm**	**Wtd AVG**
N (mg N g DW^{-1})	day	0–50	77.9 ± 5.6	92.9 ± 4.5	95.6 ± 4.4	85.9 ± 4.2	83.3 ± 0.9	90.0 ± 3.8
		50–100	71.0 ± 4.3	88.3 ± 6.3	85.7 ± 5.0	79.9 ± 5.0	74.1 ± 2.9	80.9 ± 3.5
		100–150	76.2 ± 5.3	82.3 ± 5.4	83.4 ± 4.0	77.6 ± 4.3	82.4 ± 3.1	81.3 ± 1.5
		150–200	84.5 ± 3.4	82.3 ± 3.7	78.2 ± 1.7	74.2 ± 1.7	81.0 ± 5.6	79.8 ± 1.8
		200–300	87.2 ± 2.2	92.9 ± 2.2	88.4 ± 4.2	79.5 ± 3.5	80.6 ± 6.4	86.1 ± 1.3
		300–500	85.8 ± 4.5	90.8 ± 3.9	100.5 ± 2.4	98.1 ± 3.8	86.6 ± 4.4	93.9 ± 1.6
		500–700	56.9 ± 4.4^{a}	87.1 ± 2.2^{b}	100.9 ± 2.5^{c}	98.4 ± 1.7^{c}	92.5 ± 2.2^{bc}	95.1 ± 0.7
		700–1000	52.2 ± 11.2^{a}	77.3 ± 3.7^{b}	90.5 ± 2.1^{b}	83.6 ± 1.8^{b}	89.1 ± 3.2^{b}	87.2 ± 2.2
		1000–1500	48.0 ± 8.7^{a}	61.7 ± 3.3^{a}	83.9 ± 4.8^{b}	78.9 ± 3.5^{ab}	82.6 ± 3.0^{ab}	76.1 ± 3.1
	Time	**Depth (m)**	**0.2 mm***	**0.5 mm***	**1 mm***	**2 mm***	**5 mm**	**Wtd AVG***
	night	0–50	75.8 ± 2.4	88.9 ± 1.7	91.7 ± 2.6	87.4 ± 7.8	77.9 ± 2.9	86.1 ± 3.9
		50–100	79.4 ± 5.1	90.5 ± 1.2	91.1 ± 1.6	88.4 ± 1.7	84.9 ± 2.5	88.1 ± 1.5
		100–150	75.6 ± 4.4^{a}	88.1 ± 3.2^{ab}	91.3 ± 3.1^{ab}	95.4 ± 1.3^{b}	81.2 ± 3.6^{a}	88.8 ± 0.9
		150–200	77.3 ± 2.8^{a}	86.5 ± 3.1^{a}	95.9 ± 1.9^{b}	93.9 ± 3.1^{b}	88.9 ± 4.6^{ab}	90.3 ± 1.5
		200–300	85.0 ± 1.9^{a}	91.4 ± 1.8^{ab}	97.7 ± 1.3^{b}	92.5 ± 3.7^{ab}	93.6 ± 1.5^{ab}	93.4 ± 1.7
		300–500	82.7 ± 2.4^{a}	88.0 ± 2.9^{ab}	92.7 ± 1.3^{ab}	90.2 ± 1.5^{ab}	93.5 ± 1.1^{b}	90.6 ± 0.8
		500–700	55.9 ± 3.7^{a}	76.1 ± 1.6^{b}	83.9 ± 1.7^{b}	82.6 ± 2.7^{b}	90.2 ± 6.9^{b}	83.7 ± 1.5
		700–1000	39.9 ± 7.3^{a}	75.2 ± 4.2^{b}	86.7 ± 2.7^{b}	82.1 ± 2.1^{b}	81.8 ± 3.4^{b}	78.9 ± 2.0
		1000–1500	49.6 ± 7.8^{a}	71.2 ± 3.1^{b}	80.6 ± 1.8^{b}	81.7 ± 3.1^{b}	80.3 ± 3.7^{b}	77.3 ± 1.3
Variable	**Time**	**Depth (m)**	**0.2 mm***	**0.5 mm***	**1 mm***	**2 mm***	**5 mm**	**Wtd AVG***
C:N (mol:mol)	day	0–50	5.18 ± 0.20	4.74 ± 0.15	4.57 ± 0.10	4.73 ± 0.10	4.94 ± 0.21	4.75 ± 0.07
		50–100	5.43 ± 0.16	4.83 ± 0.11	4.76 ± 0.06	4.78 ± 0.09	4.91 ± 0.11	4.92 ± 0.03
		100–150	5.32 ± 0.16	4.91 ± 0.07	4.86 ± 0.09	4.83 ± 0.14	4.83 ± 0.11	4.90 ± 0.03
		150–200	5.12 ± 0.07^{a}	5.06 ± 0.05^{a}	4.92 ± 0.04^{ab}	5.08 ± 0.10^{a}	4.69 ± 0.09^{b}	5.01 ± 0.01

(continued on next page)

Table A.1 (*continued*)

Variable	Time	Depth (m)	0.2 mm	0.5 mm	1 mm*	2 mm*	5 mm	Wtd AVG
		200–300	5.03 ± 0.05	4.85 ± 0.03	4.84 ± 0.04	4.82 ± 0.11	4.73 ± 0.15	4.88 ± 0.05
		300–500	5.36 ± 0.09[a]	4.86 ± 0.06[b]	4.49 ± 0.05[c]	4.42 ± 0.03[c]	4.56 ± 0.05[c]	4.60 ± 0.04
		500–700	7.54 ± 0.34[a]	5.52 ± 0.11[b]	4.78 ± 0.08[c]	4.63 ± 0.04[c]	4.61 ± 0.06[c]	4.80 ± 0.02
		700–1000	8.14 ± 1.00[a]	6.08 ± 0.23[b]	5.35 ± 0.09[b]	5.40 ± 0.22[b]	4.75 ± 0.17[b]	5.12 ± 0.12
		1000–1500	8.10 ± 0.92[a]	6.07 ± 0.35[b]	5.72 ± 0.29[b]	5.55 ± 0.15[b]	4.56 ± 0.09[b]	5.36 ± 0.30
	Time	**Depth (m)**	**0.2 mm***	**0.5 mm***	**1 mm***	**2 mm***	**5 mm**	**Wtd AVG***
	night	0–50	5.25 ± 0.11[a]	4.79 ± 0.04[b]	4.64 ± 0.05[b]	4.77 ± 0.04[b]	4.76 ± 0.03[b]	4.78 ± 0.01
		50–100	5.23 ± 0.11[a]	4.83 ± 0.05[b]	4.69 ± 0.05[b]	4.68 ± 0.02[b]	4.65 ± 0.09[b]	4.77 ± 0.04
		100–150	5.30 ± 0.12[a]	4.88 ± 0.08[b]	4.74 ± 0.06[bc]	4.52 ± 0.03[c]	4.72 ± 0.09[bc]	4.74 ± 0.06
		150–200	5.30 ± 0.08[a]	5.05 ± 0.07[a]	4.64 ± 0.04[b]	4.49 ± 0.04[b]	4.45 ± 0.11[b]	4.68 ± 0.07
		200–300	5.22 ± 0.04[a]	5.02 ± 0.05[ab]	4.86 ± 0.07[b]	4.51 ± 0.11[c]	4.48 ± 0.10[c]	4.76 ± 0.01
		300–500	5.73 ± 0.12[a]	5.31 ± 0.08[b]	5.22 ± 0.07[b]	4.77 ± 0.04[c]	4.54 ± 0.07[c]	4.90 ± 0.07
		500–700	8.14 ± 0.26[a]	6.56 ± 0.12[b]	5.90 ± 0.17[bc]	5.36 ± 0.21[c]	4.70 ± 0.07[c]	5.45 ± 0.13
		700–1000	10.03 ± 1.05[a]	6.31 ± 0.42[b]	5.62 ± 0.13[b]	5.76 ± 0.15[b]	4.63 ± 0.08[b]	5.53 ± 0.25
		1000–1500	8.90 ± 1.08[a]	6.35 ± 0.35[b]	5.91 ± 0.28[b]	5.65 ± 0.27[b]	4.83 ± 0.20[b]	5.59 ± 0.27

Table A.2
Zooplankton total particulate phosphorus (TPP), particulate inorganic phosphorus (PIP) and particulate organic phosphorus (POP) content, and zooplankton C:TPP, N:TPP, C:POP, and N:POP molar ratios at Sta. ALOHA. P composition is given as the mean ± standard error of the mean for data pooled across winter and spring seasons. Asterisks (*) after each size indicate a significant increase or decrease with depth (Linear regression, $p < 0.05$). Letters in superscript indicate significant differences in elemental composition within each depth interval (Kruskal-Wallis test, $p < 0.05$). n.d. = no data.

Variable	Time	Depth (m)	0.2 mm	0.5 mm*	1 mm*	2 mm*	5 mm	Wtd AVG*
TPP	day	0–50	6.40 ± 0.73	8.02 ± 0.67	8.84 ± 0.58	10.39 ± 1.26	9.77 ± 1.20	8.51 ± 0.59
(mg P g DW^{-1})		50–100	6.26 ± 0.31	8.46 ± 0.50	9.10 ± 0.24	9.37 ± 1.14	8.75 ± 1.23	8.31 ± 0.39
		100–150	7.78 ± 0.59	8.71 ± 0.65	9.21 ± 1.03	8.71 ± 0.76	7.51 ± 1.16	8.32 ± 0.45
		150–200	8.32 ± 0.58	8.60 ± 0.96	9.59 ± 0.25	9.98 ± 1.05	8.13 ± 0.52	8.82 ± 0.28
		200–300	8.45 ± 0.71	9.25 ± 0.40	9.62 ± 0.61	9.72 ± 0.43	7.83 ± 1.82	8.92 ± 0.48
		300–500	7.47 ± 0.97	9.07 ± 0.94	9.95 ± 0.24	10.82 ± 0.34	9.82 ± 0.93	9.70 ± 0.28
		500–700	5.07 ± 0.33[a]	8.86 ± 0.64[b]	8.57 ± 0.86[b]	11.3 ± 0.43[b]	11.01 ± 0.76[b]	10.35 ± 0.25
		700–1000	n.d.	6.55	7.30 ± 0.35	8.02 ± 0.52	6.56 ± 1.97	7.16 ± 0.08
		1000–1500	n.d.	4.49 ± 0.93	6.74 ± 0.58	6.63 ± 0.76	6.94 ± 2.43	6.44 ± 1.43
	Time	**Depth (m)**	**0.2 mm**	**0.5 mm**	**1 mm**	**2 mm***	**5 mm**	**Wtd AVG**
	night	0–50	7.03 ± 0.48	9.10 ± 0.31	8.43 ± 1.33	10.38 ± 0.63	9.80 ± 0.63	8.94 ± 0.85
		50–100	7.90 ± 0.14	9.25 ± 0.26	8.01 ± 1.27	12.35 ± 0.96	8.06 ± 1.58	8.72 ± 1.15
		100–150	6.93 ± 0.47	8.71 ± 0.38	8.80 ± 0.35	10.17 ± 0.59	7.88 ± 1.34	8.70 ± 0.14
		150–200	5.23	5.99	10.00 ± 0.17	8.48 ± 1.33	7.05	8.56 ± 1.27
		200–300	8.91 ± 0.07	8.12 ± 0.64	11.59 ± 3.54	7.60 ± 0.72	10.06 ± 2.90	9.35 ± 2.08
		300–500	7.73 ± 0.33	9.50 ± 0.27	7.63 ± 1.42	9.66 ± 1.00	11.46 ± 0.69	9.56 ± 0.63
		500–700	5.16	7.36 ± 0.71	6.66 ± 0.06	6.64 ± 0.68	8.68 ± 1.45	7.25 ± 0.92
		700–1000	n.d.	7.78	7.76 ± 1.19	8.87 ± 0.37	12.28	9.38 ± 1.71
		1000–1500	n.d.	7.33	6.34 ± 0.55	7.00 ± 0.99	10.06 ± 2.93	8.06 ± 1.20
Variable	**Time**	**Depth (m)**	**0.2 mm***	**0.5 mm**	**1 mm**	**2 mm**	**5 mm**	**Wtd AVG**
PIP	day	0–50	2.91 ± 0.31	3.90 ± 0.27	4.62 ± 0.38	5.30 ± 0.85	3.62	4.18 ± 0.59
(mg P g DW^{-1})		50–100	2.96 ± 0.11	4.24 ± 0.29	4.70 ± 0.42	4.58 ± 0.51	4.77 ± 0.93	4.08 ± 0.49
		100–150	3.32 ± 0.35	4.01 ± 0.53	4.32 ± 0.59	4.11 ± 0.33	3.44 ± 0.03	3.80 ± 0.36
		150–200	3.83 ± 0.43	3.90 ± 0.54	4.28 ± 0.12	5.59 ± 0.98	2.91	4.09 ± 0.14
		200–300	4.13 ± 0.41	4.57 ± 0.27	4.71 ± 0.66	5.06 ± 0.38	3.83 ± 0.98	4.42 ± 0.35
		300–500	4.10 ± 0.74	4.97 ± 0.85	5.52 ± 0.09	6.40 ± 0.08	5.42 ± 0.63	5.44 ± 0.23
		500–700	n.d.	5.74 ± 0.28	5.28 ± 0.83	7.36 ± 0.42	6.79 ± 0.5	6.56 ± 0.13
		700–1000	n.d.	3.06	3.81 ± 0.03	4.13 ± 0.16	2.21	3.95 ± 0.04
		1000–1500	n.d.	n.d.	3.70 ± 0.29	3.88 ± 0.96	1.58	3.43 ± 1.25
	Time	**Depth (m)**	**0.2 mm**	**0.5 mm**	**1 mm**	**2 mm***	**5 mm**	**Wtd AVG**
	night	0–50	3.50 ± 0.62	4.90 ± 0.64	4.36 ± 1.09	5.79 ± 0.72	5.52 ± 0.51	4.84 ± 0.54
		50–100	4.41 ± 0.27	5.11 ± 0.64	4.48 ± 1.22	6.94 ± 0.49	4.48 ± 1.22	4.80 ± 0.83
		100–150	3.40 ± 0.53	4.50 ± 0.42	5.17 ± 0.39	6.28 ± 0.04	4.33 ± 1.05	5.00 ± 0.02
		150–200	2.51	3.34	7.32	3.13	3.83	3.98
		200–300	4.07	3.96 ± 0.61	6.79 ± 3.85	3.87 ± 0.80	5.49 ± 2.90	4.58 ± 1.87
		300–500	4.41 ± 0.12	4.85 ± 0.22	4.31 ± 0.82	6.34 ± 0.58	7.21 ± 0.14	6.03 ± 0.10
		500–700	2.95	3.81	3.81	4.63 ± 0.56	5.12 ± 0.84	4.77 ± 1.09
		700–1000	n.d.	n.d.	5.14 ± 1.06	4.73 ± 0.34	6.82	5.38 ± 0.97
		1000–1500	n.d.	n.d.	3.33 ± 1.06	3.60 ± 1.68	5.43	4.01 ± 0.04
Variable	**Time**	**Depth (m)**	**0.2 mm**	**0.5 mm**	**1 mm***	**2 mm***	**5 mm**	**Wtd AVG***
POP	day	0–50	3.49 ± 0.44	4.12 ± 0.40	4.22 ± 0.74	5.09 ± 0.44	4.25	4.28 ± 0.05
(mg P g DW^{-1})		50–100	3.30 ± 0.31	4.22 ± 0.22	4.40 ± 0.26	4.79 ± 0.77	3.99 ± 0.43	4.23 ± 0.10
		100–150	4.46 ± 0.27	4.70 ± 0.14	4.89 ± 0.45	4.60 ± 0.43	4.07 ± 1.13	4.52 ± 0.09

(*continued on next page*)

Table A.2 (*continued*)

Variable	Time	Depth (m)	0.2 mm	0.5 mm*	1 mm*	2 mm*	5 mm	Wtd AVG*
		150–200	4.49 ± 0.73	4.69 ± 0.43	5.31 ± 0.36	5.02 ± 0.21	4.7	4.79 ± 0.20
		200–300	4.32 ± 0.41	4.68 ± 0.20	4.91 ± 0.14	4.66 ± 0.43	4.00 ± 0.88	4.50 ± 0.13
		300–500	3.37 ± 0.41	4.10 ± 0.31	4.44 ± 0.33	4.42 ± 0.42	4.40 ± 0.37	4.26 ± 0.04
		500–700	n.d.	3.71 ± 0.10	3.29 ± 0.54	3.94 ± 0.76	4.22 ± 0.47	4.06 ± 0.56
		700–1000	n.d.	3.48	3.49 ± 0.34	3.88 ± 0.66	2.38	3.62 ± 0.46
		1000–1500	n.d.	5.43	2.69 ± 0.37	2.75 ± 0.63	2.94	3.12 ± 0.17
	Time	**Depth (m)**	**0.2 mm**	**0.5 mm**	**1 mm**	**2 mm**	**5 mm**	**Wtd AVG**
	night	0–50	3.53 ± 0.17	4.21 ± 0.63	4.07 ± 0.67	4.60 ± 0.11	4.28 ± 0.14	4.10 ± 0.31
		50–100	3.48 ± 0.41	4.13 ± 0.38	3.53 ± 0.40	5.41 ± 0.53	3.58 ± 0.36	3.93 ± 0.33
		100–150	3.53 ± 0.20	4.21 ± 0.03	3.63 ± 0.10	3.89 ± 0.62	3.55 ± 0.34	3.70 ± 0.12
		150–200	2.72	2.65	3.01	4.02	3.22	3.31
		200–300	4.91	4.16 ± 0.18	6.26 ± 0.70	3.73 ± 0.09	4.56 ± 0.01	4.47 ± 0.09
		300–500	3.55 ± 0.46	4.65 ± 0.15	3.33 ± 0.60	3.32 ± 0.45	4.24 ± 0.80	3.65 ± 0.64
		500–700	2.22	4.26	2.92	2.58 ± 0.02	3.56 ± 0.61	3.39 ± 0.74
		700–1000	n.d.	n.d.	3.44 ± 0.17	4.14 ± 0.04	5.46	4.43 ± 0.33
		1000–1500	n.d.	n.d.	3.02 ± 0.51	3.41 ± 0.80	1.71	2.88 ± 0.02
Variable	**Time**	**Depth (m)**	**0.2 mm***	**0.5 mm***	**1 mm***	**2 mm***	**5 mm**	**Wtd AVG***
C:TPP (mol:mol)	day	0–50	139.2 ± 14.5^{a}	124.2 ± 8.4^{ab}	114.1 ± 8^{ab}	89.4 ± 9.3^{b}	92.0 ± 9.4^{ab}	114.1 ± 3.2
		50–100	139.3 ± 5.1	114.6 ± 6.2	107.0 ± 3.7	97.1 ± 7.6	99.7 ± 14.2	113.1 ± 4.1
		100–150	123.5 ± 10.0	109.7 ± 5.9	97.2 ± 5.7	96.9 ± 5.8	115.7 ± 17.6	108.2 ± 1.4
		150–200	113.7 ± 5.1	105.4 ± 5.8	90.1 ± 1.5	86.3 ± 8.3	106.0 ± 16.2	101.5 ± 1.3
		200–300	117.6 ± 7.9	105.6 ± 5.4	96.3 ± 3.8	90.7 ± 4.3	117.4 ± 25.3	106.2 ± 3.7
		300–500	136.3 ± 11.7^{a}	111.2 ± 8.6^{ab}	101.7 ± 1.6^{ab}	87.2 ± 1.5^{b}	91.8 ± 9.5^{b}	100.7 ± 0.1
		500–700	207.1 ± 8.3^{a}	126 ± 7.9^{b}	125.8 ± 7.5^{b}	90.8 ± 3.8^{c}	82.6 ± 3.3^{c}	101.8 ± 0.6
		700–1000	n.d.	160.6	146.7 ± 6.2	121.4 ± 10.2	150.6 ± 48.8	142.1 ± 3.5
		1000–1500	n.d.	172.4 ± 2.5	152.3 ± 6.6	146.4 ± 4.8	122.1 ± 35.0	140.2 ± 14.4
	Time	**Depth (m)**	**0.2 mm***	**0.5 mm***	**1 mm***	**2 mm***	**5 mm**	**Wtd AVG**
	night	0–50	127.2 ± 7.8	106.6 ± 6.4	121.2 ± 19.4	98.7 ± 12.2	85.7 ± 2.2	107.7 ± 4.7
		50–100	124.2 ± 1.3	106.2 ± 4.4	124.1 ± 18.4	76.5 ± 4.6	118.5 ± 19.5	114.8 ± 13.1
		100–150	129.2 ± 5.6	109.2 ± 1.8	108.6 ± 2.6	93.1 ± 5.4	114.1 ± 17.7	109.0 ± 1.7
		150–200	174.1	168.1	96.8 ± 1.9	108.1 ± 21.7	124.5	112.0 ± 19.6
		200–300	111.6 ± 6.0	127.9 ± 13.5	105.2 ± 24.3	94.0 ± 32.1	108.0 ± 37.3	114.7 ± 26.1
		300–500	137.1 ± 9.3^{ab}	113.2 ± 3.8^{ab}	152.0 ± 29.7^{a}	99.7 ± 11.4^{ab}	80.7 ± 3.6^{b}	107.9 ± 5.4
		500–700	201	151.5 ± 16.4	160.9 ± 7.5	148.1 ± 13.9	117.9 ± 12.4	141.2 ± 5.9
		700–1000	n.d.	142.6	141.6 ± 26.2	116.6 ± 7.7	70.2	113.2 ± 29.9
		1000–1500	n.d.	153.8	174.4 ± 4.1	148.5 ± 16.5	82.6 ± 18.0	122.4 ± 1.8
Variable	**Time**	**Depth (m)**	**0.2 mm***	**0.5 mm***	**1 mm***	**2 mm***	**5 mm**	**Wtd AVG***
N:TPP (mol:mol)	day	0–50	26.0 ± 2.0	25.9 ± 0.7	25.5 ± 1.7	19.2 ± 1.7	19.2 ± 2.2	24.1 ± 0.4
		50–100	25.7 ± 1.1	24.0 ± 1.2	22.8 ± 1.2	20.3 ± 1.3	20.5 ± 2.4	23.2 ± 1.3
		100–150	24.4 ± 1.9	22.8 ± 1.0	19.6 ± 1.0	19.4 ± 0.9	23.2 ± 2.9	22.0 ± 0.4
		150–200	22.6 ± 1.4	20.8 ± 0.9	18.1 ± 0.4	16.9 ± 1.2	22.2 ± 3.0	20.3 ± 0.2
		200–300	23.5 ± 1.5	21.7 ± 1.2	19.9 ± 0.8	18.2 ± 0.8	23.9 ± 4.1	21.5 ± 0.6
		300–500	25.8 ± 1.8	23.3 ± 1.7	22.8 ± 0.04	19.8 ± 0.2	20.2 ± 2.0	22.0 ± 0.2
		500–700	32.2 ± 0.4^{a}	23.6 ± 1.8^{b}	25.9 ± 1.8^{ab}	19.7 ± 0.8^{bc}	17.9 ± 0.7^{c}	21.2 ± 0.0
		700–1000	n.d.	27.3	27.6 ± 1.7	23.1 ± 0.7	31.7 ± 10.5	27.0 ± 1.6
		1000–1500	n.d.	31.5 ± 1.7	27.2 ± 1.5	27.2 ± 1.4	27.7 ± 7.7	28.4 ± 4.6
	Time	**Depth (m)**	**0.2 mm**	**0.5 mm**	**1 mm**	**2 mm**	**5 mm**	**Wtd AVG**
	night	0–50	24.0 ± 1.2	22.3 ± 1.4	26.1 ± 4.4	20.9 ± 2.7	17.9 ± 0.5	22.6 ± 1.1
		50–100	24.5 ± 0.2	21.6 ± 0.9	26.3 ± 4.2	16.4 ± 1.1	25.6 ± 4.3	24.2 ± 3.2
		100–150	24.6 ± 1.1	22.0 ± 0.9	22.9 ± 0.6	20.6 ± 1.1	24.7 ± 3.8	23.1 ± 0.8
		150–200	33.6	35.0	20.9 ± 0.5	24.0 ± 5.3	28.3	24.4 ± 4.4
		200–300	21.3 ± 1.1	25.4 ± 3.0	22.2 ± 5.4	21.0 ± 7.3	23.2 ± 7.0	24.0 ± 5.7
		300–500	24.3 ± 0.9	21.7 ± 0.7	29.4 ± 6.6	20.7 ± 2.4	18.3 ± 0.8	22.0 ± 1.6
		500–700	27	23.4 ± 2.2	26.3 ± 0.6	28.2 ± 2.6	24.6 ± 3.0	26.5 ± 2.2
		700–1000	n.d.	25.2	26.1 ± 5.2	20.7 ± 1.6	14.9	21.0 ± 4.6
		1000–1500	n.d.	23.2	29.5 ± 3.4	27.7 ± 4.2	16.9 ± 5.7	23.1 ± 1.8
Variable	**Time**	**Depth (m)**	**0.2 mm**	**0.5 mm**	**1 mm***	**2 mm***	**5 mm**	**Wtd AVG***
C:POP (mol:mol)	day	0–50	257.1 ± 30.7	243 ± 20.0	256.7 ± 56.1	179.8 ± 10.2	202.2	231.0 ± 16.6
		50–100	266.4 ± 17.5	229.5 ± 11.6	222.0 ± 10.5	193.2 ± 22.4	216.3 ± 28.4	222.3 ± 7.8
		100–150	214.3 ± 13.9	201.5 ± 1.4	182.1 ± 7.1	183.8 ± 12	225.6 ± 62.0	199.7 ± 5.4
		150–200	220.7 ± 37.0	191.9 ± 8.3	163.8 ± 8.6	171.0 ± 9.5	197.9	192.2 ± 6.4
		200–300	231.1 ± 19.9	209.0 ± 11.5	188.0 ± 7.4	191.1 ± 13.9	232.7 ± 58.6	210.0 ± 0.2
		300–500	301.1 ± 26.8	246.1 ± 26.4	230.2 ± 14.3	216.0 ± 13.7	203.6 ± 15.1	228.0 ± 7.5
		500–700	n.d.	304.1 ± 13.2	340.2 ± 55.5	279.0 ± 51.4	220.1 ± 26.2	262.5 ± 41.0
		700–1000	n.d.	301.9	310.3 ± 26.3	262.7 ± 43.5	384.3	289.1 ± 36.5
		1000–1500	n.d.	175	370.2 ± 33.7	406.5 ± 133.1	241.3	337.0 ± 72.4
	Time	**Depth (m)**	**0.2 mm***	**0.5 mm**	**1 mm***	**2 mm***	**5 mm***	**Wtd AVG***

(*continued on next page*)

Table A.2 (*continued*)

Variable	Time	Depth (m)	0.2 mm	0.5 mm*	1 mm*	2 mm*	5 mm	Wtd AVG*
	night	0–50	253.0 ± 18.8	238.8 ± 30.4	249.9 ± 35.0	222.5 ± 27.6	195.7 ± 6.5	231.8 ± 3.3
		50–100	288.0 ± 27.2	238.8 ± 18.8	274.5 ± 28.7	175.9 ± 14.7	253.8 ± 21.5	249.7 ± 11.2
		100–150	255.2 ± 23.8	226.2 ± 15.4	263.2 ± 9.3	255.3 ± 42.6	244.5 ± 27.0	253.2 ± 2.6
		150–200	334.6	379.5	327.7	230.9	272.3	287.6
		200–300	193.1	246.1 ± 9.3	170.5 ± 16.2	217.6 ± 34.2	214.4 ± 13.9	219.3 ± 5.7
		300–500	290.9 ± 21.8	231.4 ± 6.8	347.5 ± 66.6	294.3 ± 42.8	230.7 ± 37.5	281.7 ± 42.5
		500–700	468.2	255.8	389.1	377.1 ± 4.1	289.3 ± 34.6	307.3 ± 50.4
		700–1000	n.d.	n.d.	294.3 ± 34.2	248.3 ± 8.5	157.8	227.0 ± 29.6
		1000–1500	n.d.	n.d.	381.0 ± 87.9	337.2 ± 92.8	421.1	365.8 ± 24.6
Variable	**Time**	**Depth (m)**	**0.2 mm**	**0.5 mm**	**1 mm***	**2 mm***	**5 mm**	**Wtd AVG***
N:POP (mol:mol)	day	0–50	48.0 ± 4.0	50.7 ± 2.1	57.5 ± 12.6	38.6 ± 1.6	42.1	49.0 ± 4.1
		50–100	49.0 ± 1.9	48.0 ± 2.3	47.3 ± 2.0	40.2 ± 3.7	44.5 ± 4.4	45.6 ± 0.7
		100–150	42.3 ± 2.7	41.9 ± 0.2	36.8 ± 1.1	36.7 ± 2.0	45.0 ± 11.1	40.5 ± 0.8
		150–200	44.1 ± 8.2	38.0 ± 1.4	33.0 ± 1.9	33.7 ± 0.2	40.8	38.6 ± 1.6
		200–300	46.3 ± 4.1	42.9 ± 2.6	38.8 ± 1.5	38.2 ± 2.5	47.2 ± 9.7	42.6 ± 0.2
		300–500	57.0 ± 3.9	51.7 ± 5.9	51.6 ± 2.7	49.1 ± 3.2	44.9 ± 3.4	49.8 ± 1.1
		500–700	n.d.	56.0 ± 2.9	70.5 ± 12.7	60.6 ± 11.2	47.8 ± 5.7	55.9 ± 8.0
		700–1000	n.d.	51.2	58.3 ± 5.4	49.5 ± 5.9	81.4	53.3 ± 3.5
		1000–1500	n.d.	29.8	68.2 ± 0.3	74.4 ± 22.5	54.4	64.8 ± 8.3
	Time	**Depth (m)**	**0.2 mm**	**0.5 mm**	**1 mm**	**2 mm**	**5 mm***	**Wtd AVG**
	night	0–50	48.1 ± 5.2	50.1 ± 7	53.9 ± 8.0	47.1 ± 6.2	41.0 ± 1.8	48.7 ± 0.9
		50–100	57.0 ± 5.9	48.7 ± 3.8	58.0 ± 6.4	37.6 ± 3.4	54.8 ± 4.5	52.5 ± 3.1
		100–150	48.9 ± 5.7	45.6 ± 4.2	55.6 ± 3.0	56.3 ± 9.0	52.9 ± 5.7	53.9 ± 1.5
		150–200	64.7	79.0	70.9	52.3	61.8	62.8 ± 0.0
		200–300	37.0	48.8 ± 2.1	36.2 ± 4.3	48.6 ± 6.9	46.6 ± 0.7	46.6 ± 0.9
		300–500	53.4 ± 3.7	44.4 ± 0.7	67.3 ± 14.8	61.0 ± 9.1	52.3 ± 8.4	58.6 ± 9.8
		500–700	62.9	40.3	63	74.4 ± 2.8	60.4 ± 8.2	62.1 ± 9.5
		700–1000	n.d.	n.d.	53.1 ± 6.5	44.1 ± 2.2	33.5	41.5 ± 2.8
		1000–1500	n.d.	n.d.	63.0 ± 8.9	61.5 ± 15.0	94.4	70.8 ± 1.8

References

Abramson, L., Lee, C., Liu, Z., Wakeham, S.G., Szlosek, J., 2010. Exchange between suspended and sinking particles in the northwest Mediterranean as inferred from the organic composition of in situ pump and sediment trap samples. Limnol. Oceanogr. 55, 725–739. https://doi.org/10.4319/lo.2009.55.2.0725.

Alldredge, A.L., 1972. Abandoned larvacean houses: a unique food source in the pelagic environment. Science 177, 885–887.

Alonso-Gonzalez, I.J., Aristegui, J., Lee, C., Sanchez-Vidal, A., Calafat, A., Fabres, J., Sangra, P., Masque, P., Hernandez-Guerra, A., Benitez-Barrios, V., 2010. Role of slowly settling particles in the ocean carbon cycle. Geophys. Res. Lett. 37, L13608. https://doi.org/10.1029/2010GL043827. doi: 10.1029/2010GL043827.

Ambler, J.W., Miller, C.B., 1987. Vertical habitat-partitioning by copepodites and adults of subtropical oceanic copepods. Mar. Biol. 94, 561–577.

Aspila, K., Agemian, H., Chau, A., 1976. A semi-automated method for the determination of inorganic, organic and total phosphate in sediments. Analyst 101, 187–197.

Baker, C.A., Henson, S.A., Cavan, E.L., Giering, S.L.C., Yool, A., Gehlen, M., Belcher, A., Riley, J.S., Smith, H.E.K., Sanders, R., 2017. Slow-sinking particulate organic carbon in the Atlantic Ocean: Magnitude, flux, and potential controls. Glob. Biogeochem. Cycles 31, 1051–1065. https://doi.org/10.1002/2017GB005638.

Baltar, F., Aristegui, J., Gasol, J.M., Sintes, E., Herndl, G.J., 2009. Evidence of prokaryotic metabolism on suspended particulate organic matter in the dark waters of the subtropical North Atlantic. Limnol. Oceanogr. 54, 182–193. https://doi.org/10.4319/lo.2009.54.1.0182.

Båmstedt, U., 1986. Chemical composition and energy content. In: The Biological Chemistry of Marine Copepods. Clarendon Press, Oxford, pp. 1–58.

Beers, J.R., 1966. Studies on the chemical composition of the major zooplankton groups in the Sargasso Sea off Bermuda. Limnol. Oceanogr. 11, 520–528.

Benitez-Nelson, C., Buesseler, K.O., Karl, D.M., Andrews, J., 2001. A time-series study of particulate matter export in the North Pacific Subtropical Gyre based on 234Th:238U disequilibrium. Deep-Sea Res. I 48, 2595–2611.

Benitez-Nelson, C.R., Madden, L.P.O., Styles, R.M., Thunell, R.C., Astor, Y., 2007. Inorganic and organic sinking particulate phosphorus fluxes across the oxic/anoxic water column of Cariaco Basin, Venezuela. Mar. Chem. 105, 90–100. https://doi.org/10.1016/j.marchem.2007.01.007.

Bishop, J.L.K.B., Lam, P.J., Wood, T.J., 2012. Getting good particles: Accurate sampling of particles by large volume in-situ filtration. Limnol. Oceanogr. Methods 10, 681–710. https://doi.org/10.4319/lom.2012.10.681.

Böttger-Schnack, R., 1997. Vertical structure of small metazoan plankton, especially non-calanoid copepods. II. Deep Eastern Mediterranean (Levantine sea). Oceanol. Acta 20, 399–419.

Böttger-Schnack, R., 1996. Vertical structure of small metazoan plankton, especially non-calanoid copepods. I. Deep Arabian Sea. J. Plankton Res. 18, 1073–1101. https://doi.org/10.1093/plankt/18.7.1073.

Bradley, C.J., Madigan, D.J., Block, B.A., Popp, B.N., 2014. Amino acid isotope incorporation and enrichment factors in Pacific bluefin tuna, *Thunnus orientalis*. Plos One 9, e85818. https://doi.org/10.1371/journal.pone.0085818.

Bradley, C.J., Wallsgrove, N.J., Choy, C.A., Drazen, J.C., Hetherington, E.D., Hoen, D.K., Popp, B.N., 2015. Trophic position estimates of marine teleosts using amino acid compound specific isotopic analysis. Limnol. Oceanogr.-Methods 13, 476–493. https://doi.org/10.1002/lom3.10041.

Brodeur, R.D., Yamamura, O., 2005. Micronekton of the North Pacific (PICES Scientific Report No. 30). North Pacific Marine Science Organization (PICES), Canada.

Buesseler, K.O., Boyd, P.W., 2009. Shedding light on processes that control particle export and flux attenuation in the twilight zone of the open ocean. Limnol. Oceanogr. 54, 1210–1232. https://doi.org/10.4319/lo.2009.54.4.1210.

Buesseler, K.O., Lamborg, C.H., Boyd, P.W., Lam, P.J., Trull, T.W., Bidigare, R.R., Bishop, J.K.B., Casciotti, K.L., Dehairs, F., Elskens, M., Honda, M., Karl, D.M., Siegel, D.A., Silver, M.W., Steinberg, D.K., Valdes, J., Van Mooy, B., Wilson, S., 2007. Revisiting carbon flux through the ocean's twilight zone. Science 316, 567–570.

Calbet, A., Landry, M.R., 1999. Mesozooplankton influences on the microbial food web: direct and indirect trophic interactions in the oligotrophic open ocean. Limnol. Oceanogr. 44, 1370–1380.

Casciotti, K.L., Trull, T.W., Glover, D.M., Davies, D., 2008. Constraints on nitrogen cycling at the subtropical North Pacific Station ALOHA from isotopic measurements of nitrate and particulate nitrogen. Deep-Sea Res. Part Ii-Top. Stud. Oceanogr. 55, 1661–1672. https://doi.org/10.1016/j.dsr2.2008.04.017.

Checkley, D.M., Miller, C.A., 1989. Nitrogen isotope fractionation by oceanic zooplankton. Deep-Sea Res. I 36, 1449–1456.

Chikaraishi, Y., Ogawa, N.O., Kashiyama, Y., Takano, Y., Suga, H., Tomitani, A., Miyashita, H., Kitazato, H., Ohkouchi, N., 2009. Determination of aquatic food-web structure based on compound-specific nitrogen isotopic composition of amino acids. Limnol. Oceanogr. Methods 7, 740–750.

Chikaraishi, Y., Ogawa, N.O., Ohkouchi, Naohiko, 2010. Further evaluation of the trophic level estimation based on nitrogen isotopic composition of amino acids. In: Ohkouchi, N., Tayasu, I., Koba, K. (Eds.), Earth, Life and Isotopes. Kyoto University Press, pp. 37–51.

Choy, C.A., Davison, P.C., Drazen, J.C., Flynn, A., Gier, E.J., Hoffman, J.C., McClain-Counts, J.P., Miller, T.W., Popp, B.N., Ross, S.W., Sutton, T.T., 2012. Global trophic position comparison of two dominant mesopelagic fish families (Myctophidae, Stomiidae) using amino acid nitrogen isotopic analyses. PLoS ONE 7. https://doi.org/10.1371/journal.pone.0050133.

Choy, C.A., Popp, B.N., Hannides, C.C.S., Drazen, J.C., 2015. Trophic structure and food resources of epipelagic and mesopelagic fishes in the North Pacific Subtropical Gyre ecosystem inferred from nitrogen isotopic compositions. Limnol. Oceanogr. 60,

1156–1171. https://doi.org/10.1002/lno.10085.
Christian, J.R., Lewis, M.R., Karl, D.M., 1997. Vertical fluxes of carbon, nitrogen and phosphorus in the North Pacific Subtropical Gyre near Hawaii. J. Geophys. Res. 102, 15667–15677.
Church, M.J., Lomas, M.W., Muller-Karger, F., 2013. Sea change: Charting the course for biogeochemical ocean time-series research in a new millennium. Deep-Sea Res. Part II-Top. Stud. Oceanogr. 93, 2–15. https://doi.org/10.1016/j.dsr2.2013.01.035.
Church, M.J., Mahaffey, C., Letelier, R.M., Lukas, R., Zehr, J.P., Karl, D.M., 2009. Physical forcing of nitrogen fixation and diazotroph community structure in the North Pacific subtropical gyre. Glob. Biogeochem. Cycles 23. https://doi.org/10.1029/2008GB003418.
Clarke, T.A., 1978. Diel feeding patterns of 16 species of mesopelagic fishes from Hawaiian waters. Fish. Bull. 76, 495–513.
Close, H.G., Hannides, C.C.S., Drazen, J.C., Popp, B.N., 2015. Degradative transformations of stable isotope ratios in sinking and suspended organic matte, from surface to upper bathypelagic depths, Station ALOHA. Presented at the Aquatic Sciences Meeting, Grenada, Spain.
Close, H.G., Shah, S.R., Ingalls, A.E., Diefendorf, A.F., Brodie, E.L., Hansman, R.L., Freeman, K.H., Aluwihare, L.I., Pearson, A., 2013. Export of submicron particulate organic matter to mesopelagic depth in an oligotrophic gyre. Proc. Natl. Acad. Sci. USA 110, 12565–12570. https://doi.org/10.1073/pnas.1217514110.
Conroy-Dalton, S., Huys, R., 1999. New genus of Aegisthidae (Copepoda : Harpacticoida) from hydrothermal vents on the Galapagos Rift. J. Crustac. Biol. 19, 408–431. https://doi.org/10.2307/1549248.
Doney, S.C., Ruckelshaus, M., Duffy, J.E., Barry, J.P., Chan, F., English, C.A., Galindo, H.M., Grebmeier, J.M., Hollowed, A.B., Knowlton, N., Polovina, J., Rabalais, N.N., Sydeman, W.J., Talley, L.D., 2012. Climate change impacts on marine ecosystems. Annu. Rev. Mar. Sci. 4, 11–37. https://doi.org/10.1146/annurev-marine-041911-111611.
Dore, J.E., Brum, J.R., Tupas, L.M., Karl, D.M., 2002. Seasonal and interannual variability in sources of nitrogen supporting export in the oligotrophic subtropical North Pacific Ocean. Limnol. Oceanogr. 47, 1595–1607.
Duret, M.T., Lampitt, R.S., Lam, P., 2019. Prokaryotic niche partitioning between suspended and sinking marine particles. Environ. Microbiol. Rep. 11, 386–400. https://doi.org/10.1111/1758-2229.12692.
Durkin, C.A., Estapa, M.L., Buesseler, K.O., 2015. Observations of carbon export by small sinking particles in the upper mesopelagic. Mar. Chem. 175, 72–81. https://doi.org/10.1016/j.marchem.2015.02.011.
Flood, P.R., 2003. House formation and feeding behaviour of Fritillaria borealis (Appendicularia: Tunicata). Mar. Biol. 143, 467–475. https://doi.org/10.1007/s00227-003-1075-y.
Fuller, B.T., Petzke, K.J., 2017. The dietary protein paradox and threonine ^{15}N-depletion: Pyridoxal-5'-phosphate enzyme activity as a mechanism for the δ^{15}N trophic level effect. Rapid Commun. Mass Spectrom. 31, 705–718. https://doi.org/10.1002/rcm.7835.
Gallienne, C.P., Robins, D.B., 2001. Is Oithona the most important copepod in the world's oceans? J. Plankton Res. 23, 1421–1432. https://doi.org/10.1093/plankt/23.12.1421.
Giering, S.L.C., Sanders, R., Lampitt, R.S., Anderson, T.R., Tamburini, C., Boutrif, M., Zubkov, M.V., Marsay, C.M., Henson, S.A., Saw, K., Cook, K., Mayor, D.J., 2014. Reconciliation of the carbon budget in the ocean's twilight zone. Nature 507, 480–483. https://doi.org/10.1038/nature13123.
Gloeckler, K., Choy, C.A., Hannides, C.C.S., Close, H.G., Goetze, E., Popp, B.N., Drazen, J.C., 2017. Stable isotope analysis of micronekton around Hawaii reveals suspended particles are an important nutritional source in the lower mesopelagic and upper bathypelagic zones. Limnol. Oceanogr.
Gonzalez, H.E., Smetacek, V., 1994. The possible role of the cyclopoid copepod Oithona in retarding vertical flux of zooplankton fecal material. Mar. Ecol. Prog. Ser. 113, 233–246.
Gutiérrez-Rodríguez, A., Décima, M., Popp, B.N., Landry, M.R., 2014. Isotopic invisibility of protozoan trophic steps in marine food webs. Limnol. Oceanogr. 59, 1590–1598. https://doi.org/10.4319/lo.2014.59.5.1590.
Hannides, C.C.S., 2014. Migrant solution to the anammox mystery. Proc. Natl. Acad. Sci. USA 111, 15604–15605. https://doi.org/10.1073/pnas.1418296111.
Hannides, C.C.S., Drazen, J.C., Popp, B.N., 2015. Mesopelagic zooplankton metabolic demand in the North Pacific Subtropical Gyre. Limnol. Oceanogr. 60, 419–428. https://doi.org/10.1002/lno.10032.
Hannides, C.C.S., Popp, B.N., Choy, C.A., Drazen, J.C., 2013. Midwater zooplankton and suspended particle dynamics in the North Pacific Subtropical Gyre: a stable isotope perspective. Limnol. Oceanogr. 58, 1931–1946. https://doi.org/10.4319/lo.2013.58.6.1931.
Hannides, C.C.S., Popp, B.N., Landry, M.R., Graham, B.S., 2009. Quantification of zooplankton trophic position in the North Pacific Subtropical Gyre using stable nitrogen isotopes. Limnol. Oceanogr. 54, 50–61.
Hayes, J.M., Freeman, K.H., Popp, B.N., Hoham, C.H., 1990. Compound specific isotope analysis: a novel tool for reconstruction of ancient biochemical processes. Org Geochem. 16, 1115–1128.
Hayward, T.L., 1980. Spatial and temporal feeding patterns of copepods from the North Pacific Central Gyre. Mar. Biol. 58, 295–309.
Heatherington, E.D., Kurle, C.M., Ohman, M.D., Popp, B.N., 2019. Effects of chemical preservation on bulk and amino acid isotope ratios of zooplankton, fish, and squid tissues. Rapid Commun. Mass Spectrom. 33, 935–945. https://doi.org/10.1002/rcm.8408.
Hebel, D.V., Karl, D.M., 2001. Seasonal, interannual, and decadal variations in particulate matter concentrations and composition in the subtropical North Pacific Ocean. Deep Sea Res. II 48, 1669–1696.
Hessen, D.O., Elser, J.J., Sterner, R.W., Urabe, J., 2013. Ecological stoichiometry: an elementary approach using basic principles. Limnol. Oceanogr. 58, 2219–2236. https://doi.org/10.4319/lo.2013.58.6.2219.
Ikeda, T., Sano, F., Yamaguchi, A., Matsuishi, T., 2007. RNA : DNA ratios of calanoid copepods from the epipelagic through abyssopelagic zones of the North Pacific Ocean. Aquat. Biol. 1, 99–108. https://doi.org/10.3354/ab00011.
Ikeda, T., Sano, F., Yamaguchi, A., Matsuishi, T., 2006a. Metabolism of mesopelagic and bathypelagic copepods in the western North Pacific Ocean. Mar. Ecol. Prog. Ser. 322, 199–211. https://doi.org/10.3354/meps322199.
Ikeda, T., Torres, J.J., Hernández-Léon, S., Geiger, S.P., 2000. Metabolism. In: Harris, R.P., Wiebe, P., Lenz, J., Skjoldal, H.R., Huntley, M. (Eds.), ICES Zooplankton Methodology Manual. Academic Press, San Diego, pp. 455–532.
Ikeda, T., Yamaguchi, A., Matsuishi, T., 2006b. Chemical composition and energy content of deep-sea calanoid copepods in the western North Pacific Ocean. Deep-Sea Res. Part -Oceanogr. Res. Pap. 53, 1791–1809. https://doi.org/10.1016/j.dsr.2006.08.002.
Jackson, G.A., Checkley, D.M., 2011. Particle size distributions in the upper 100 m water column and their implications for animal feeding in the plankton. Deep-Sea Res. Part -Oceanogr. Res. Pap. 58, 283–297. https://doi.org/10.1016/j.dsr.2010.12.008.
Jarman, C.L., Larsen, T., Hunt, T., Lipo, C., Solsvik, R., Wallsgrove, N., Ka'apu-Lyons, C., Close, H.G., Popp, B.N., 2017. Diet of the prehistoric population of Rapa Nui (Easter Island, Chile) shows environmental adaptation and resilience. Am. J. Phys. Anthropol. 164, 343–361. https://doi.org/10.1002/ajpa.23273.
Karl, D.M., 1999. A sea of change: biogeochemical variability in the North Pacific Subtropical Gyre. Ecosystems 2, 181–214.
Karl, D.M., Christian, J.R., Dore, J.E., Hebel, D.V., Letelier, R.M., Tupas, L.M., Winn, C.D., 1996. Seasonal and interannual variability in primary production and particle flux at Station ALOHA. Deep-Sea Res. II 43, 539–569.
Karl, D.M., Church, M.J., 2014. Microbial oceanography and the Hawaii Ocean Time-series programme. Nat. Rev. Microbiol. 12, 699–713. https://doi.org/10.1038/nrmicro3333.
Karl, D.M., Church, M.J., Dore, J.E., Letelier, R.M., Mahaffey, C., 2012. Predictable and efficient carbon sequestration in the North Pacific Ocean supported by symbiotic nitrogen fixation. Proc. Natl. Acad. Sci. USA 109, 1842–1849. https://doi.org/10.1073/pnas.1120312109.
Karl, D.M., Lukas, R., 1996. The Hawaii Ocean Time-series (HOT) program: background, rationale and field implementation. Deep Sea Res Part II Top. Stud. Oceanogr. 43, 129–156.
Koppelmann, R., Bottger-Schnack, R., Mobius, J., Weikert, H., 2009. Trophic relationships of zooplankton in the eastern Mediterranean based on stable isotope measurements. J. Plankton Res. 31, 669–686. https://doi.org/10.1093/plankt/fbp013.
Koppelmann, R., Weikert, H., Lahajnar, N., 2003. Vertical distribution of mesozooplankton and its δ15N signature at a deep-sea site in the Levantine Sea (eastern Mediterranean) in April 1999. J. Geophys. Res.-Oceans 108, 8118. https://doi.org/10.1029/2002JC001351.
Laakmann, S., Auel, H., 2010. Longitudinal and vertical trends in stable isotope signatures (δ^{13}C and δ^{15}N) of omnivorous and carnivorous copepods across the South Atlantic Ocean. Mar. Biol. 157, 463–471. https://doi.org/10.1007/s00227-009-1332-9.
Lam, P.J., Doney, S.C., Bishop, J.K.B., 2011. The dynamic ocean biological pump: Insights from a global compilation of particulate organic carbon, $CaCO_3$, and opal concentration profiles from the mesopelagic. Glob. Biogeochem. Cycles 25. https://doi.org/10.1029/2010GB003868.
Landry, M.R., Al-Mutairi, H., Selph, K.E., Christensen, S., Nunnery, S., 2001. Seasonal patterns of mesozooplankton abundance and biomass at Station ALOHA. Deep Sea Res. Part II Top. Stud. Oceanogr. 48, 2037–2061.
Lee, R.F., Hagen, W., Kattner, G., 2006. Lipid storage in marine zooplankton. Mar. Ecol. Prog. Ser. 307, 273–306. https://doi.org/10.3354/meps307273.
Letelier, R.M., Karl, D.M., Abbott, M.R., Bidigare, R.R., 2004. Light driven seasonal patterns of chlorophyll and nitrate in the lower euphotic zone of the North Pacific Subtropical Gyre. Limnol. Oceanogr. 49, 508–519.
Liu, S., Wang, W.X., Huang, L.M., 2006. Phosphorus dietary assimilation and efflux in the marine copepod *Acartia erythraea*. Mar. Ecol. Prog. Ser. 321, 193–202.
Longhurst, A.R., Bedo, A., Harrison, W.G., Head, E.J.H., Horne, E.P., Irwin, B., Morales, C., 1989. NFLUX: a test of vertical nitrogen flux by diel migrant biota. Deep Sea Res. Part Oceanogr. Res. Pap. 36, 1705–1719. https://doi.org/10.1016/0198-0149(89)90067-8.
Mauchline, J., 1998. Advances in Marine Biology. The Biology of Calanoid Copepods, vol. 33 Academic Press, San Diego.
Mayor, D., Sanders, R., Giering, S., Anderson, T., 2014. Microbial gardening in the ocean's twilight zone: Detritivorous metazoans benefit from fragmenting, rather than ingesting, sinking detritus. Bioessays. https://doi.org/10.1002/bies.201400100.
McClelland, J.W., Montoya, J.P., 2002. Trophic relationships and the nitrogen isotopic composition of amino acids in plankton. Ecology 83, 2173–2180.
McGowan, J.A., Walker, P.W., 1985. Dominance and diversity maintenance in an oceanic ecosystem. Ecol. Monogr. 55, 103–118.
McGowan, J.A., Walker, P.W., 1979. Structure in the copepod community of the North Pacific central gyre. Ecol. Monogr. 49, 195–226.
Metz, C., 1998. Feeding of Oncaea curvata (Poecilostomatoida, Copepoda). Mar. Ecol. Prog. Ser. 169, 229–235. https://doi.org/10.3354/meps169229.
Moran, X.A.G., Lopez-Urrutia, A., Calvo-Diaz, A., Li, W.K.W., 2010. Increasing importance of small phytoplankton in a warmer ocean. Glob. Change Biol. 16, 1137–1144. https://doi.org/10.1111/j.1365-2486.2009.01960.x.
Nielsen, J.M., Popp, B.N., Winder, M., 2015. Meta-analysis of amino acid stable nitrogen isotope ratios for estimating trophic position in marine organisms. Oecologia 178, 631–642. https://doi.org/10.1007/s00442-015-3305-7.
O'Connell, T.C., 2017. "Trophic" and "source" amino acids in trophic estimation: a likely metabolic explanation. Oecologia 184, 317–326. https://doi.org/10.1007/s00442-

017-3881-9.
Ohkouchi, N., Chikaraishi, Y., Close, H.G., Fry, B., Larsen, T., Madigan, D.J., McCarthy, M.D., McMahon, K.W., Nagata, T., Naito, Y.I., Ogawa, N.O., Popp, B.N., Steffan, S., Takano, Y., Tayasu, I., Wyatt, A.S.J., Yamaguchi, Y.T., Yokoyama, Y., 2017. Advances in the application of amino acid nitrogen isotopic analysis in ecological and biogeochemical studies. Org Geochem. 113, 150–174. https://doi.org/10.1016/j.orggeochem.2017.07.009.
Ohtsuka, S., Kubo, N., Okada, M., Gushima, K., 1993. Attachment and feeding of pelagic copepods on larvacean houses. J. Oceanogr. 49, 115–120.
O'Neil, J.M., 1998. The colonial cyanobacterium Trichodesmium as a physical and nutritional substrate for the harpacticoid copepod Macrosetella gracilis. J. Plankton Res. 20, 43–59. https://doi.org/10.1093/plankt/20.1.43.
Paffenhöfer, G.A., Mazzocchi, M.G., 2002. On some aspects of the behaviour of Oithona plumifera (Copepoda: Cyclopoida). J. Plankton Res. 24, 129–135. https://doi.org/10.1093/plankt/24.2.129.
Pasulka, A.L., Landry, M.R., Taniguchi, D.A.A., Taylor, A.G., Church, M.J., 2013. Temporal dynamics of phytoplankton and heterotrophic protists at station ALOHA. Deep-Sea Res. Part II-Top. Stud. Oceanogr. 93, 44–57. https://doi.org/10.1016/j.dsr2.2013.01.007.
Popp, B.N., Graham, B.S., Olson, R.J., Hannides, C.C.S., Lott, M.J., López-Ibarra, G.A., Galván-Magña, F., Fry, B., 2007. Insight into the trophic ecology of yellowfin tuna, *Thunnes albacares*, from compound-specific nitrogen isotope analysis of proteinaceous amino acids. In: Dawson, T.D., Siegwolf, R.T.W. (Eds.), Stable Isotopes as Indicators of Ecological Change, Terrestrial Ecology Series. Elsevier, San Diego, pp. 173–190.
Postel, L., Fock, H., Hagen, W., 2000. Biomass and abundance. In: Harris, R.P., Wiebe, P.H., Lenz, J., Skjoldal, H.R., Huntley, M.E. (Eds.), ICES Zooplankton Methodology Manual. Academic Press, San Diego, CA, pp. 83–192.
Puigcorbe, V., Benitez-Nelson, C.R., Masque, P., Verdeny, E., White, A.E., Popp, B.N., Prahl, F.G., Lam, P.J., 2015. Small phytoplankton drive high summertime carbon and nutrient export in the Gulf of California and Eastern Tropical North Pacific. Glob. Biogeochem. Cycles 29, 1309–1332. https://doi.org/10.1002/2015GB005134.
Richardson, T.L., Jackson, G.A., 2007. Small phytoplankton and carbon export from the surface ocean. Science 315, 838–840. https://doi.org/10.1126/science.1133471.
Robison, B.H., 2004. Deep pelagic biology. J. Exp. Mar. Biol. Ecol. 300, 253–272. https://doi.org/10.1016/j.jembe.2004.01.012.
Scharek, R., Latasa, M., Karl, D.M., Bidigare, R.R., 1999a. Temporal variations in diatom abundance and downward vertical flux in the oligotrophic North Pacific gyre. Deep-Sea Res. I 46, 1051–1075.
Scharek, R., Tupas, L.M., Karl, D.M., 1999b. Diatom fluxes to the deep sea in the oligotrophic North Pacific gyre at Station ALOHA. Mar. Ecol. Prog. Ser. 182, 55–67.
Sheridan, C.C., Landry, M.R., 2004. A 9-year increasing trend in mesozooplankton biomass at the Hawaii Ocean Time-series Station ALOHA. ICES J. Mar. Sci. 61, 457–463.
Sheridan, C.C., Steinberg, D.K., Kling, G.W., 2002. The microbial and metazoan community associated with colonies of Trichodesmium spp.: a quantitative survey. J. Plankton Res. 24, 913–922.
Sommer, S.A., Van Woudenberg, L., Lenz, P.H., Cepeda, G., Goetze, E., 2017. Vertical gradients in species richness and community composition across the twilight zone in the North Pacific Subtropical Gyre. Mol. Ecol. 26, 6136–6156. https://doi.org/10.1111/mec.14286.
Steinberg, D.K., Carlson, C.A., Bates, N.R., Goldthwait, S.A., Madin, L.P., Michaels, A.F., 2000. Zooplankton vertical migration and the active transport of dissolved organic and inorganic carbon in the Sargasso Sea. Deep Sea Res. I 47, 137–158.
Steinberg, D.K., Cope, J.S., Wilson, S.E., Kobari, T., 2008a. A comparison of mesopelagic mesozooplankton community structure in the subtropical and subarctic North Pacific Ocean. Deep-Sea Res. Part II 55, 1615–1635. https://doi.org/10.1016/j.dsr2.2008.04.025.
Steinberg, D.K., Landry, M.R., 2017. Zooplankton and the Ocean Carbon Cycle. In: Annual Review of Marine Sciences, vol. 9. Annual Reviews, Palo Alto, pp. 413–444.
Steinberg, D.K., Van Mooy, B.A.S., Buesseler, K.O., Boyd, P.W., Kobari, T., Karl, D.M., 2008b. Bacterial vs. zooplankton control of sinking particle flux in the ocean's twilight zone. Limnol. Oceanogr. 53, 1327–1338.
Taylor, G.T., Muller-Karger, F.E., Thunell, R.C., Scranton, M.I., Astor, Y., Varela, R., Troccoli Ghinaglia, L., Lorenzoni, L., Fanning, K.A., Hameed, S., Doherty, O., 2012. Ecosystem responses in the southern Caribbean Sea to global climate change. Proc. Natl. Acad. Sci. USA 109, 19315–19320. https://doi.org/10.1073/pnas.1207514109.
Trull, T.W., Bray, S.G., Buesseler, K.O., Lamborg, C.H., Manganini, S., Moy, C., Valdes, J., 2008. In situ measurement of mesopelagic particle sinking rates and the control of carbon transfer to the ocean interior during the Vertical Flux in the Global Ocean (VERTIGO) voyages in the North Pacific. Deep-Sea Res. Part II-Top. Stud. Oceanogr. 55, 1684–1695. https://doi.org/10.1016/j.dsr2.2008.04.021.
Umhau, B., Benitez-Nelson, C.R., Close, H.G., Hannides, C.C.S., Motta, L.C., Popp, B.N., Blum, J.D., Drazen, J.C., 2019. Seasonal and spatial changes in carbon and nitrogen fluxes estimated using 234Th: 238U disequilibria in the North Pacific Subtropical Gyre. Mar. Chem.
Valencia, B., Landry, M.R., Decima, M., Hannides, C.C.S., 2016. Environmental drivers of mesozooplankton biomass variability in the North Pacific Subtropical Gyre. J. Geophys. Res.-Biogeosci. 121, 3131–3143. https://doi.org/10.1002/2016JG003544.
Wiebe, P.H., Morton, A.W., Bradley, A.M., Backus, R.H., Craddock, J.E., Barber, V., Cowles, T.J., Flierl, G.R., 1985. New developments in the MOCNESS, an apparatus for sampling zooplankton and micronekton. Mar. Biol. 87, 313–323. https://doi.org/10.1007/BF00397811.
Wiggert, J.D., Haskell, A.G.E., Paffenhofer, G.A., Hofmann, E.E., Klinck, J.M., 2005. The role of feeding behavior in sustaining copepod populations in the tropical ocean. J. Plankton Res. 27, 1013–1031. https://doi.org/10.1093/plankt/fbi090.
Wilson, S.E., Steinberg, D.K., 2010. Autotrophic picoplankton in mesozooplankton guts: evidence of aggregate feeding in the mesopelagic zone and export of small phytoplankton. Mar. Ecol.-Prog. Ser. 412, 11–27. https://doi.org/10.3354/meps08648.
Yamaguchi, A., Watanabe, Y., Ishida, H., Harimoto, T., Furusawa, K., Suzuki, S., Ishizaka, J., Ikeda, T., Masayuki, M.T., 2002. Community and trophic structures of pelagic copepods down to greater depths in the western subarctic Pacific (WEST-COSMIC). Deep-Sea Res. Part -Oceanogr. Res. Pap. 49, 1007–1025. https://doi.org/10.1016/S0967-0637(02)00008-0.
Zalkina, A.V., 1970. Vertical distribution and diurnal migration of some Cyclopoida (Copepoda) in the tropical region of the Pacific Ocean. Mar. Biol. 5, 275–282.